MULLARD LIMITED
Mullard House
Torrington Place
London, W.C.1

CONTENTS

Infrared Detectors and their Applications 75–82

Fire Alarm System using Infrared Flame Detector 82–86

Simple Heat Locator using Infrared Detector 86–88

Passive Intruder Alarm using Infrared Detector 88–90

Radiation Thermometer for Temperatures Greater than 100°C 91–98

Room Temperature Radiation Thermometer 98–101

Infrared Microscope for Temperature Measurement of Small Areas 101–107

Closed Circuit Infrared Television System 108–120

VOL. 10 No. 93 MAY 1968

Mullard Technical Communications

VOLUME 10 NUMBER 93

May 1968

Mullard Technical Communications

VOLUME 10 NUMBER 93 May 1968

Contents

Infrared Detectors and their Applications *F. D. Morten* 75

Fire Alarm System using Infrared Flame Detector *P. R. D. Coleby* 82

Simple Heat Locator using Infrared Detector *P. R. D. Coleby* 86

Passive Intruder Alarm using Infrared Detector *R. A. Lockett* 88

Radiation Thermometer for Temperatures Greater than 100°C *P. R. D. Coleby* 91

Room Temperature Radiation Thermometer *R. A. Lockett* 98

Infrared Microscope for Temperature Measurement of Small Areas *T. J. Jarratt* 101

Closed Circuit Infrared Television System *M. H. Jervis* 108

Mullard Technical Communications contains information on the performance or application of Mullard products such as semiconductor devices, integrated circuits, electronic valves and tubes, and electrical and magnetic components. It is issued free-of-charge to equipment designers, research organisations, reference libraries, and educational establishments. Applications to be added to the circulation list should be made under an official letter head to Central Technical Services.

Abstracts, or references to an article, should mention both the source, *Mullard Technical Communications*, and the authors. Requests for republication or translation should be made to the Editor in writing.

All articles in *Mullard Technical Communications* are indexed in *British Technology Index*. Abstracts appear in *Current Papers in Physics, Electrotechnology, and Control.*

The issue of the information contained in this publication does not imply any authority or licence for the utilisation of any patented feature.

'Mullard' is the trade mark of Mullard Limited and is registered in most of the principal countries of the world.

Editor: F. A. Sowan
Assistant Editors: E. G. Evans A. Perry

Published by
Central Technical Services
Mullard Limited, Mullard House, Torrington Place, London, W.C.1
Telephone: 01-580 6633 Telex: 264341

© Mullard Limited, 1968

Made and Printed in England by
WIGHTMAN AND COMPANY LIMITED, 1/3 BRIXTON ROAD, LONDON, S.W.9

THERMOMETRY AND INSTRUMENTATION USING INFRARED DETECTORS

Temperature measurements with accuracies from about ±0·2degC at 25°C to ±5degC at 500°C are now attainable with electronic infrared detectors and their associated circuits. No contact is necessary between the detector and the area whose temperature is being measured; the response time can be as low as 1ms, and the object itself can even be in motion.

The presence or the arrival of an object whose temperature is significantly different from that of the background can be detected with other arrangements of infrared detectors and their circuits. The output can be used for control or alarm applications.

A complete thermal picture to indicate the superficial temperature over a given area of a scene can be provided by more complex infrared detection systems. This thermal image can be presented on a normal cathode ray tube (for example, in an oscilloscope).

Infrared detection, infrared measurement and infrared imaging are finding increasingly numerous and varied uses in industry and medicine. The articles on pages 75 to 120 give a brief account of the relevant theory of infrared detection and several typical applications. Circuits of prototypes are provided.

Mullard Limited manufacture and supply the infrared detectors that are used, but not the equipments described.

ACKNOWLEDGEMENT

Each of the authors of the articles on pages 75 to 120 wishes to thank J. Ingham of Mullard Limited for assistance in the work done and in the preparation of the articles.

Infrared Detectors and their Applications

F. D. Morten
Mullard Limited

INTRODUCTION

The nature of infrared radiation is discussed first in this article, and then follow descriptions of methods of detection and a number of applications of the Mullard range of detectors.

Infrared radiation is physically of the same form as visible radiation (light), but in many of its interactions with matter it behaves rather differently. The wavelength of infrared radiation is longer than that of radiation in the visible region, causing it to lie 'beyond the red' when a spectrum is formed by a prism from an incandescent source. It was in this way that the existence of infrared radiation was deduced by Sir William Herschel in 1800. The similarity of the natures of infrared and visible radiation was shown by the fact that both could be polarised; the wavelength of infrared radiation was determined by interferometric measurements soon after 1830. Subsequent work showed that there is no upper limit to the wavelength of such radiation, and it has now been studied at wavelengths where it merges with electromagnetic radiation generated by microwave techniques.

The essential property which distinguishes infrared radiation from light is thus its wavelength. A convenient unit for measurement is the micrometre (µm) which is 10^{-6} metre. (The micrometre is equal to the micron, µ, a term still used but now deprecated. Similarly deprecated is the term millimicron, mµ, being 10^{-3} micron.) In the shorter wavelength region, the nanometre (10^{-9} metre) may be used.

The Ångstrom unit, Å, which is 10^{-10} metre, is commonly used in optical physics. These units of wavelength are compared in Table 1, which must be read from the lefthand side.

TABLE 1

Comparison of Units of Length

	Å	nm	µm	mm	cm	m
Å =	1	10^{-1}	10^{-4}	10^{-7}	10^{-8}	10^{-10}
nm =	10	1	10^{-3}	10^{-6}	10^{-7}	10^{-9}
µm =	10^{4}	10^{3}	1	10^{-3}	10^{-4}	10^{-6}
mm =	10^{7}	10^{6}	10^{3}	1	10^{-1}	10^{-3}
cm =	10^{8}	10^{7}	10^{4}	10	1	10^{-2}
m =	10^{10}	10^{9}	10^{6}	10^{3}	10^{2}	1

The infrared region begins at the wavelength which is just too long for the eye to see (0·75µm); its other limit is not clearly defined, but it is often taken to be 1000µm, where the microwave region begins. This limit depends on whether optical or microwave techniques are being considered. Fig. 1 illustrates the relation of the infrared region to other parts of the electromagnetic spectrum.

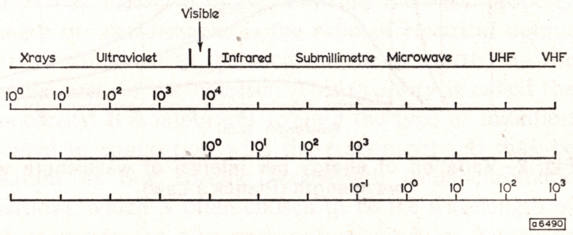

Fig. 1—Electromagnetic spectrum

The infrared region is often divided into 'near' (0·75 to 1·5µm), 'intermediate' (1·5 to 10µm) and 'far' (beyond 10µm) regions, and the region beyond 300µm is often referred to as the 'submillimetre' region.

SOURCES OF INFRARED RADIATION

Electromagnetic radiation is emitted by any object at any temperature above the absolute zero (−273°C), but the amount emitted and its distribution with wavelength depend on the temperature and emissivity of the body. The emissivity denotes the ratio of the actual emission from the body to that from a hypothetical source called a 'black body' at the same temperature. The emissivity generally varies with wavelength.

The properties of a 'black body' radiator may be calculated theoretically. Three points about it are of particular importance:

1) The total energy radiated (W_{tot}) is proportional to the fourth power of the absolute temperature T (°C+273):

$$W_{tot} = \sigma T^4$$

where σ is Stefan's constant, which is approximately equal to $5{\cdot}67 \times 10^{-12}\mathrm{Wcm^{-2}deg^{-4}K}$.

2) The curve of variation of energy per interval of wavelength ($W\lambda d\lambda$) is always of the same shape, following Planck's law:

$$W\lambda d\lambda = \frac{C_1\lambda^{-5}d\lambda}{\exp(C_2/\lambda T)-1}$$

where C_1 and C_2 are constants, given by

$$C_1 = 3{\cdot}7 \times 10^{-12}\,\mathrm{Wcm}^2$$
$$C_2 = 1{\cdot}44\,\mathrm{cm\ deg.}$$

This is plotted in Fig. 2 for some typical source temperatures.

3) The wavelength of the peak emission is a simple function of the absolute temperature (Wien's displacement law). The wavelength in μm is:

$$\lambda_{pk} = \frac{2900}{T}.$$

Many real objects are similar to the hypothetical 'black body', and it is possible to make an experimental source approaching the theoretical very closely by taking an almost complete hollow sphere or a narrow cone at a uniform temperature.

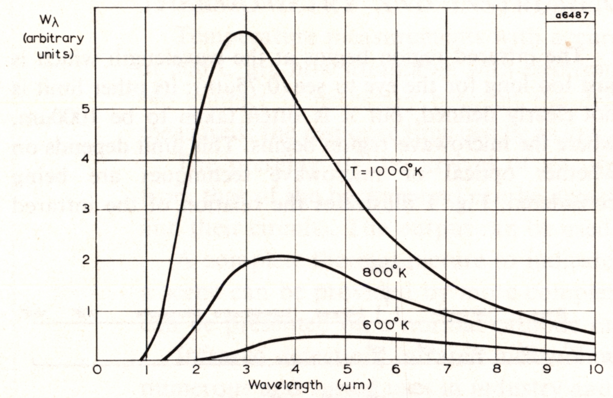

Fig. 2—Variation of energy per interval of wavelength with wavelength (Planck's Law)

Application of the equation for peak wavelength to the sun (at 6000°K) shows peak emission at 0·5μm or 5000Å, in the visible region. An object at, say, 900°K (common for a furnace) will emit most at about 3μm, one at room temperature (300°K), at 10μm. Thus the range from the visible limit to 10μm is a very suitable wavelength region for measuring radiation from common objects, and hence detecting their presence or determining their temperature.

Although many interesting sources of infrared radiation are close to 'black body' sources, some sources such as flames and lasers emit over a narrow wavelength range. Normal tungsten filament lamps, although producing visible radiation, emit peak radiation in the near-infrared region. Gallium arsenide electroluminescent diodes, when forward-biased, produce monochromatic radiation at 0·9μm which may be modulated at very high frequencies.

TRANSMISSION OF INFRARED RADIATION

Although infrared radiation is similar to light, it is important to realise that, because something is transparent or opaque in the visible region, it is not necessarily so in the infrared. Thus, for example, ordinary clear glass is transparent up to only about 2·5μm in the infrared region. On the other hand, semiconductor materials such as germanium and silicon, opaque in the visible, are transparent in the infrared region beyond 1·8 and 1μm respectively.

An important factor in transmission over long distances is the atmosphere, and Fig. 3 shows typical transmission percentages over a path of one mile. The 'transparent' regions in this figure (in for example, 8 to 13μm) are referred to as 'windows'.

Interference filters which enable narrow bands of radiation to be selected, or 'cut-on' and 'cut-off' characteristics of any form to be achieved, are important components often used in infrared systems.

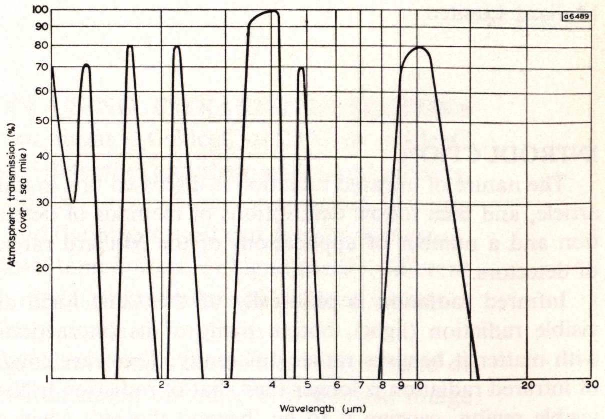

Fig. 3—Atmospheric transmission of infrared radiation over one sea mile

DETECTION OF INFRARED RADIATION

As infrared radiation is a form of electromagnetic energy, it is, of course, possible to detect it by absorbing it and hence converting the energy to heat. This is the basis of early experiments using a blackened thermometer bulb. However, this is slow, insensitive and inconvenient; a device that gives an electrical output is more desirable.

Thermal Detectors

Detectors which measure the change of temperature of an absorber are called thermal detectors. The output obtained from them may be in the form of a thermal e.m.f. (thermocouple detector), a change in resistance of a conductor (bolometer), or the movement of a diaphragm caused by the expansion of a gas (pneumatic detector) which may lead to the change in illumination of a subsidiary photocell (Golay Cell). Such detectors can be made to respond to radiation over a very wide wavelength range. However, because the temperature of the sensing object must change, they are either slow in response, taking one-hundredth to one-tenth of a second, or are fragile.

Quantum Detectors

The alternative method of detecting infrared radiation depends on the interaction of the radiation with electrons in a solid, causing the electrons to be excited to a higher energy state. These effects depend on the quantum nature of radiation, and detectors using them are called quantum detectors.

The quantum theory states that radiation of a given wavelength λ is composed of 'particles' each of individual energy proportional to 1/λ. Hence, if a transition of electrons from one state to another, requiring an energy W, is considered, it will only occur if the wavelength is such that λ is less than some critical value. The idealised response of a quantum detector is as shown in Fig. 4.

The rising form of the curve is due to the fact that, as the wavelength increases, the number of quanta for a given amount of energy increases, and since the output is controlled by the number of electrons excited, it also rises. Fig. 4 also shows the idealised response of a thermal detector; as this type of detector measures the energy directly, the response per watt is constant.

To use this quantum effect, it is necessary to be able to excite electrons from one state to another in which their electrical properties are different. One way is by photoemission, when electrons are given enough energy to escape from a solid and flow through a vacuum to give a current. However, surfaces require rather high energies for the release of electrons, and this effect can only be used in the visible and near infrared (to about 1μm). However, inside a semiconducting material, the properties of an electron in the valence band are very different from when it is in the conduction band: in an n-type semiconducting material, the electrons in the valence band are unable to contribute to the conduction. If excited to the conduction band, however, they can do so, as also can the 'hole' left behind in the valence band. Thus the conductivity is increased, and the material may be used as a photoconductor to detect radiation. If the absorption occurs near a p-n junction, the excited carriers are swept away by the junction electric field and give a current in the external circuit. Devices using such effects are known as photodiodes and phototransistors.

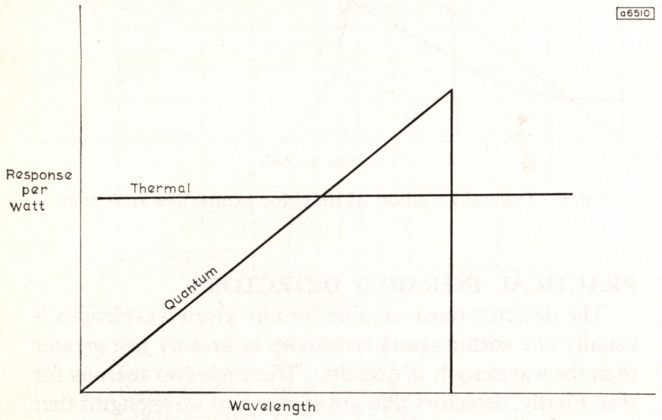

Fig. 4—Idealised response characteristic for quantum and thermal dectectors

If it is desired to detect radiation at long wavelengths in the infrared region, a small amount of excitation energy is required. Some detectors make use of the release of an electron from an added impurity atom, which needs less energy than for an excitation across the band gap. Such devices are impurity photoconductors. The energies required for several types of quantum detector are compared in Fig. 5.

The fact that smaller energies are required at the longer wavelengths for quantum detectors has one important consequence. The smaller energy requirement allows the excitation of electrons by thermal agitation of the solid, and this is a random effect that gives rise to electrical noise in the output. Thus, for good sensitivity, it is necessary to cool the semiconducting element. This may necessitate only a thermoelectric cooler to maintain a temperature just below room temperature, or it may demand the use of liquid helium, boiling at 4·2°K, depending on the application.

SOME IMPORTANT DETECTOR PROPERTIES

Responsivity

The purpose of a detector is to convert infrared radiation into an electrical signal, and thus the basic property defining the performance is the ratio of electrical output (volts or amperes) to the incident energy (watts) on the sensitive area of the detector. This quantity is called the responsivity. It is important to note the type of radiation specified in connection with the responsivity. It may be radiation at one specific wavelength (monochromatic radiation), which is often chosen to be the wavelength of peak sensitivity (to give peak responsivity), or it may be black-body radiation from a source at a specified temperature, often 500°K (to give black-body responsivity). In this case, some of the incident radiation is in wavelength regions where the detector is not sensitive, but the whole of the radiation is counted in calculating this responsivity. Of course, the black-body responsivity is always less than the peak responsivity. The responsivity will also vary with modulation frequency of the radiation because of the finite time-constant of the photo-effect.

Noise Equivalent Power, N.E.P.

The importance of cooling to reduce noise has been mentioned. Such electrical noise sets a limit to the smallest radiation level that can be detected. The noise of a detector is usually quoted as the root mean square value of the electrical output measured in a bandwidth of 1Hz at some specified centre frequency, under typical operating conditions for the detector. This quantity may be independent of frequency over some range, when it is said to show white noise in that range, or it may vary with

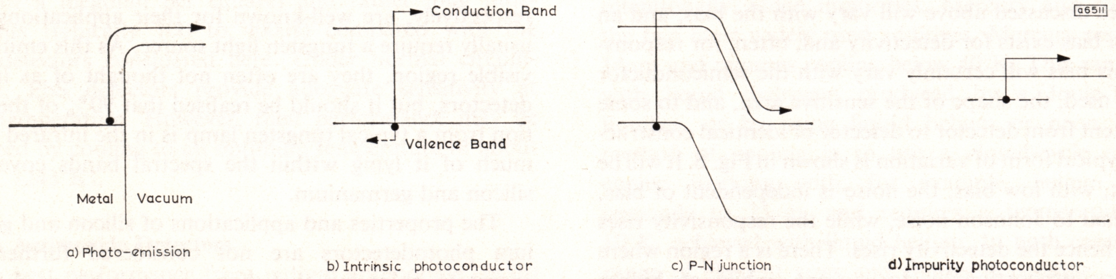

a) Photo-emission b) Intrinsic photoconductor c) P-N junction d) Impurity photoconductor

Fig. 5—Energy transitions in quantum detectors

frequency. For white noise, the magnitude measured is proportional to the square root of the bandwidth, so the performance is often quoted as volts per unit bandwidth ($\mathrm{VHz}^{-\frac{1}{2}}$).

Although a low noise enables smaller energies to be detected, it may make the design of suitable amplifiers difficult. To get the best performance, the amplifier noise must be low. It is thus often of importance to know the ratio of the detector noise to the value of Johnson noise in a resistance, at room temperature, of magnitude equal to that of the detector. This ratio may be quoted as a noise factor.

In testing a detector intended for measuring small quantities of radiation, the signal-to-noise ratio may be measured. This depends on a number of test conditions, such as the radiation energy used, the frequency of modulation of the energy and of the noise measured, and the bandwidth. A more useful quantity is the Noise Equivalent Power, or N.E.P. This is the amount of energy that will give a signal equal to the noise in a bandwidth of 1Hz. It is, in general, a function of the wavelength and of the frequency of measurement. It is equal to the noise (per unit bandwidth) divided by the responsivity.

Area Normalised Detectivity, D*

As one might expect, all the above quantities vary with the size and shape of the sensitive area of detectors, even if made of the same material prepared by the same process. However, it is found (and supported by theory) that for similarly made detectors, the N.E.P. is often proportional to the square root of the area of the detector. Thus a quantity called the area normalised detectivity, with symbol D*, and equal to $(\mathrm{Area})^{\frac{1}{2}}/\mathrm{N.E.P.}$, is commonly used to compare and specify detectors. From what has been stated, it will be seen that this quantity depends on the wavelength or black-body temperature of radiation used, and the frequency of measurement of signal and noise. It is therefore written as, for example, D* (5μm, 800, 1), implying a value at a wavelength of 5μm and a frequency of 800Hz, the '1' indicating the normalisation to unit bandwidth. Alternatively, if a black-body radiation source is concerned, the definition may be, for example, D* (500°K, 90, 1). The dimensions of this commonly used quantity are $\mathrm{cmHz}^{\frac{1}{2}}\mathrm{W}^{-1}$, and, as opposed to the N.E.P., it has the merit of taking a higher value for better-performance cells.

OPTIMUM PERFORMANCE CONDITIONS

Photoconductive cells must have a bias current passed through them to make the changes of resistance appear as a voltage; photodiodes may also require bias. All the properties discussed above will vary with the bias, and an optimum bias exists for detectivity and, often, for responsivity. This bias will certainly vary with the semiconductor material used, the shape of the sensitive area, and to some small extent from detector to detector of identical construction. A typical form of variation is shown in Fig. 6. It will be seen that, with low bias, the noise is independent of bias, being equal to Johnson noise, while the responsivity rises linearly, hence the detectivity rises. There is a region where both vary proportionally to current, while at higher operating currents, the noise tends to rise more rapidly than linearly, and the signal less rapidly than linearly. The most suitable operating range for optimum signal-to-noise can be seen in Fig. 6.

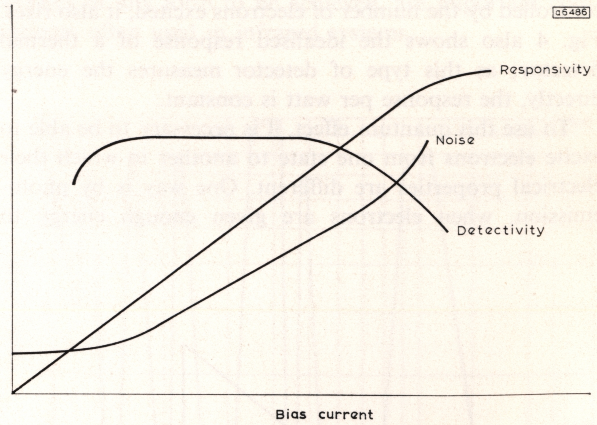

Fig. 6—Typical variation of detector properties with bias

PRACTICAL INFRARED DETECTORS

The detector most suitable for any given wavelength is usually one with its peak sensitivity at or only just greater than the wavelength in question. There are two reasons for this. Firstly, detectors that are sensitive to wavelengths that are much longer than are necessary require more cooling to reduce internal thermal noise. Secondly, there is a theoretical limit to the detectivity set by the amount of radiation the detector receives in its sensitive band from the thermal background radiation, usually at 300°K. This radiation is noisy in nature, gives rise to a limiting noise in the detector, and limits the attainable detectivity to what is called the background limited, or BLIP, value. For wavelengths up to 10μm, this limiting value falls with wavelength, and so any sensitivity beyond the required wavelength is likely to be detrimental.

The graph in Fig. 7 shows this limitation together with the performance of some typical detectors that are discussed below. The materials used are stated, together with the operating temperature and the field of view (F.O.V.). It will be seen that some detectors show performance above the theoretical limit. This is because these have a cooled aperture restricting their field of view and hence the amount of background radiation received.

Silicon and Germanium Photodetectors

Silicon and germanium, sensitive up to 1μm and 1·8μm respectively, are well-known for their applications which usually require a tungsten light source. As this emits in the visible region, they are often not thought of as infrared detectors, but it should be realised that 90% of the radiation from a typical tungsten lamp is in the infrared region, much of it lying within the spectral bands covered by silicon and germanium.

The properties and applications of silicon and germanium photodetectors are not considered further here, except to point out that they are available as diodes or transistors, and that many specialised forms of silicon diode are available, such as cells having high operating speeds, and solar cells.

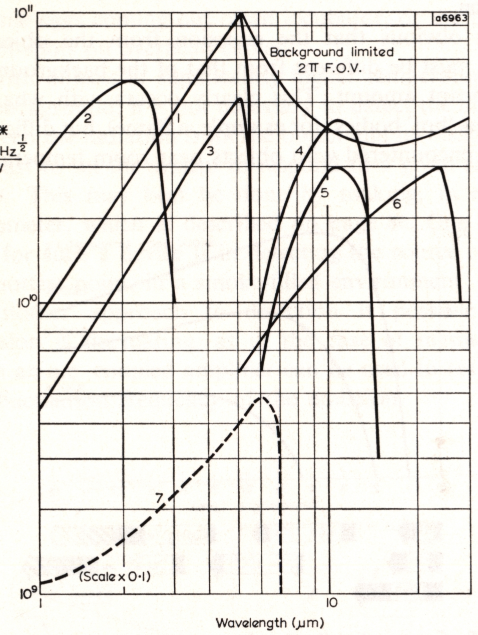

Fig. 7—Typical infrared response curves
Curve 1—InSb, 77°K, 60° F.O.V.
Curve 2—PbS, 300°K, 2π F.O.V.
Curve 3—InSb, 77°K, 2π F.O.V.
Curve 4—Ge:Hg, 35°K, 30° F.O.V.
Curve 5—Ge:Hg, 35°K, 60° F.O.V.
Curve 6—Ge:Cu, 4·2°K, 60° F.O.V.
Curve 7—(scale × 0·1) InSb, 300°K, 2π F.O.V.

Lead Sulphide Detectors

Next in increasing wavelength of peak sensitivity is lead sulphide (PbS). This material must be prepared in a way very different from silicon and germanium to give good photosensitivity. It may be deposited by evaporation, in which case a small vacuum capsule is used. The layer is treated during and after deposition to give a high sensitivity. The typical detectivity D* (2·2μm, 800, 1) at the peak wavelength is $6\times10^{10}\mathrm{cmHz}^{\frac{1}{2}}\mathrm{W}^{-1}$.

The evaporation technique is limited in the size and shape of the elements that can conveniently be made. An alternative process is to deposit the lead sulphide layer by means of a chemical reaction on to a suitable insulating substrate. This enables the formation of a layer which can be cut into a wide range of shapes and sizes, including arrays of elements.

All lead sulphide cells have a high impedance (of the order of a megohm per square) and rather long time-constants (typically 100 to 400μs) compared with the other detectors considered here. Under normal circumstances, PbS detectors provide adequate sensitivity at room temperature. However, their performance may be enhanced by cooling to an optimum temperature of about −30°C (243°K).

Indium Antimonide Detectors

The best performance from indium antimonide (InSb) is achieved by cooling to liquid nitrogen temperature (77°K), when detectivities near the background-limited value can be obtained. However, indium antimonide also has many uses at higher temperatures. It is the only currently available semiconductor material that will respond to 7μm at room temperature.

Photoconductive detectors are made from doped single crystals, prepared in a way similar to that used for germanium and silicon. These crystals are then cut into elements of the required size and made as thin as possible. At room temperature, the resistivity is low, giving detectors with resistances of about 5Ω per square. The most useful forms are thus either long thin strips, or areas made up of a number of such strips laid in parallel but connected electrically in series. The effect of temperature on performance is rather large at these temperatures, and a good heatsink is required for the element. Cooling to, say, 0°C gives improved performance, and these detectors are ideally suited to thermoelectric refrigeration. The response time is very low (about 50ns) and the detectivity D* (6μm, 800, 1) is up to $8\times10^{8}\mathrm{cm\ Hz}^{\frac{1}{2}}\mathrm{W}^{-1}$.

Cooled detector elements are made in a similar way, the main difference being in the doping of the single crystal material. The sensitive element must be mounted in an enclosure suitable for cooling. This is usually a small glass dewar vessel with infrared transmitting window, and the cooling may be achieved either by using liquid nitrogen at 77°K (either simply pouring liquid nitrogen into a vessel, or alternatively using a liquid nitrogen transfer system for continuous operation) or by means of a miniature Joule-Thomson expansion liquifier.

Cooling increases the resistance to a more convenient value (about 2kΩ per square) and elements covering a wide range of shapes and sizes may be made. This includes arrays of elements as small as 100μm square with as many as 100 in one assembly. Detectors are 'background limited' and hence the use of a cooled aperture as part of the assembly improves the detectivity. Without such apertures, a value of D* (5·3μm, 800, 1) of $5\times10^{10}\mathrm{cm\ Hz}^{\frac{1}{2}}\mathrm{W}^{-1}$ is achieved. With a restricted field of view, values of over $1\times10^{11}\mathrm{cm\ Hz}^{\frac{1}{2}}\mathrm{W}^{-1}$ are possible.

Doped Germanium Detectors

For wavelengths greater than 5μm, detectors using controlled impurities in germanium are the most highly developed. In these, the radiation is absorbed by electrons in the impurities, and this leads to a lower absorption coefficient, hence the need for thicker specimens. It is also essential to cool the element so that the electrons are initially in the impurity centres ready to be excited.

The germanium must be extremely pure apart from the intentionally added impurities. Mercury and copper are the two most widely used additives. Mercury responds to 14μm and requires cooling below 40°K. This can be done with liquid hydrogen produced by a Joule-Thomson liquifier, or by using liquid helium or neon. Another method of cooling is to use a closed-cycle expansion engine working with, for example, helium. Copper responds to 25μm, and requires a temperature below 10°K, achieved with liquid helium. In both cases, a wide range of element sizes and shapes is possible. A cooled aperature is usually essential, and with a field of view of 60°, peak wavelength detectivities of over $10^{10}\text{cmHz}^{\frac{1}{2}}\text{W}^{-1}$ are obtained.

Indium Antimonide Extrinsic Detectors

For the specialised applications of infrared radiation, beyond 50µm, detectors have been developed which are faster than thermal detectors. One such device uses impurity levels in indium antimonide, giving a very low activation energy. It is necessary to operate such devices at a temperature below that of helium boiling at atmospheric pressure, and so the helium must be in a low-pressure container. The response of such devices extends through to the submillimetre and microwave regions.

Future Developments

The detectors described above will be seen to give a coverage over the whole of the infrared spectrum. However, other semiconductor materials are of interest because they may give better performance or be more convenient to use. One such material is a mixed crystal of cadmium telluride and mercury telluride, which can be made to have its peak response over a wide range of wavelengths. The chief interest in this material is for use at about 10µm; this corresponds to the peak of thermal emission from objects at room temperature, and also lies in a 'window' in the atmospheric transmission. The doped germanium detectors currently available for this wavelength require cooling below liquid nitrogen temperature (77°K), which has disadvantages, but with an intrinsic photoconductor, operation at higher temperatures is possible. It is expected that this material will find many applications.

APPLICATIONS OF INFRARED DETECTORS

The range of infrared detectors currently available gives coverage of the whole infrared spectrum. Although the applications of these detectors are numerous, they fall into two general classes. One depends on the properties of black-body radiation for purposes of measurement and control, the other depends on the optical properties of materials (solid, liquid and gaseous) in the infrared region as aids to analysis and control. These two classes are discussed below.

BLACK-BODY OBJECTS

In the first class, the applications use the black-body emission which is emitted from all objects at temperatures above the absolute zero. Fig. 8 shows the distribution of energy from black-bodies at three temperatures, showing the rapid increase in total radiation, and the shift of the peak of the energy distribution to shorter wavelengths, Also shown in Fig. 8 is the useful spectral range of the types of detector most commonly available. This indicates the desirability of choosing a detector to match the spectral output of the source of interest. For example, for a source at 300°K, a detector responding to at least 10µm is desirable although, for practical reasons, a detector of, say, indium antimonide may be preferred. A lead sulphide detector is unlikely to be of any use.

A detector responding in the correct wavelength region can be used in three types of application. It can be used for detection of an object, measurement of its temperature, or to form a thermal picture. These will be considered in turn.

Detection

It is obvious that the emission from the object of interest must be different from that of the background by a significant amount. This clearly occurs with what are known as 'hot' bodies (for example, a flame), but difficulties may be encountered with objects near room temperature; some objects, assumed here to approximate to a black body, are listed in Table 2 with their radiation outputs indicated. Whether or not one of these objects can be detected against the room temperature background depends on whether or not enough of the radiation can be focused onto the detector to give a change of signal greater than the noise of the detector and amplifier, and greater than any extraneous noise. It might be necessary, therefore, to use a large aperture in the collecting optical system for the greatest sensitivity. A narrow bandwidth, giving a long response time, will decrease the noise and lead to a greater sensitivity. It will also be necessary to detect a change in the output to indicate the presence of the object. Such a system can be made either to detect the passing of objects whose temperatures are within a few degrees of the background temperature or, by 'scanning' the optical system over the scene, to detect a stationary object. The principles of the system are shown in Fig. 9.

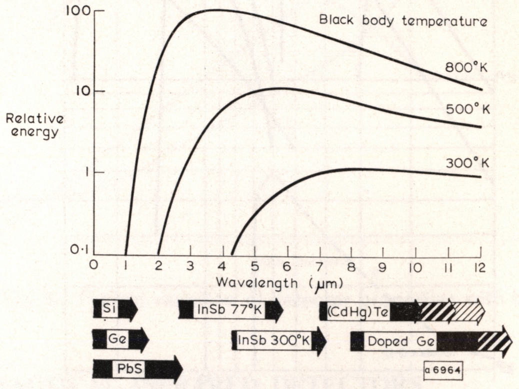

Fig. 8—Energy distribution from a black body at three temperatures

TABLE 2
Radiation from Various Objects

Object	Temperature	Total energy	Energy between 0 and 5µm
	(°C)	(W/m²)	(W/m²)
Ice	0	320	2·2
Room temperature	22	430	5·2
Human face	34	505	7·7
A cup of tea	60	700	24·5

Some of the known applications of such systems are the detection of human beings, the occurrence of an overheated part of a mechanical system (overheated axle-boxes on trains, for example), the difference between fertile and infertile eggs coming out of an incubator, or the presence of hot spots on overhead cables.

With objects at significantly higher temperatures than the background, it is not necessary to detect the difference between the radiation from the object and its background, but just to set the system to respond to a given radiation input. This may best be done by making, in effect, a radiometer, which is described on page 86. One application for such a device is in detecting the source of a fire, the hottest point, in a smoke-filled environment.

Another approach to detection is possible if the emission is fluctuating, as in the case of many flames. Then an a.c. coupled amplifier can be used to respond to the fluctuation frequency of the emission.

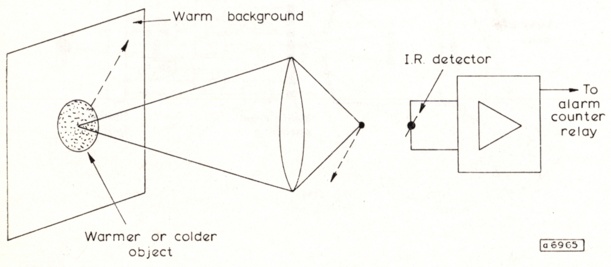

Fig. 9—Detection of moving object with temperature different from that of the background

There are many extensions to the techniques mentioned. For example, the output may be used for counting, to control a servo-system in a tracking mode or, using two channels, to measure time intervals and hence speed.

Temperature Measurements

To attain the accuracy essential for temperature measurement using the emitted infrared radiation, it is usually necessary to measure the difference in detector output when viewing the object and a reference source alternately. This is because the voltage across the detector is usually a function of the temperature of the detector itself, as well as that of the object being viewed, and drifts in the detector temperature could mask the output produced by the object. The measurement of the difference between the test source and the reference can be effected by using a radiation 'chopper', often a rotating segmented disc. In this case, the output a.c. signal is related to the difference between the emission of the object and that of the chopper blade. For objects above 100°C, the radiation from a room-temperature chopper can usually be ignored, although this depends to some extent on the wavelength response of the detector used. For lower temperatures, the output is related to the difference between object temperature and chopper blade temperature unless the image of a reference source is reflected by the chopper blade back onto the detector when the object is obscured. Fig. 10 illustrates the basis of a simple system.

Chopping the radiation has the further advantage that a.c. amplifiers can be used, and the bandwidth limited to reduce the noise. The frequency of chopping can be chosen such that the noise figure of detector and amplifier is lowest.

It may be necessary, for absolute measurements, to take account of the fact that the emissivity of the object is not unity. However, because of the rapid change of emission with temperature, the absence of such a correction does not always have a very marked effect on the temperature indicated.

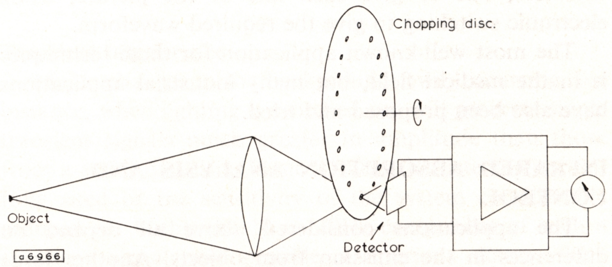

Fig. 10—Basic radiometer system

The advantages of radiation measurements of temperature lie primarily in the fact that no contact need be made with the object under investigation. Thus the temperature of the object is not seriously disturbed, and moving objects present no difficulty. Furthermore, in many cases, no special surface preparation is necessary, unless the surface has a very low emissivity.

The applications for these techniques are too numerous to list here. Two extreme examples may be mentioned; these are the determination of temperatures of parts of integrated circuits in operation, and the measurement of the temperatures of blast furnace walls.

Thermal Imaging

The need for thermal imaging frequently arises when the location of those parts of an object where the temperature is of interest are not specified. Measurements could be made point by point with a radiometer, but it is often more convenient or essential to have a picture of the emission differences, and hence of temperature differences, presented directly. Thus there is considerable interest in devices that give such thermal pictures.

The requirement may be for an indication of the hot areas, or for actual temperature measurements of selected points in the picture. A television type of display tube is the most convenient method of displaying the picture. The information to make up this picture can be obtained in a number of ways, as illustrated in Fig. 11. One technique scans an image (produced by lens or mirror system) using a disc containing a spiral of holes known as a Nipkow disc. A detector behind the disc generates an electrical waveform which can be used as the video signal for the display. In a second system, the image of the scene is made to move in a television-raster type of movement over a small detector by the synchronised movements of two mirrors giving line and frame scans. In a third method,

Fig. 11—Methods of obtaining information for television display
(a) Nipkow disc scanner
(b) Double mirror scanner
(c) Multi-element detector scanner

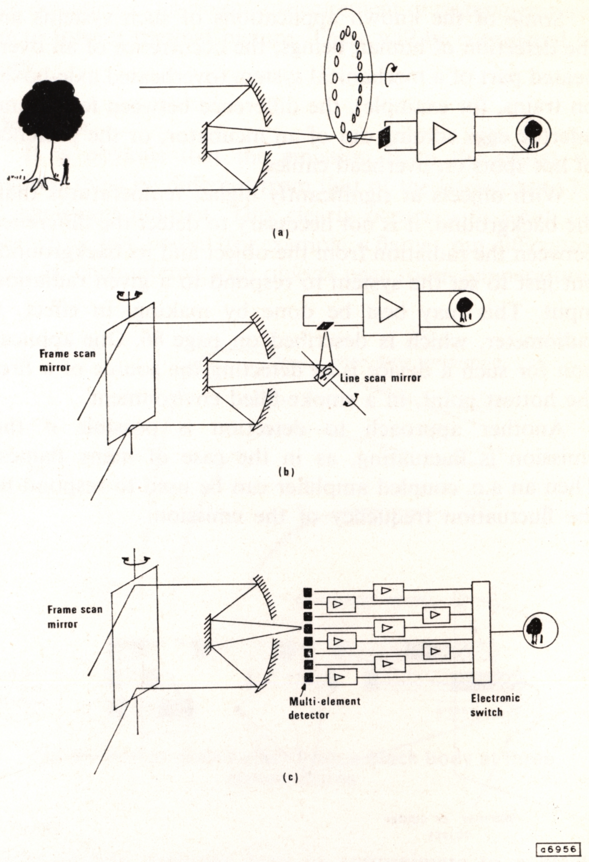

greater sensitivity may be achieved by using an array of detectors, one to give each line of the picture, using electronic switching to give the required waveform.

The most well-known application for these techniques is in the medical field, but many industrial applications have also been proposed and tried.

INFRARED ABSORPTION ANALYSIS AND CONTROL

The applications considered above all depend on differences in the emission from objects. Another large class of applications depends on the change of absorption produced by materials, in either the solid, liquid or gaseous form. The field of chemical analysis by infrared absorption spectroscopy is now well known and depends on the fact that the absorption, particularly of organic materials, is characteristic of a particular compound or type of chemical structure. Application of such techniques outside the laboratory is expected to grow rapidly with the availability of rugged and sensitive semiconductor detectors. Improvements of sensitivity, speed of response and wavelength coverage are expected to widen still further the scope of this type of measurement. Much work is being done to improve gas analysis, which must often be performed in situ and give a rapid read-out. Such measurements are of growing importance in control systems as widely varying as those for power station exhaust gases, and anaesthetics. Other applications, not involving 'on-line' control, include detecting leaks in piped gas systems or hermetically 'sealed' electronic equipment.

Fire Alarm System using Infrared Flame Detector

P. R. D. Coleby
Mullard Limited

INTRODUCTION

Commercially available fire alarms are usually one of two basic types, namely 'heat' detectors and 'smoke' detectors. With heat detectors, a dual-action thermostat operates the alarm either at a predetermined temperature (approximately 65°C) or when the rate of rise of temperature exceeds a given level. The basic limitation of this system is that the fire must generally be well-established before the alarm is given. The optical smoke detector relies on the presence of smoke particles in the atmosphere to operate the alarm. Since most fires produce an appreciable volume of smoke in their early stages this system has the major advantage of producing an early warning. Its limitations are set by the environment and the nature of the fire.

The system to be described here is a 'flame' detector in which the infrared radiation from a flame results in an alarm signal from an infrared detector. The major advantage of this type of system is that an alarm signal will be produced as soon as a flame occurs in the field of view of the detector.

BASIC FIRE ALARM SYSTEM

A practical form of flame-detector fire alarm system using an infrared detector has been designed using the 119CPY, a small lead sulphide cell with a sensitive area of 1×1mm having a peak spectral response at 2·2μm. As an infrared detecting system, the fire alarm is very simple, requiring no mechanical chopping or elaborate optical system. Fig. 12 shows the overall scheme of the system.

An amplifying stage is incorporated with a cell to form a composite detector head. This has the advantage that a large signal is generated at source so that the system is less prone to electrical interference between the source and the central alarm position. The detectors are sited, either singly or in groups, to provide a protected zone as covered by their field of view, which in this case is about 150° cone angle per detector. The operating range obviously depends on the size of flame which may be tolerated before the alarm operates.

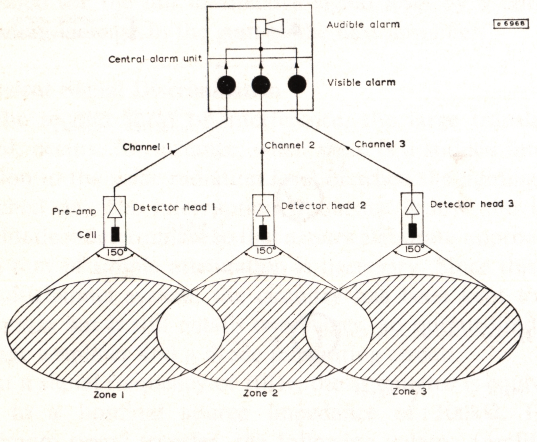

Fig. 12—System schematic diagram of fire alarm, showing protected areas

Alarm signals from each zone are fed to separate channels in the central alarm position so that the location of the fire may rapidly be determined. A common form of audible alarm indicates the outbreak of a fire, while zone location is provided by indicator lamps. The prototype, a three-channel system illustrated in Fig. 12, is powered from a 24V supply, which could be derived from mains or batteries.

DESIGN PRINCIPLES

The flame detector is based on the principle that a flickering flame acts as an intermittent source of high-energy infrared radiation to which a lead sulphide cell is extremely responsive. However, the infrared detector cannot discriminate between sources of infrared radiation so that, when used as a flame detector in a fire alarm, it is necessary to devise methods of discriminating between 'true' and 'spurious' signals. For design purposes, spurious signals are classified as either continuous, such as those generated by the 100Hz radiation from a mains-powered tungsten filament lamp, or isolated transients, such as those generated by a sudden change in the background radiation level. The methods used in the fire alarm system described here to discriminate between the two main classes of interference are as follows.

Continuous Interference

The major source of continuous interference signals is the 100Hz radiation from mains-powered lighting systems. This type of radiation is particularly significant with tungsten filament lamps. As emitted radiation is not polar, lighting systems powered by 50Hz mains supply emit radiation fluctuating at 100Hz. Since this frequency is considerably higher than the typical flame flicker frequency (10 to 20Hz), the necessary discrimination is provided by making the system frequency-selective.

Transient Interference

Major changes in the background level, occurring, for instance, when lighting is switched on, will generate single transient signals much greater in amplitude than those from a small flickering flame. Unless the detector is carefully sited or the sensitivity of the system considerably reduced (or both), the 10 to 20Hz component of such a transient signal will provide a spurious alarm. Such limitations are not desirable on a general purpose system. Therefore 'transient' discrimination is provided by means of an 'integrating' circuit. The output signals from the amplifier preceding this stage are limited to such an amplitude that any single pulse will not trigger the alarm, whereas a short train of pulses such as that produced by a flickering flame will quickly build up to the trigger level.

DESIGN OF DETECTOR HEAD

On the prototype system a complete detector head has been assembled in a standard metal envelope such as that used for the Mullard 61SV lead sulphide detector; it is 22mm in diameter and 41mm long. The circuit diagram is shown in Fig. 13. The circuit design is considerably influenced by the limitation of volume of the envelope.

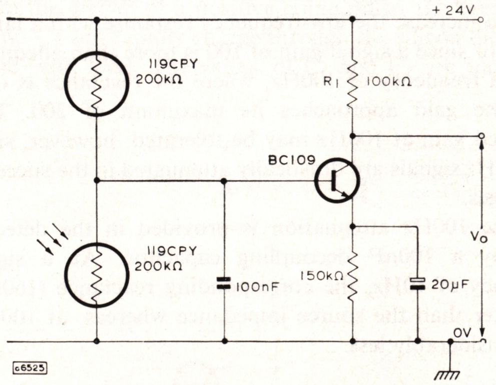

Fig. 13—Detector head amplifier

The circuit uses two 119CPY lead sulphide cells, one of which is used as a temperature-compensating load for the active element and is covered so that it receives no radiation. The cells track with temperature changes, so that a constant voltage bias is always maintained across the active element. There is the further advantage that the cell may be directly coupled to the amplifier.

To obtain maximum signal transfer from the cell to the following voltage amplifier, the input resistance of the transistor should be kept high. If it is assumed that the cell resistances are 200kΩ, that is, a source resistance of 100kΩ, an input resistance greater than 100kΩ is desirable.

In this circuit, there is a compromise between simplicity and sensitivity; an input resistance comparable with 100kΩ has been obtained by operating a high gain transistor at a low current.

Typical operating conditions with 200kΩ cells are as follows:

Supply
V_s = 24V
119CPY
I_{cell} = (24/400 000) A = 60μA
V_{cell} = 12V
BC109
V_{EE} = 11·4V
$I_e = I_c$ = (11·4/150 000) A = 75μA
V_{CE} = 16·5V
r_e(= 24/I_e in mA) = 330Ω
h_{FE} = 300
R_{in} (= $h_{FE}r_e$) ≥ 100kΩ

The gain of the amplifier ($A = R_1/Z_2$) is frequency-dependent since the total emitter impedance Z_2 depends on frequency. Under d.c. conditions, where the emitter decoupling is not effective, the emitter resistor of 150kΩ restricts the gain to less than unity ($A = 100/150 = 2/3$). This ensures that the amplifier has a poor response to slow transients.

Ideally, at a flicker frequency of 10Hz, the emitter decoupling should be completely effective, so that the gain is virtually determined by r_e and is therefore equal to 100 000/330, or 300. However, with the space limitations, a 20μF capacitor was the maximum possible. This value provides a reactance value of 800Ω at 10Hz, which limits the gain to approximately 100. No attempt has been made to increase the low-frequency response with a larger capacitor since a signal gain of 100 is more than adequate.

At a frequency of 100Hz, where the reactance is only 80Ω, the gain approaches its maximum of 300. This increased gain at 100Hz may be tolerated, however, since the 100Hz signals are drastically attenuated in the succeeding stages.

Some 100Hz attenuation is provided in the detector head by a 100nF decoupling capacitor. At a signal frequency of 10Hz, the corresponding reactance (160kΩ) is greater than the source impedance whereas, at 100Hz, it is considerably less.

CENTRAL ALARM UNIT

The Central Alarm Unit provides both visual and audible alarm signals. Provision is made to connect each detector to a separate channel so that the location of the fire may be readily determined. Each channel contains a bistable element which switches to the ON state on receipt of an alarm pulse. In this state, both an indicator lamp and an audible alarm are activated. A suitable type of bistable circuit, which may be driven directly from a detector, is shown in Fig. 14. It merely consists of two transistors connected as a p-n-p-n device.

On receiving an alarm pulse greater than the threshold voltage of the n-p-n transistor (that is, 500mV), the p-n-p-n element switches to a stable ON state. In this state, both the channel indicating lamp (15V, 750mW) and the audible alarm (Mallory 'Sonalert') are activated.

With the 24V supply allowing for 1·5V across the p-n-p-n switch and 15V across the lamp, there is 7·5V available for the 'Sonalert'. This is a suitable operating voltage for this alarm but, since it is a high-impedance element (2kΩ), its corresponding current requirement is low (3·5mA). Most of the 50mA lamp current must therefore be diverted via a shunt path. By using a 7·5V reference diode, more than one lamp circuit can operate at the same time and yet the correct operating voltages for the lamps are maintained. The channel is reset by short-circuiting the input to the n-p-n transistor to the 0V line, cutting off the bistable circuit.

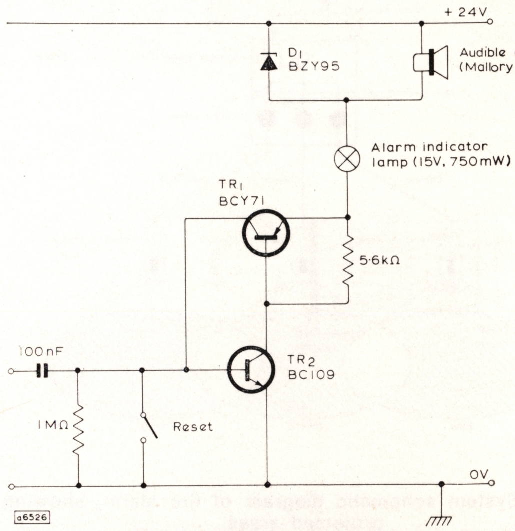

Fig. 14—Central alarm bistable circuit

With the high gain transistors used, the base current required to switch on is negligible (< 1μA) so that the switch does not load the detector. However, at high ambient temperatures, transistor leakage may be sufficient to give a spurious switch on. This spurious effect is eliminated by shunting the emitter base diode of the p-n-p transistor so that it does not switch on below a pre-determined current level. With 5·6kΩ shunt a level of 100μA is required for switch on.

In this simple form, use of the system is restricted since the circuit cannot discriminate between a flame and any other spurious pulse. The circuits described below overcome this difficulty.

CENTRAL-ALARM DISCRIMINATING CIRCUITS

Under normal operating conditions, it is essential that the system is able to discriminate between the desired flame flicker and the two major classes of interference signal. These are dealt with separately below.

100Hz Discrimination

Under some operating conditions, there may be a very high level of continuous radiation from the ambient lighting system. For example, if the detector faces a 60W tungsten lamp at a range of 2m, a 1·6V output signal will be generated. So that the detector can operate in such an environment, further 100Hz attenuation must be introduced into the system at an early stage.

A simple method of producing the necessary voltage attenuation is by means of an RC filter. The values used (150kΩ, 100nF) provide a nominal 20dB attenuation at 100Hz and 3dB at 10Hz. With three filters (Fig. 15) 60dB of 100Hz attenuation is introduced. If required, this may be increased by further filters. Since there has been prior amplification in the detector head (40dB), the loss of signal caused by this filter may be tolerated. There is no loss in overall sensitivity because compensation may be provided for the fall in effective signal level by a corresponding increase in the gain of the next amplifier.

Transient Signal Discrimination

The second form of interference, the large transient signal, occurs, for instance, when there is a sudden interruption in the solar radiation level or when the lighting is switched on. The interruption frequency is low and the amplitude indeterminate so that a more elaborate approach than that of simple attenuation is necessary. Since this is a multichannel system, the circuitry has been kept to a minimum but it still entails two stages, an output-limited voltage amplifier and a diode integrating circuit.

At a signal frequency of 10Hz, the attenuator is equivalent to a nominal source impedance of 100kΩ. For maximum signal transfer, the following voltage amplifier should have an input resistance greater than this value. However, as high gain is available, some loss of signal may be tolerated, and this allows some simplification of the circuit.

A low operating current level is used as a simple means of providing high input resistance. At a current of 100μA, r_e is 250Ω, so that with a suitable high gain transistor ($h_{FE} > 300$), an input resistance ($h_{FE}r_e$) of 75kΩ may be obtained. In conjunction with the high-impedance bias chain, this gives an overall input resistance of 60kΩ which does not lead to an excessive loss of signal.

With the bias chain setting the base potential at 5V, and the 39kΩ emitter resistor defining a current of 100μA, a collector load of 180kΩ may be tolerated before the transistor bottoms. In practice, the load may be preset between the limits 12 and 112kΩ by means of the variable resistor R_1 (100kΩ). With the emitter load effectively decoupled, the gain of the amplifier may be set between the corresponding limits 12 000/250 or 48 and 112 000/250, or 450. With the gain set such that a small flame flicker signal has the required detection level, large transients will be of such an amplitude as to overload the amplifier. All large transient signals must have a standard amplitude prior to being fed to the 'integrating circuit', therefore some form of amplitude limiting is necessary.

The method used is to connect the output from the amplifier via a 100nF coupling capacitor to the two silicon diode chains D_1, D_2 and D_3, D_4. The forward voltage drop of the two series diodes defines the limit level to approximately 1V, while the reverse connection ensures that conduction occurs on both positive and negative half cycles. With this circuit, the input to the integrator is a waveform which has a maximum amplitude of ±1V with respect to the 24V supply line.

In the initial d.c. state, with no input signal, the input to the integrating circuit will be 24V. However, because the leakage resistance of the polyester capacitor C_1 is far greater than that of the germanium diode D_5, the input potential to the bistable circuit (TR_3) will nevertheless be effectively zero.

On the arrival of a positive-going pulse, the capacitors C_1 and C_2 will rapidly charge through the silicon diode D_6 to the peak level. The values of C_1 and C_2 are such that

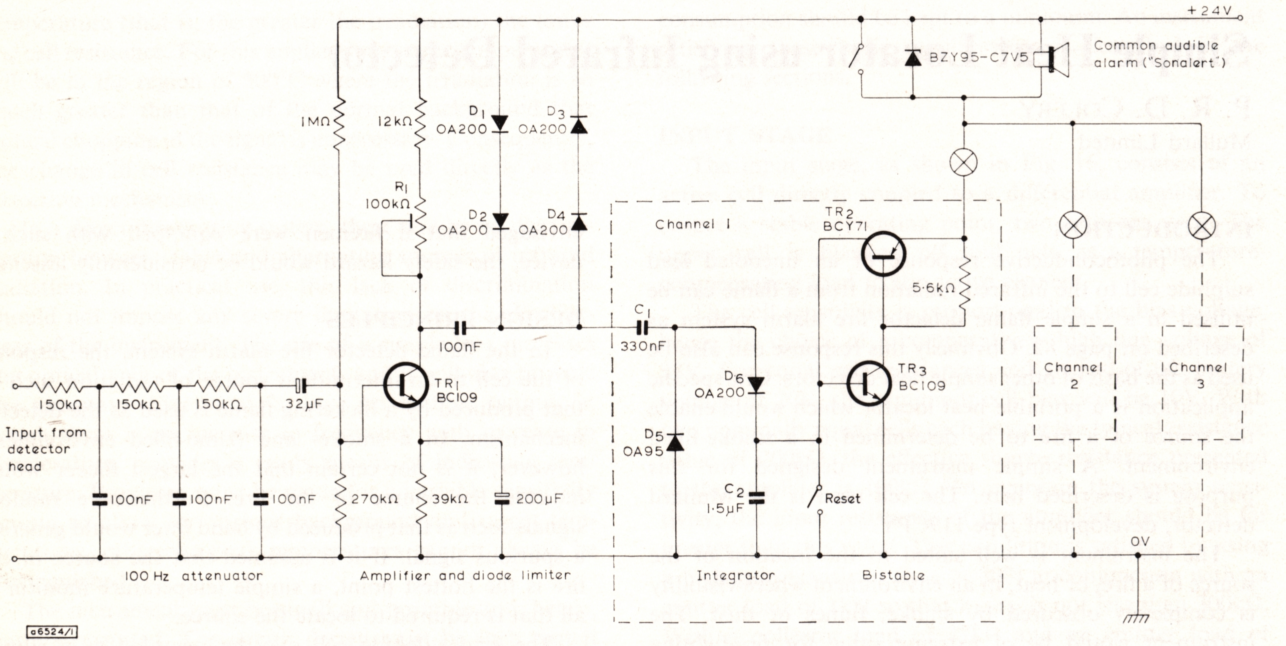

Fig. 15—Central alarm unit, with channel 1 only shown in detail

they form a capacitive attenuator of 6 to 1 so that, even for the maximum input pulse of 2·0V (23 to 25V) the corresponding potential rise across C_2 (allowing for a forward voltage drop of 0·5V), is only 250mV. This level of input to the bistable stage is insufficient to switch it on.

At the end of the pulse, C_1 discharges rapidly through the now forward-biased diode D_5 while C_2 discharges slowly through the reverse-biased diode D_6. Within a period of approximately one second, both capacitors will discharge, and the circuit will revert to its initial state. However, if within this period, further pulses arrive, C_2 will progressively charge towards the peak value of the input. Once the input to TR_3 reaches a level of approximately 700mV the bistable stage will switch to its stable ON state.

Sensitivity

A sensitivity control has been incorporated to enable optimum sensitivity to be realised for the prevailing conditions of ambient lighting. To form a reliable fire alarm system, the sensitivity must not be set so high as to exceed an acceptable false alarm rate.

With the minimum gain setting of the system, it is possible to detect approximately 8cm of flame flicker at a range of 6m within each detector head cone angle of 150°. Under favourable environmental conditions where maximum sensitivity may be used, the range is approximately doubled to 12m for an 8cm flame flicker.

Current Consumption

In the normal quiescent condition, the total current drawn per channel is less than 1mA. However, with the indicator lamps used in the demonstration model, 50mA will be demanded from the supply when the channel is activated. For this reason it may be preferable to arrange mains, rather than battery, operation. A single-channel alarm system using a 'Sonalert' as the indicator would only require a maximum of 10mA when activated, and therefore a portable battery-operated alarm would be more feasible.

Optical Filter

Discrimination against interference signals in the visible spectrum may be provided by means of an optical filter. Under those conditions where this results in an improvement in the false alarm rate, the system gain may be increased. However, the overall improvement in the system 'sensitivity' will depend on the amount of attenuation that the filter produces on the required infrared signal. For low signal attenuation, a germanium ($\lambda c = 1{\cdot}8\mu m$) or silicon ($\lambda c = 1{\cdot}2\mu m$) filter should be used.

Simple Heat Locator using Infrared Detector

P. R. D. Coleby
Mullard Limited

INTRODUCTION

The photoconductive response of an uncooled lead sulphide cell to the infrared radiation from a flame can be utilised in a simple flame detector fire alarm system as described on page 82. Obviously this response can also be used as the basis of other simple heat detectors. One specific application is a portable heat locator which would enable the source of a fire to be determined in a smoke-filled environment. A simple instrument designed for this purpose is described here. The cell used is the Mullard detector, development type 119CPY.

The instrument is well suited to the location of the source of a fire, or heat, in an environment where visibility is completely obscured by smoke, fumes or dust. The instrument would be of extreme value for fire-fighting personnel: the obvious use is for fire location, and it is envisaged that if firemen were equipped with such a device, the safety hazard would be considerably lessened.

DESIGN PRINCIPLES

In the flame detector fire alarm system, the response of the cell to an intermittent source of radiation such as that produced by a flickering flame is used as the detector mechanism. In a smoke- and flame-filled environment, however, it is not certain that the largest flicker would indicate the source of the fire. Furthermore random signals such as that produced by hand jitter would generate a spurious signal. If it is assumed that the source of the fire is the hottest point, a simple temperature monitor is all that is required to locate the source.

The lead sulphide cell may be regarded as a simple radiation-sensitive resistor in which the higher the target temperature (that is, the greater the irradiation) the lower the cell resistance. For this application, target temperatures will be in the region of 500°C where the irradiation is so much greater than that of the normal background that optical chopping of the signal is unnecessary. Consequently, the change in cell resistance may be used directly as the detection mechanism.

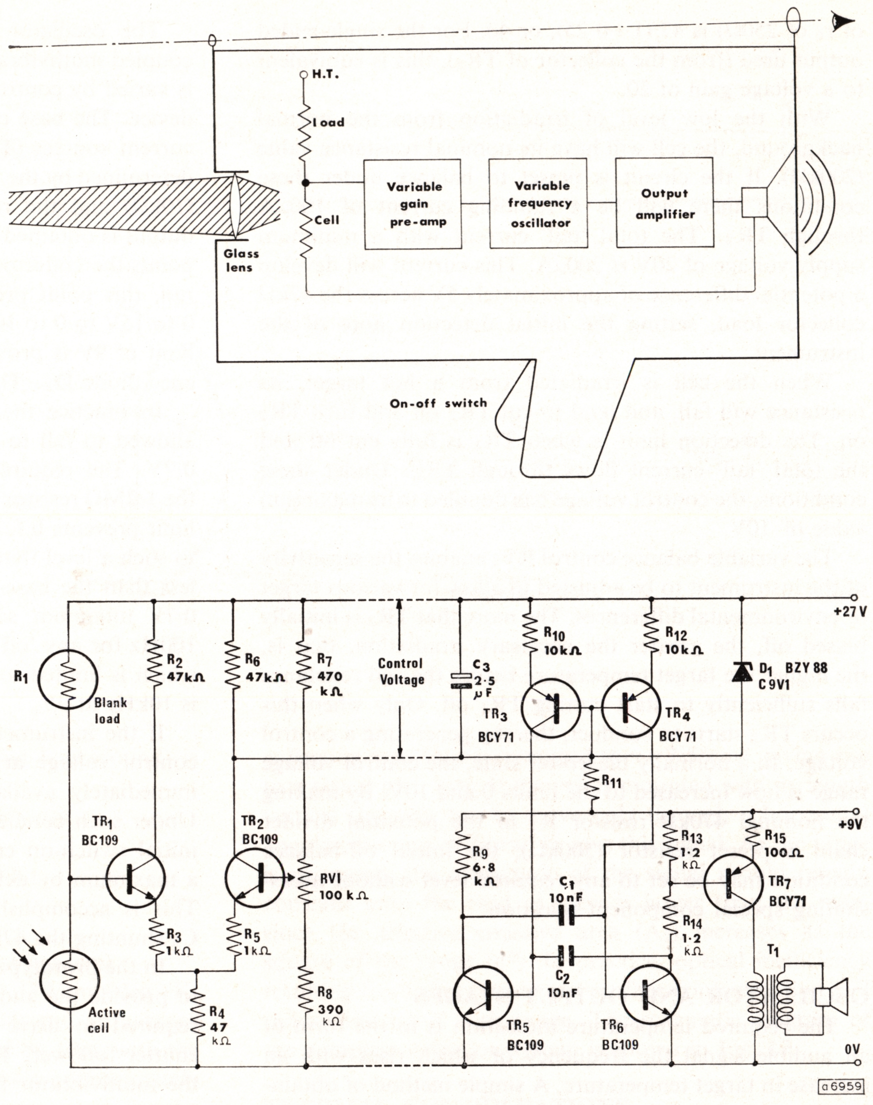

Fig. 16—Schematic diagram of heat locator, and circuits of input amplifier, oscillator and output stages

In a direct-monitoring system, there will be no discrimination between stable and alternating sources of infrared radiation. In practical use, this lack of discrimination should not impose any severe limitation on the effectiveness of the instrument. The use of a simple lens increases the optical gain of the instrument, and it will also provide the necessary directional facility. An audible output, in which there is an increase in frequency with increase in temperature, provides a ready means of indicating temperature. Provision must be made for a variable sensitivity setting to allow for various background and target temperatures, otherwise peak temperatures cannot always be distinguished.

The instrument must be small and portable and, hence, battery-operated. The circuit design must be such that it functions adequately until the end of battery life. Current consumption should be kept to a minimum. An instrument satisfying these basic requirements is described in the following sections.

INPUT STAGE

The input stage, as shown in Fig. 16, consists of an active cell directly coupled to a differential amplifier. To ensure a stable operating point, two cells are used. The upper cell is blanked off and acts as a temperature-compensating load to the active element.

The cell sensitivity is proportional to the bias voltage, hence the choice of a comparatively high line voltage of 27V. For equal cell resistances and an end-of-life battery voltage of 20V, the minimum cell bias will be 10V. With two nominally equal cells each having the typical resistance value of 200kΩ, the effective source resistance presented to the amplifier is 100kΩ. To maintain the system sensitivity, the input resistance of the amplifier should be far greater than this value. This condition is satisfied by using a high gain transistor ($h_{FE} \geqslant 300$) in conjunction with an emitter load of 1kΩ so that $h_{FE}r_E$ is not less than 300kΩ. With a collector load of 47kΩ and an emitter load of 1kΩ the voltage gain of the amplifier (assuming a value of r_e of 250Ω) is 47/(1+0·25), or 40. For the single-ended output used (from the collector of TR$_2$), this is equivalent to a voltage gain of 20.

With the low level of irradiation from the normal background, the cell will have its nominal resistance value (200kΩ). If the circuit is preset to balance under these conditions there will be a standing current of 100μA through TR$_2$. The total 'tail' current with a minimum supply voltage of 20V is 200μA. This current will develop a potential difference of approximately 5V across the 47kΩ collector load, setting the initial detection note of the instrument.

When the cell is irradiated from a hot target, its resistance will fall, and tend to cut TR$_1$ off and turn TR$_2$ on. The detection limit is when TR$_1$ is fully cut off and the total 'tail' current flows through TR$_2$. Under these conditions, the control voltage has doubled to its maximum value of 10V.

The variable balance control RV$_1$ enables the sensitivity of the instrument to be adjusted to allow for various target or environmental differences. The more that TR$_2$ is initially biased off, the greater the necessary irradiation, that is, the higher the target temperature before the cell resistance falls sufficiently to start cutting TR$_1$ off. Only when this occurs TR$_2$ starts to conduct, thereby generating a control voltage. In a normally biased-off state, the control voltage range is now increased to the limits 0 and 10V. By making the nominal 470kΩ resistor R$_7$ in the potential divider chain a preset resistor (500kΩ), the initial off-balance condition may be set to any required level without necessitating special component selection.

OSCILLATOR AND OUTPUT STAGES

The required temperature indication is in the form of an audible signal the frequency of which rises with an increase in target temperature. A simple method of obtaining the wide frequency range necessary is by means of a relaxation oscillator. The output does not need to be a pure tone, so the square-wave generated by this type of circuit is satisfactory.

The oscillator used is a symmetrical collector-base coupled multivibrator (TR$_5$, TR$_6$) in which the frequency is varied by controlling the base current available in each device. The base currents are derived from two constant-current sources (TR$_3$, TR$_4$) in which the current level is determined by the value of the emitter resistors (R$_{10}$, R$_{12}$) (10kΩ) and the relevant base potential. A symmetrical output is obtained by connecting both bases to a common point, the collector of TR$_2$. With reference to the +27V rail, this point produces a control voltage ranging from 0 to 15V to 0 to 10V, depending on the supply. An upper limit of 9V is provided by clamping with a voltage reference diode D$_1$. This limits the current to 0·9mA.

In practice the lower limit of control voltage is not allowed to fall to zero, but is clamped to approximately 0·7V. The required maintaining current is provided by the 1·2MΩ resistor R$_{11}$ connected to the 9V line. This lower limit prevents h.f. instability occurring when TR$_2$ cuts off to such a level that the resultant control voltage would be less than the base-emitter voltage of the transistors. The 0·7V minimum sets a low-note limit of approximately 100Hz for any 'off' condition. The upper frequency limit, which is limited to a degree by the coupling components, is 10kHz at 9V.

If the instrument is preset to produce a high level of control voltage at initial switch on, sufficient current is immediately available to bottom both TR$_5$ and TR$_6$. Under such conditions, the circuit will not oscillate. The initial switch-on current is therefore slowly increased to a maximum by delaying the rise of the control potential. This is accomplished by means of the 2·5μF capacitor C$_3$ shunting the 47kΩ load, R$_6$.

In the prototype, a miniature 0·5W loudspeaker is used to provide the audible alarm. The necessary current gain required to drive the loudspeaker is provided by the emitter follower, TR$_7$. This device is directly coupled to the multivibrator from the split collector load. With the 100Ω emitter resistor R$_{15}$, this limits the current through TR$_7$ to approximately 6mA. This defines the current which flows through the primary of the 5·5:1 transformer driving the 150Ω loudspeaker.

Passive Intruder Alarm using Infrared Detector

R. A. LOCKETT
Mullard Limited

INTRODUCTION

The intruder alarm was designed and constructed to show the ability of an uncooled indium antimonide photoconductive element in an unchopped system to detect objects with temperatures ten or twenty Celsius degrees above room temperature moving across the field of view against a steady background at room temperature.

The detector is a Mullard ORP10 element, which is a.c. coupled to a low-drift differential amplifier driving an alarm circuit. The radiation from the field of view is collected by a front-silvered concave mirror and is reflected back to be focused on the cell by a smaller plane mirror. A sufficient increase in radiation at a rate greater than the circuit time-constant causes the alarm to be sounded.

OPTICAL SYSTEM

The change in radiation (δE) falling on the cell, without the optical system, when a warm object appears in the field of view against a cooler background (assuming emissivities of unity for both object and background) is given by

$$\delta E = \sigma(T_2^4 - T_1^4)A_1A_2/\pi d^2 \text{watts}$$

where T_2 = object temperature (°K)
T_1 = background temperature (°K)
A_1 = area of cell (cm^2)
A_2 = area of object (cm^2)
d = distance between cell and object (cm)
σ = Stefan's constant $\simeq 5{\cdot}7\times10^{-12}$Wcm^{-2}deg^{-4}K.

For the ORP10 ($A_1 = 0{\cdot}6\times0{\cdot}05$cm^2) and an average man (A_2 = 7000cm^2) at 35°C separated by 10m, with the background at 25°C, the radiation signal is approximately 0·4μW. From the spectral response curve given for the ORP10 and the black body emission curve for 35°C, it is seen that approximately 4% of the incident radiation has effect on the cell. Thus the accepted radiation is approximately 0·016μW, giving rise to an electrical signal of 0·016μV, if the cell is typical and biased at 50mA. A signal of this level superimposed on the bias potential across the cell is very difficult to detect since not only is the amplitude small, but the rate at which the signal appears is also necessarily small.

Some improvement in signal rate may be achieved by using a system of grids so that radiation from an object in the field of view is chopped by virtue of the movement of the object. Nevertheless the amplitude remains unaltered.

The amplitude of the signal may be improved significantly, at the expense of field of view, by the use of an optical system; at the same time, the signal rate is improved beyond that effected by a grid system if the field of view is small. The alarm system described here utilises a front-silvered concave mirror having a diameter and focal length of 15cm. With the cell at the focus, the field of view is approximately 3×36mrad. Thus, for comparison, with the same man at 10m, although the effective emissive area (A_2) is now only 3×36cm^2, the optical collecting area (A_1) is increased to $\pi\times7{\cdot}5^2$cm^2, giving rise to a signal of 1·2μV. If the cell is mounted with its length vertical the man has to move only through a horizontal angular distance of 3mrad to give this signal. As the range is increased, the magnitude of the signal should remain constant until the field of view is larger than the man, since the effective emissive area (A_2) increases as the square of the range (d^2). In practice, optical inefficiency resulting from aberrations and surface contamination will reduce the signal with range. The schematic diagram of the complete detection system is shown in Fig. 17.

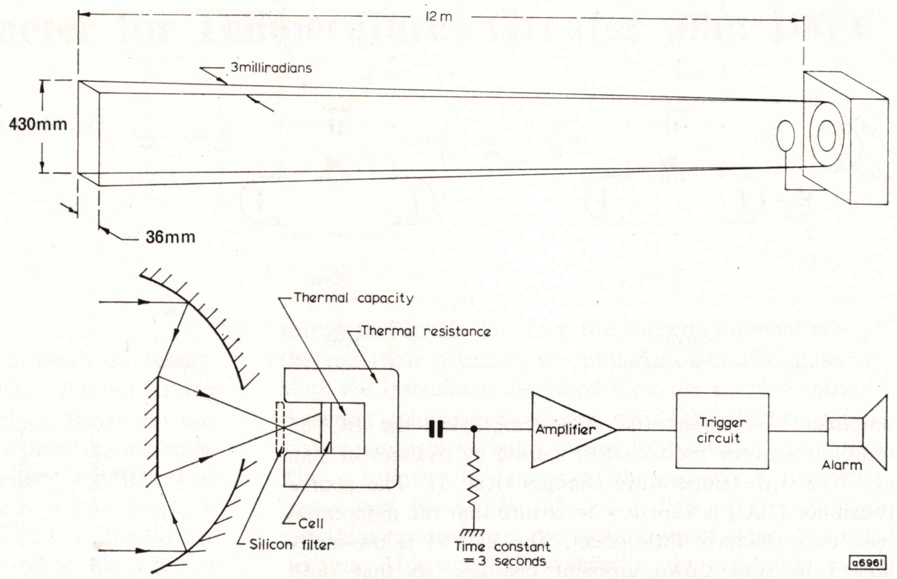

Fig. 17—Schematic diagram of intruder alarm

THERMAL CONSIDERATIONS

The resistance of the cell falls at a rate of approximately 1·5% for each Celsius degree rise in temperature. Thus, for instance, if the cell is biased at one volt, this potential will fall 15mV for one degree rise. Even if this change takes place over 1000s the rate is 15μV/s which is ten times larger than the signal rate. Hence very small changes in ambient temperature will produce spurious outputs unless some precaution is taken.

To this end the cell is mounted on a copper block to provide thermal capacitance, and this is surrounded by s.r.b.f. to provide thermal resistance. The thermal capacitance slows down temperature changes of the cell resulting from the flow of heat between cell and ambient, and the thermal resistance impedes the flow of heat. In this alarm system the mass of copper used is 100g, and it is surrounded by s.r.b.f. 6mm thick. The rate of change of cell temperature is approximately 10^{-3}degC/s for each degree difference between cell and ambient temperature, corresponding to a signal rate of 15μVs^{-1}deg^{-1}C. This is further reduced by the case of the instrument and the use of cotton wool. A thin sheet of polythene was placed in front of the filter to reduce direct draught on the filter.

Temperature changes will also cause drifts in the pre-

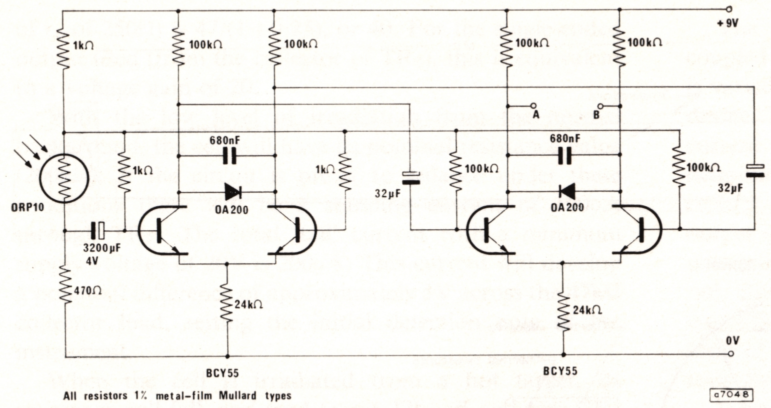

Fig. 18—Amplifier, and voltage level trigger circuit

amplifier. A differential stage employing the BCY55 double transistor reduces drift caused by changes in V_{BE} and h_{FE} with temperature changes (Ref. 1). The source resistance (1kΩ) is kept low to ensure that the differential base currents have little effect. The BCY55 is thermally lagged to slow down ambient changes, so that both transistor junctions keep in step with the temperature of the heatsink.

Further sources of drift with temperature are the cell load resistor and the capacitor coupling the cell to the pre-amplifier. The resistor must therefore be of high stability, and all the resistors in the pre-amplifier are high stability types. The capacitor is assisted by its bulk to impede the rate of change of temperature.

ELECTRICAL CONSIDERATIONS

Pre-amplifier

The minimum angular speed required to be detected by an intruder alarm is approximately 1mrad/s. This occurs for example with a linear velocity of 1cm/s at 10m at right-angles to the beam. As the cell is mounted vertically, giving a horizontal field of view of 3mrad, the signal from the cell must be held by a coupling capacitor to the amplifier for approximately three seconds. Thus for a biasing resistance of 1kΩ, a 3200μF capacitor is used (Fig. 18). The capacitor holds one side of the differential amplifier with respect to the negative end of the cell, and the signal from the positive end is fed to the other input via the biasing resistor. The gain of the first stage is 100, with each transistor biased to an emitter current of 50μA.

The second stage is not so critical in terms of temperature sensitivity, and a 100kΩ biasing resistor may be tolerated. This allows the use of much smaller coupling capacitors (32μF) and also does not load the signal source excessively. The gain of this stage is also 100. The capacitors in the collector circuits of these two differential stages serve to limit the high frequency response to 16Hz, thus reducing high frequency noise to a minimum. The diodes in parallel with these capacitors are forward-biased only when the instrument is first switched on, so that following stages are allowed to stabilise simultaneously.

Amplifier

The differential output is fed to a single-ended amplifier (Fig. 19) by using a second battery: that is, one collector output is connected to the negative line and the other to the input of the single stage. This method of coupling uses all the available signal (rather than half) and obviates the necessity of decoupling the supply for the cell, which would require very large capacitors. The two differential stages dictate no special decoupling since the current drawn from the battery is independent of signal. The resistors in this stage were chosen so that, with no signal, the collector voltage referred to the negative line remains fixed as the battery discharges. The gain of this stage is 200, giving an overall gain of 2×10^6.

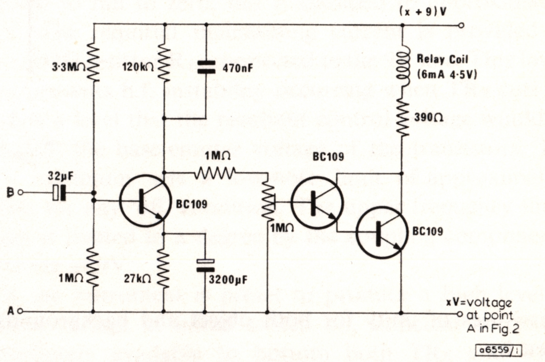

Fig. 19—Pre-amplifier

Level Detector

The final stage is a simple level detector driving a small reed relay coil. The potentiometer provides the adjustment of sensitivity required to differentiate between true signals and spurious signal levels which differ in various types of environment.

Battery Consumption and Life

The cell supply battery (PP9) discharges at the rate of approximately 2μV/s when the bias current is 10mA. The equivalent input signal due to this effect is tapped down to 0·2μV/s across the cell. The use of smaller-capacity batteries is, however, likely to upset the operation of the circuit.

The gain of the first two stages will drop to half the original overall value when the battery voltage has fallen to 6·6V. This occurs after 485 hours at a discharge rate of 10mA for 12hours/day.

REFERENCE

1. 'Directly-coupled Amplifiers—BCY55'. Mullard Limited, August 1967, TP700/1.

Radiation Thermometer for Temperatures Greater than 100°C

P. R. D. Coleby
Mullard Limited

INTRODUCTION

A radiation thermometer provides a means of measuring the surface temperature of an object without having to make physical contact with the surface. It has obvious applications where normal temperature detecting methods, which rely on physical contact, are either impractical or uneconomical. A radiation thermometer determines temperature by measuring the energy emitted from the surface of the object. Its ability to do so is based on the fact that every object above absolute zero temperature emits radiation energy and that the intensity of the radiation is a function of temperature.

One class of radiation thermometers is that based on thermal detectors in which the absorbed radiation heats the detector and causes a change in some observable property, for example, its resistance. Such detectors respond to all wavelengths but, relying on a heating effect, their response is slow (one millisecond to ten seconds). The other class of radiation thermometers is that based on quantum detectors in which all incident photons having the minimum necessary energy free a bound electron. Such detectors respond to a limited range of wavelengths but their response is fast (one picosecond to one millisecond). The portable radiation thermometer described here is of the latter type using the infrared detector type 61SV.

The basic elements of the radiation thermometer are shown in Fig. 20. They are the collecting optical system, the radiation detector, an amplifier, and the indicator. With the instrument described here, the simplest infrared detecting techniques have been used. The collecting optical system consists of either a simple light-pipe or a lens. This is followed by an optical chopper which alternately passes and blocks the infrared radiation. The chopped radiation results in an alternating output signal from the detector. This signal is amplified in the pre-amplifier and then fed to the main amplifier. The output from the main amplifier, which has an amplitude proportional to the source temperature, is demodulated and registered on a meter.

The instrument is calibrated on a perfect radiator (that is a black body) which has an emissivity of 1. Provision is made for practical target emissivities ranging from 0·1 to 1.

RADIATION DETECTOR

The choice of radiation detector has considerable influence on the design and performance of the complete instrument. For this particular portable equipment, it is desirable that the detector has a high infrared sensitivity when operated at normal room temperatures. This entails the use of a detector designed to measure energy at short wavelengths where the higher photon energy ($E = hc/\lambda$) obviates the need to reduce thermal noise by means of cell cooling. The cell used is the Mullard 61SV, a lead sulphide

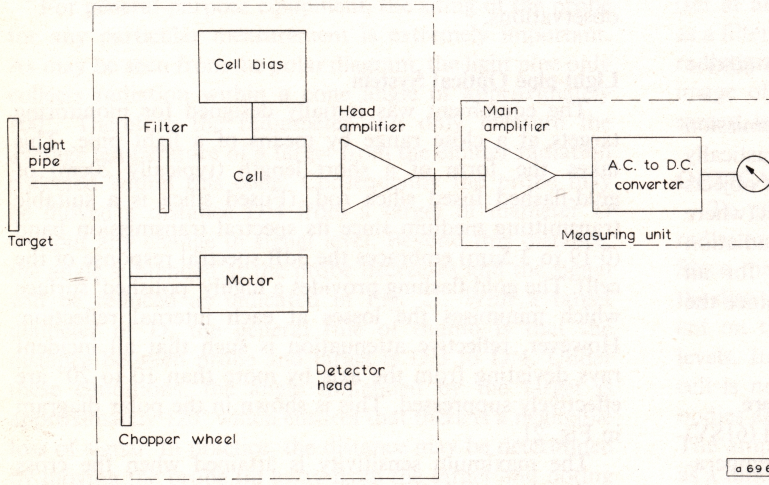

Fig. 20—Schematic layout of radiation thermometer (PbS)

photoconductive cell with a 3dB spectral response from 1·8 to 2·8μm which has a high infrared sensitivity at room temperature.

Collecting Optical System

The spectral transmission band of glass, extending typically to 2·7μm, embraces the spectral response of the cell. An optical glass lens may therefore be used as the collecting system for those applications where the target is remote from the measuring instrument. An alternative optical system may be used for those applications where the target is at a short range: this is the light-pipe, consisting of a short length of fused silica rod within a metal casing giving a transmission band from 0·19 to 3·5μm.

Optical Filter

Interference due to short wavelength radiation, such as solar radiation, may be attenuated by an optical filter. Semiconductor filters which have a high absorption below a critical wavelength (λ_c) are extremely suitable in this respect. If a germanium filter ($\lambda_c = 1{\cdot}8\mu m$) or silicon filter ($\lambda_c = 1{\cdot}2\mu m$) is used in conjunction with this cell, a narrow spectral response is obtained, free from solar and other visible background interference.

Lower Limit of Target Temperature

The peak spectral emission from a perfect radiator, or black body, is a function of its absolute temperature. From the Wien displacement formula ($\lambda_m T = 2893$), it may be seen that the lower the temperature, the longer the wavelength. The general rule is therefore that the spectral emission shifts to longer wavelengths as the temperature of the body to be detected decreases. This imposes a fundamental limitation on the minimum temperature that may be detected with the short-wavelength detector used. In practice, with simple techniques, a lower limit of 100°C may be realised.

Radiation from Ambient Bodies

The power per unit area radiated into a hemisphere by a perfect radiator or black body is given by

$$W_{bb} = \sigma T^4,$$

where σ is the Stefan-Boltzmann constant ($5{\cdot}6693 \times 10^{-8} Wm^{-2} deg^{-4} K$).

The fall in power and the shift in peak spectral emission to longer wavelengths both have the effect of drastically reducing the sensitivity of the lead sulphide cell for objects at room temperature. For this particular application (where the minimum target temperature is 100°C) the radiation from the chopper disc itself may be regarded, for all practical purposes, as an effective zero reference, since the disc blocks the incoming radiation.

Change in Cell Sensitivity with Ambient Temperature

One limitation of the photon detector employed (61SV) is that the sensitivity is a function of the ambient temperature. For a portable radiation thermometer it is impracticable either to cool or to heat the cell to provide a constant operating temperature. Therefore a constant cell sensitivity cannot be realised. However, with the 61SV, the change in signal sensitivity is consistent and may be expressed, over the range −10 to +50°C, as:

$$\frac{S_T}{S_{20}} = 1{\cdot}4 - \frac{T}{50}$$

where S_T and S_{20} are the sensitivities at T°C and 20°C. Thus the sensitivity changes 2% of its value at 20°C for every degC change in temperature. Therefore, a constant sensitivity may be simulated if a suitable compensating circuit is used to increase the gain of the amplifier by a corresponding amount, that is, by 2% for every degC rise in temperature.

The gain compensation is made by means of a negative temperature coefficient thermistor, which of necessity must track with the cell. Since the cell and thermistor do not have the same thermal time-constant, both elements are encased in a metal block. This provides a large, common thermal mass, so that the temperature tracking is greatly improved.

Cell Bias

The 61SV exhibits ohmic behaviour in that the signal for a given irradiation is linearly proportional to the applied voltage. With this instrument, a separate h.t. supply has been used to attain sufficient sensitivity to keep the signal clear of interference and noise at low irradiation levels. Since the 61SV is a high-impedance element (1 to 4MΩ) the current drain on this supply is low.

For a specified supply voltage the optimum signal voltage is generated across the cell when the load resistor has a value equal to that of the cell (1MΩ is a convenient load). This provides a high source impedance (about 500kΩ). A compromise may be made between signal level and reduced source impedance by using a lower load resistance (470kΩ) with the cell.

OPTICAL SYSTEM

The optical system preceding the radiation detector can have one of two forms: a light pipe system for close-range measurements and a lens system for longer-range observations.

Light-pipe Optical System

The equipment was initially designed for monitoring targets at a close range by means of a light pipe. This takes the form of a short length (typically 20cm) of gold-flashed fused silica rod. (Fused silica is a suitable transmitting medium since its spectral transmission band (0·19 to 3·5μm) embraces the 3dB spectral response of the cell). The gold-flashing provides a highly 'polished' surface which minimises the losses at each internal reflection. However, reflective attenuation is such that all incident rays deviating from the axis by more than 10 to 20° are effectively suppressed. This is shown in the polar diagram in Fig. 21.

The maximum sensitivity is attained when the cross sectional area of the rod is comparable with the effective area of the cell. For this particular application, a 5mm diameter rod has been used with a 6mm square cell. For high-temperature applications, where some degree of optical attenuation is actually desirable, a smaller diameter rod, or a tapered probe, may be used.

This simple light pipe is extremely fragile and, for use with a general-purpose instrument, such as this portable thermometer, some form of protection is desirable. A stainless steel sheath, which does not deteriorate with use in high-temperature environments, has been found to be suitable. For other applications, where protection is deemed unnecessary, for example, in an enclosed control system, the rod may be bent or tapered to any desired form to suit the particular requirement.

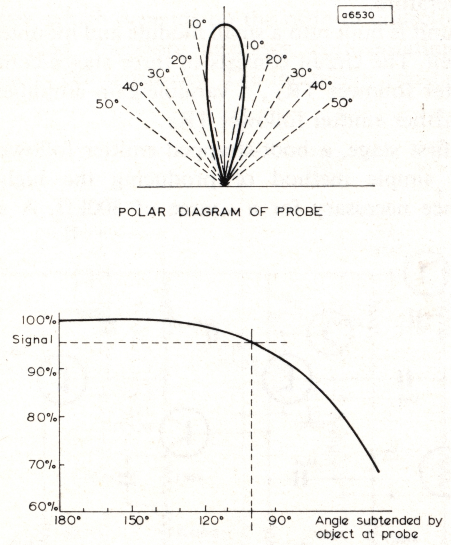

POLAR DIAGRAM OF PROBE

Fig. 21—Directivity of optical system

High-temperature measurements have also been made using a stainless steel tube as a light pipe. The open-ended tube proved unsatisfactory in that the internal surface deteriorated with life. This limitation could be overcome by inserting fused silica plugs at each end.

For general-purpose equipment, the siting of the probe for any particular measurement is extremely important. As may be seen from the polar diagram, the light pipe only collects radiation within a cone angle of approximately 100°. Therefore the radiometer can only measure the average temperature of a target from the emitter radiation collected within this cone. Consequently the probe may be moved a distance D/4 from a target of diameter D without any change in signal level. Beyond this distance, the angle subtended at the probe decreases and the signal will be reduced as indicated in Fig. 21. With a target diameter of D, the general rule of thumb is that the distance between probe and target is D/3 to D/4. Under these conditions, the angle subtended by the target is approximately 120° which ensures that there is a negligible loss of signal. In practice, the distance may be determined by moving the probe tip away from the target and noting if there is any significant reduction in the observed temperature reading.

Lens Optical System

Although the initial design was for a light pipe optical system, an alternative long-range collecting system, consisting of a double convex lens, also proved satisfactory. With a lens 38mm in diameter and having a 60mm focal length, the collecting area is increased so that the overall sensitivity should be improved by a factor of 25. This is achieved in practice and a black-body target at 100°C gives an indication two scales higher after the lens has been fitted. With this optical system, scale A (the highest gain amplifier setting) is completely inoperative since normal room radiation produces a standing signal level of 10% of the full scale B deflection. Under these conditions, the lowest temperature that could be detected is 70°C corresponding to 20% full scale B deflection.

With a 6×6mm cell and a lens with a focal length of 60mm, although the instrument has increased sensitivity, the target-diameter-to-distance ratio is only 1:10. For those applications where a lower sensitivity may be tolerated, the effective area of the cell may be reduced to improve the target-diameter-to-distance ratio. With a 1·5mm aperture in front of the cell, the diameter-to-distance ratio is reduced to 1:40 while the basic sensitivity (100°C minimum) is retained.

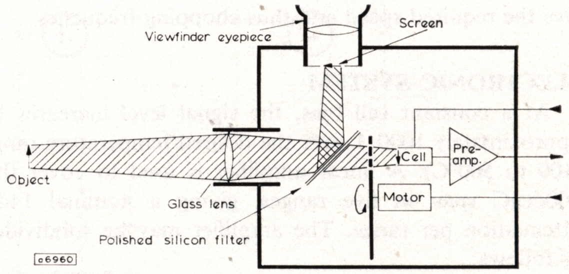

Fig. 22—Remote focusing head

A variable focus sighting system is employed to ensure that the target completely fills the effective cell aperture. The transmission properties of the bloomed silicon filter (set at an angle of 45°) are utilised by employing it both as a filter to the cell and as a reflective mirror to the visible radiation (Fig. 22). To facilitate sighting, a magnified image of the target, which is focused onto the viewing screen, is provided by a further lens.

OPTICAL CHOPPER

To generate an alternating signal across the cell, the radiation from a target is interrupted by a chopper disc. Since the disc itself will radiate energy corresponding to the disc temperature, the amplitude of the signal is dependent on the energy difference between the two radiation levels. In this application, the sensitivity is such that the cell is not responsive to radiation from low-temperature bodies and so the radiation from the disc may be ignored. The amplitude of the signal may therefore be considered as a function of the target temperature alone. The chopper disc is made of metal and has suitably positioned holes around its circumference. The hole diameter is not critical, but should be comparable with the cell width. A signal waveform approximating to a sine wave is produced by spacing the holes with a separation distance equal to the hole diameter. If the effective area of the cell in the design using the lens system is reduced to improve the target-diameter-to-distance ratio, then there must be a corresponding reduction in the hole diameter to maintain this sinusoidal output.

For a 16-hole disc, a motor speed of 3000 rev/min is required to produce a chopping frequency of 800Hz. The current drain of the motor is the main load on the battery supply and, hence, increased battery life can be obtained by underrunning the motor. There is the further advantage that 'brush' noise is reduced. With the prototype model, the motor does not have a completely separate supply, and 'brush' noise could be of prime importance. In practice, the chopping frequency is maintained at 350Hz. At this frequency, there is no loss in cell sensitivity, and low-frequency noise does not present a major problem.

With an ungoverned motor, the motor speed is controlled by using a constant-voltage supply. This takes the form of a simple series voltage regulator in which the e.m.f. applied to the motor is set by a potentiometer to give the required speed and thus chopping frequency.

ELECTRONIC SYSTEM

At a constant cell bias, the signal level increases by approximately 1000:1 over the desired temperature range (100 to 500°C). A linear amplifier is used to cover this 400degC span in five ranges, giving a nominal 14dB attenuation per range. The amplifier may be subdivided as follows:

1) Head Amplifier, which is mounted close to the cell and performs two basic functions, that of gain compensation, to correct the variation of cell sensitivity with temperature, and impedance transformation.

2) Main Amplifier, which is a comparatively low-gain stage. The gain may be preset between the limits ×20 to ×40.

3) Variable Gain Amplifier which has a variable gain (×1 to ×10), and provides a continuously variable overall gain setting to allow for target emissivities from 0·1 to 1.

4) Output Amplifier which has negative current feedback and, in conjunction with a bridge detector, provides linear a.c. to d.c. conversion for the moving-coil meter readout.

Apart from the 120V h.t. cell bias supply, all circuits are powered by a common 12V l.t. line. Since this is a battery-operated instrument, the current drain is kept as low as possible. Although a stabilised 12V supply is used, the circuit employs extensive negative feedback so that variations in the line voltage may be tolerated. The chopping frequency is low and therefore filters would tend to be rather cumbersome. It has been possible to obtain a suitable bandwidth using high- and low-frequency attenuation at various stages in the amplifier.

Head Amplifier

The head amplifier (Fig. 23) performs two main functions:

1) it provides the necessary high-impedance to low-impedance transformation;

2) in conjunction with a negative temperature coefficient thermistor, it provides variable gain to compensate for the decrease in cell sensitivity with increasing ambient temperature.

The unit is built into a small module and mounted close to the cell. The circuit consists of three stages comprising an emitter follower TR$_1$, a variable-gain amplifier TR$_2$, and a further emitter follower TR$_3$.

The first stage, a boot-strapped emitter follower, provides a simple method of producing the high input impedance necessary for a source of 300kΩ. A selected high-gain, low-noise transistor (BCY71) is used in all stages. (For an n-p-n circuit the transistor could be the BC109).

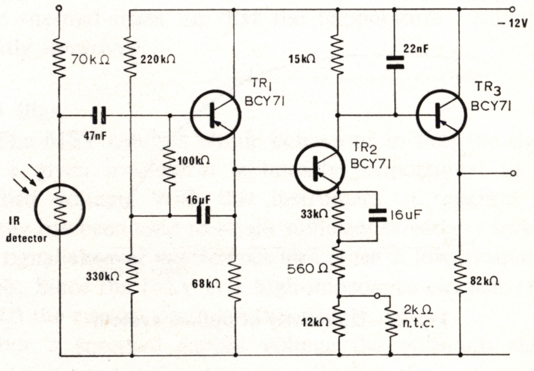

Fig. 23—Head amplifier

a6957

Low-noise conditions in the input transistor are achieved by using a low operating current (100μA) with a low collector-to-emitter voltage ($V_{CE} = 5V$). Unfortunately, it is impossible to satisfy the other optimum low-noise condition by providing a source impedance of several kΩ. For this particular application, the performance is adequate, but for lower-noise performance, a field-effect transistor would provide a better solution. The transistor is biased at approximately 7V, and the 100μA current level defined by an emitter resistor of 68kΩ. With a typical current gain of 100, the corresponding input resistance of the transistor is approximately 7MΩ.

The overall input resistance is kept high by boot-strapping the bias chain. This produces an effective increase in the value of the 100kΩ bias resistor of $1/(1-A)$. The emitter resistance R_E (68kΩ) is so much greater than r_e (250Ω) that the voltage gain A, given by $R_E/(R_E+r_e)$, approximates to unity. The output impedance ($Z = R_{source}/h_{FE}$) is low, approximately 3kΩ, and is therefore suitable for low-noise matching to the following stage.

This second stage is a variable-gain voltage amplifier incorporating negative feedback. The second stage also contributes significantly to the overall noise level and is therefore biased to low-noise conditions. With direct coupling, the base potential lies between 6 and 7V. A decoupled emitter resistor of 33kΩ sets a 200μA bias level. The decoupling capacitor of 16μF provides an impedance level of less than 50Ω at 350Hz and the 200μA bias level a low value of r_e (125Ω). Both these values are considerably lower than the undecoupled emitter resistors which therefore predominantly determine the voltage gain.

A negative temperature coefficient thermistor forms part of the emitter load, so that as the ambient temperature increases the emitter load decreases. The gain of the amplifier, which depends on the ratio of collector load to emitter load, therefore increases, compensating for the decrease in cell sensitivity. The thermistor resistance must be of the order of several kΩ to have an adequate temperature coefficient. By using a 2kΩ thermistor and a comparable value of series resistor, the necessary temperature coefficient is obtained.

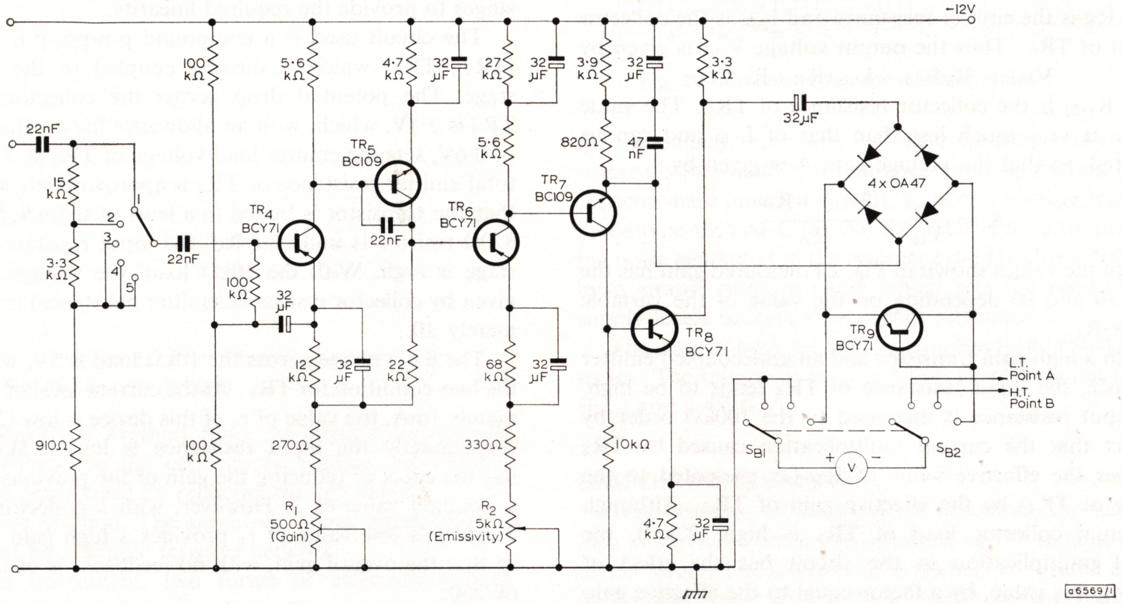

Fig. 24—Main and output amplifiers

a6569/1

The input resistance with the undecoupled emitter load is greater than 100kΩ and produces a negligible loading effect on the previous stage. With a base potential of 6 to 7V and a collector current of 200μA, the maximum value of collector load that may be tolerated is 27kΩ. Under these conditions, the transistor is close to bottoming and the signal handling capacity is reduced. Since high gain is not a prime consideration, a lower resistance (15kΩ) may be tolerated, giving a corresponding improvement in signal-handling and a lower output impedance.

With the motor noise encountered in the prototype, a considerable amount of h.f. attenuation is required. This is provided at an early stage (before the amplifier becomes over-loaded) by decoupling the collector load. In this particular case, a 22nF capacitor has been used, but at the cost of reduced gain.

It is possible to couple from this stage directly to the main amplifier. However, with the remote head, a low output impedance was deemed desirable to minimise electrical pick-up, and consequently a further stage, an emitter follower, has been added.

Main Amplifier

As with the head amplifier, the requirement for the main amplifier (Fig. 24) is to keep the design simple and compact. For this reason a circuit has been used which favours d.c. coupling between stages.

The first two stages of the main amplifier consist of a compound p-n-p/n-p-n amplifier (TR$_4$, TR$_5$) which has a high input impedance and a low output impedance. The input transistor (TR$_4$) is operated at a current level of 400μA at which the value of r_e (60Ω) is low compared with the emitter resistance. The variable control R$_1$ enables the emitter resistance to be set between the limits 270Ω and 770Ω. With a BCY71, the typical base current requirement at this level is 4μA. The bias chain current is significantly greater than this, that is, 60μA. Boot-strapping has been employed to keep the effective value of the bias resistor high.

The typical operating voltages of TR$_4$ are as follows:

at mid-point of base potential divider (V_{BB})	5·8V
at base (V_B)	5·4V
at emitter (V_E)	4·8V
at collector (V_C)	9·7V

The decoupled 12kΩ emitter resistor, being far greater than r_e, determines the current level of 400μA. The decoupling capacitor of 32μF ensures that the impedance at 350Hz (20Ω) is far less than the emitter resistance.

The 5·6kΩ collector load of TR$_4$ sets the d.c. operating levels of TR$_5$. With a collector current of 400μA, the voltage drop across this load is 2·3V. If allowance is made for a base-emitter voltage, V_{BE}, of 0·6V, the potential drop across the emitter load of TR$_5$ is 1·7V. The 4·7kΩ load in turn defines the emitter current of TR$_5$ at approximately 300μA. The output voltage level is predominantly determined by this current and the collector load of 22kΩ, and is typically 7V. The additional voltage drop is that developed across the emitter resistance of TR$_4$.

At an operating level of 300μA, the value of r_e for TR$_5$ is approximately 70Ω, which, in conjunction with the high current gain ($h_{FE} \simeq 300$), provides an input resistance of 22kΩ. The 5·6kΩ collector load of TR_4 therefore provides a low-impedance shunt path for the signal.

For simplicity, it may be assumed that all signal current flows into the base of TR_5 and that the effective current gain of the amplifier has been proportionally reduced to 75. On this assumption the voltage gain may be derived as follows:

$$I_{b(5)} = I_{c(4)} = I_{e(4)}$$

where these are respectively the base current of TR_5 and the collector and emitter currents of TR_4. Therefore the input voltage V_{in} is given by the equation,

$$V_{in} = R_E(I_{b(5)} + I_{c(5)})$$

where R_E is the emitter resistance and $I_{c(5)}$ is the collector current of TR_5. Thus the output voltage V_{out} is given by

$$V_{out} = R_E I_{b(5)} + I_{c(5)}(R_E + R_{c(5)})$$

where $R_{c(5)}$ is the collector resistance of TR_5. The value of $I_{b(5)}$ is very much less than that of $I_{c(5)}$ and can be neglected, so that the voltage gain A is given by

$$A = \frac{V_{out}}{V_{in}} = \frac{R_{c(5)} + R_E}{R_E}.$$

With the values shown in Fig. 24 measured gain has the limits 30 and 90 depending on the value of the variable resistor R_1.

With a high-gain transistor and an undecoupled emitter resistance, the input resistance of TR_4 tends to be high. The input resistance is increased to the 100kΩ order by the fact that the current multiplication caused by TR_5 increases the effective value of R_E (as presented to the emitter of TR_4) by the effective gain of TR_5. Although the actual collector load of TR_5 is high (22kΩ), the current multiplication in the circuit has the effect of reducing this value, by a factor equal to the effective gain of TR_5, to produce an output impedance of 300Ω.

The standing voltage of 7V at the output allows for direct coupling to the following stage. Initially, under the maximum-gain conditions of the complete instrument, this stage tended to be unstable. The instability was cured by connecting a 22nF capacitor between the collector and base of TR_5. This had the effect of reducing the gain limits to 20 and 40, which were tolerable but also introduced undesirable frequency selectivity. A more uniform frequency response has been obtained by introducing low-frequency attenuation at the input. This is accomplished by reducing the coupling capacitor to 22nF.

Variable Gain Stage

The output from the main amplifier is directly coupled to the following stage, which is a variable gain amplifier. The transistor (TR_6) is biased to a nominal 100μA level by the decoupled 68kΩ emitter resistor. At this current, the value of r_e is 250Ω which, in conjunction with the 330Ω resistor, sets the minimum limit of emitter resistance at 580Ω (assuming that the control R_2 is set to zero). With a current gain of 100, the corresponding input resistance is of the order of 50kΩ, so that there is a negligible loading effect on the previous stage.

The variable 5kΩ emitter resistor (R_2) enables any required value of emitter resistance to be set between the limits 580Ω and 5·6kΩ. With a 5·6kΩ collector load, the gain of the amplifier (collector resistance/emitter resistance) may be correspondingly set between the limits 10 and 1. The decoupled collector load of 27kΩ in conjunction with the 5·6kΩ provides a required voltage drop of 3·3V so that this stage in turn may be directly coupled to the output amplifier.

Output Amplifier

The output amplifier (Fig. 24) provides a moving-coil meter readout. The signal is rectified by a bridge and the integrating action of the meter produces a d.c. level corresponding to the average value of the waveform. The rectifying diodes have a non-linear characteristic and therefore negative current feedback is used in the output stages to provide the required linearity.

The circuit used is a compound p-n-p/n-p-n amplifier (TR_7, TR_8) which is directly coupled to the previous stage. The potential drop across the collector load of TR_6 is 3·3V, which, with an allowance for a value of V_{BE} of 0·6V, sets the emitter load voltage of TR_7 as 2·7V. The total emitter resistance of TR_7 is approximately 4·7kΩ, so that the transistor is biased to a level of 0·5mA. Since the 820Ω resistor is undecoupled, the input resistance of this stage is high. With the 10kΩ load, the voltage gain (as given by collector resistance/emitter resistance) is approximately 10.

The d.c. voltage across the 10kΩ load is 5V, which sets the bias condition for TR_8. At the current level of approximately 1mA, the value of r_e of this device is low (25Ω) and consequently the input resistance is low (2·5kΩ). This has the effect of reducing the gain of the previous stage to a nominal value of 2. However, with a collector load of 3·3kΩ this low value of r_e provides a high gain in TR_8, so that the overall gain, with no feedback, is of the order of 250.

At various points in the overall system, it has been necessary to introduce h.f. attenuation. By decoupling the 820Ω feedback resistor, h.f. boost is introduced, thereby improving the frequency response. This allows for a ±10% variation in chopping frequency.

Temperature Ranges

The prototype instrument covers a temperature range of 100 to 500°C. Over this range, the cell responsivity is such that the signal amplitude increases by a factor of 1000:1. This temperature span has been covered in five ranges, using linear amplification. The attenuation between each range is approximately 5:1. The first 20% of the scale reading is extremely non-linear but for the remaining region (20% to 100%) the response is more open. A range covers a typical temperature span of 80degC.

With this five-range instrument, a single linear meter scale is used in conjunction with a calibration chart. For a single- or dual-range instrument, the meter could be scaled directly in temperature.

Attenuation of the signal may be accomplished by the following methods:

1) Optical Method. The incident radiation of the cell may be attenuated by reducing the diameter of the light pipe. For targets at temperatures considerably above 500°C, this method is essential to prevent the cell from overloading.

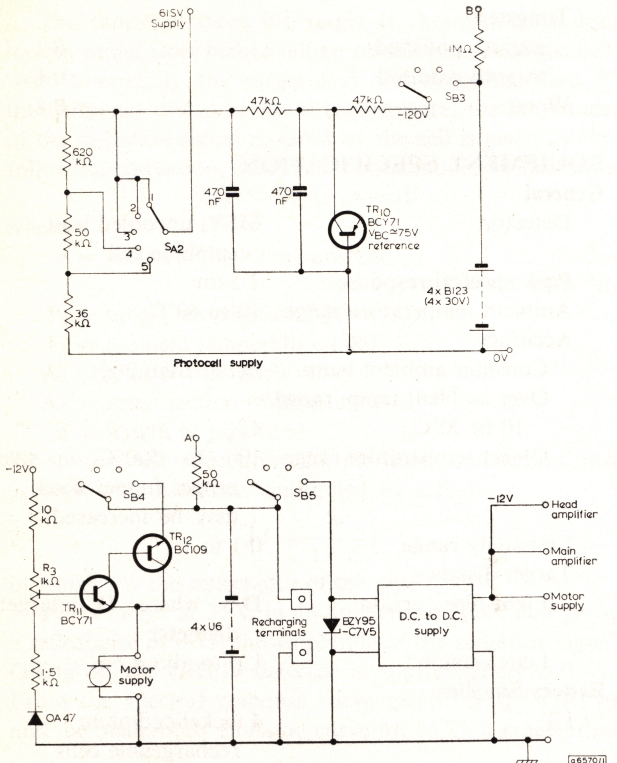

Fig. 25—Supply circuits

2) Cell Sensitivity Method. Since the sensitivity is directly proportional to the cell supply voltage, attenuation may be introduced by reducing the cell supply.

3) Resistive Method. The amplitude of the signal may be reduced by a simple resistive network.

In this instrument, two forms of attenuation have been utilised: the cell supply method has been used up to the head amplifier, and the resistive method up to the main amplifier.

On the most sensitive range, the general order of r.m.s. output signal levels is:

Cell output = 0·3mV
Head amplifier output = 1mV
Main amplifier output = 20mV

This gives 10% deflection on a 200μA meter, with an 820Ω feedback resistor providing approximately 20mV feedback. Attenuation is necessary before the head amplifier to prevent overloading. Attenuation before the main amplifier ensures that the input signal range is restricted.

Supplies

A commercial d.c. to d.c. converter (as used in the Philips portable transistorised d.c. millivoltmeter, type PM2430) is used to provide the stabilised 12V line for the electronic circuits. The converter may be operated either from four ordinary U2 (1·5V) batteries or from four rechargeable nickel-cadmium (1·3V) accumulators. Provision has been made to charge the latter type in situ. The supply circuit is shown in Fig. 25.

The battery supply also provides the source for the motor supply regulator. The reference potential for this voltage regulator is derived from the stabilised 12V line.

The cell supply is provided by four B123 (30V) batteries (Fig. 25). These may discharge to 90V without affecting the secondary reference of approximately 75V. This voltage is provided by a reference diode as formed by the collector-base junction of a BCY71 (or a voltage regulator diode type BZY94–C75). An RC filter is used to minimise the noise generated in the reference diode. This is followed by a simple resistive chain which sets the required cell supply levels necessary for signal attenuation.

The state of both h.t. and l.t. supplies is indicated on the meter. The minimum level is 88μA corresponding to 88V (h.t.) and 4·4V (l.t.).

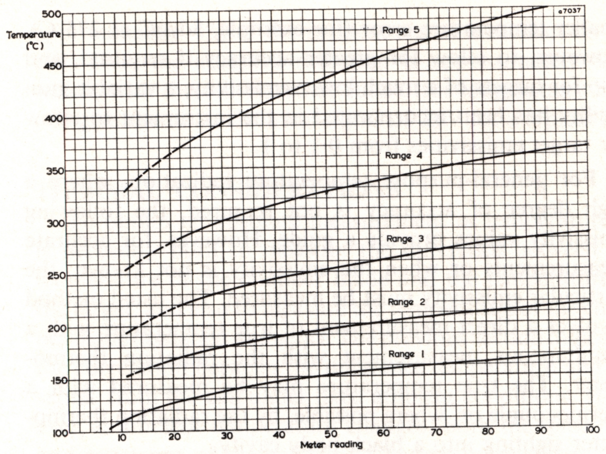

Fig. 26—Calibration graph of thermometer

USE OF INSTRUMENT

With the type of thermometer described, the temperature is derived from a measurement of the radiant power of the target. The instrument is initially calibrated against the radiant power emitted by a black-body source, that is, a perfect radiator. For such a target the radiant emission as given by the Stefan-Boltzmann law is exactly proportional to the fourth power of absolute temperature.

Since the radiant power increases much faster, proportionally, than absolute temperature, the calibration of this instrument over the temperature span 100 to 500°C is covered in five ranges (see Fig. 26). There is the advantage in this scaling that the temperature discrimination, particularly in the lower ranges, is very good.

Real bodies reflect or transmit radiation or do both, and are imperfect radiation emitters. The emittance of a real body (W) is always less than that of a black body (W_{bb}). Consequently the emissivity (ε) of a real body ($\varepsilon = W/W_{bb}$) is always less than 1.

The instrument should only be used with an emissivity setting of 1 when the target is simulating a black-body source. One standard method of doing this is to drill a hole in the target to produce a black-body cavity. This provides increased emittance because of the multiple reflections within the cavity, but to be effective, the hole depth should be typically six times the diameter. An alternative method is to apply a surface coating of a material such as colloidal graphite having a high emissivity. The emittance of a colloidal graphite is typically 0·92 hence, with an emissivity setting of 1, there will be a 10% error in the scale reading. For some applications such an error in emissivity may be tolerated since this represents a much smaller temperature error (for example, 5degC at 275°C). However, to allow for greater accuracy if required, and also for targets of a much lower emissivity, a variable gain facility has been incorporated in the instrument to allow for target emissivities from 0·1 to 1.

For general-purpose temperature indication, where a high degree of accuracy is not required, the following emissivity values provide a guide. However, for accurate measurements or when the emissivity is not known, the particular emissivity must be measured. The usual method involves a direct measurement of true temperature with a simultaneous measurement with the radiation thermometer. The true temperature may be measured with a thermocouple or, where possible, by the radiation thermometer sighting into a black-body cavity.

Material	Emissivity
Aluminium	
smooth polished	0·1
smooth oxidised	0·2
Cardboard	
light coloured	0·4 to 0·8
dark coloured	> 0·9
Ceramics	0·7 to 1·0
Copper	
smooth polished	0·04
smooth oxidised	0·7
Firebrick	0·7 to 1·0
Glass (commercial soda-lime, 150mm thick)	0·9
Graphite	0·65
Nickel	
smooth polished	0·15
smooth oxidised	0·9
Tungsten	
smooth polished	0·1
smooth oxidised	0·6
Wood	> 0·8

EQUIPMENT SPECIFICATION

General	
Detector	61SV, uncooled lead sulphide cell
Peak spectral response	2·5μm
Ambient temperature range	10 to 40°C
Accuracy	
Constant ambient temp.	Better than 2%
Over ambient temp. range, 10 to 40°C	4%
Object temperature range	100 to 500°C in five ranges (upper limit may be increased)
Emissivity range	0·1 to 1
Target distance	
Light-pipe version	D/3 where D = target diameter
Lens version	Up to about 6m
Battery Supplies	
LT	4 nickel-cadmium rechargeable cells (D.E.A.C., type BD2·5) or 4×1·5V dry cells
HT	4 dry batteries (Ever Ready, type B123) 30V
Operating Life	
LT	40 hours continuous (per charging)
HT	200 hours continuous (per set of batteries)

Room Temperature Radiation Thermometer

R. A. Lockett
Mullard Limited

INTRODUCTION

The equipment described uses the ability of the uncooled indium antimonide photoconductive element, type ORP10, to measure the temperature of objects near room temperature by means of the energy radiated from them. The radiation is interrupted at approximately 600Hz by a mechanical chopper, driven by a clockwork motor. The resulting alternating signal from the cell is amplified by a wideband amplifier of flat response so that variations in chopping frequency do not affect the amplitude. The amplified signal is then mixed with a signal corresponding to room temperature. Finally a phase-sensitive rectifier, deriving its reference signal from the interruption of a secondary beam of radiation (between a BPX25 detector and 101CAY emitter) by the chopper blade, rectifies the signal to produce a direct current through the meter.

OPTICAL SYSTEM

For demonstration purposes it was decided that the instrument be built in the form of a clinical thermometer, covering the range 30 to 40°C, intended for the measurement of the temperature of the external auditory canal (which has been shown by Bowling-Barnes (Ref. 1) to approach closely that measured orally). To define the area of measurement, a steel light-guide of diameter 10mm and length 80mm is used.

The radiation from the target is chopped by a disc having radial slots before falling on the cell. Thus the cell 'sees' alternately the target and the chopping disc. If the chopping disc is at room temperature, the amplitude of the radiation signal received by the cell is given by the following expression, which takes no account of reflections,

$$\sigma(T_2^4 - T_1^4)A_1A_2/\pi d^2$$

where

σ = Stefan-Boltzmann constant $\simeq 5{\cdot}7\times10^{-12}\text{Wcm}^{-2}\text{deg}^{-4}\text{K}$
T_2 = target temperature (°K)
T_1 = ambient temperature (°K)
A_1 = area of cell (cm^2)
A_2 = cross section of pipe (cm^2)
d = length of pipe (cm)

When internal reflections in the pipe are taken into account, this is further multiplied by a factor

$$\left(1+\frac{8r}{1-r^2}\right)$$

in which r is the reflectance of the pipe.

For a target at 35°C in an ambient of 20°C, and given a reflectance of 0·75, the amplitude of the radiation signal falling on the ORP10 detector is approximately 200μW. From the spectral response curve given for the ORP10 and the black-body emission curve for 35°C, it is seen that approximately 4% of the incident signal has effect on the cell. Thus the accepted radiation is approximately 8μW which, with the cell biased at 10mA (for long battery life), will give rise to an electrical signal of 2μV for a typical cell.

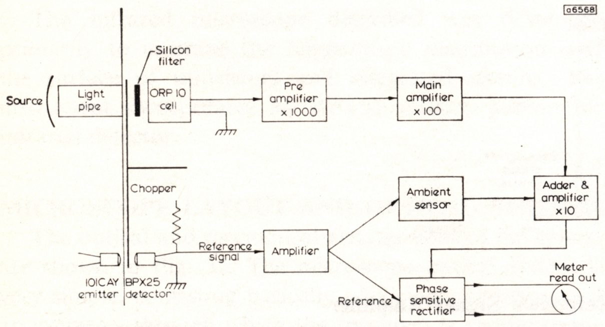

Fig. 27—Block schematic diagram of room temperature radiometer

THERMAL CONSIDERATIONS

To obtain an absolute measurement of temperature, it is necessary both to measure the difference between the temperature of the chopper blade and the temperature of the target, and also to measure the temperature of the chopper blade (assumed ambient). The previous section indicated the correlation between the difference temperature and the signal from the cell under fixed ambient conditions. However, as ambient temperature changes, both the sensitivity and resistance of the cell vary. Changes in sensitivity may be compensated by adjusting the gain of the amplifier; variations in resistance affect the gain. Preliminary investigations show that these effects tend to cancel approximately, and the residual variation was within the error of experiments.

The measurement of ambient temperature is performed by an n.t.c. thermistor in an attenuating network.

ELECTRICAL CONSIDERATIONS

Since the a.c. signal from the detector (Fig. 27) is small, the system as a whole must not introduce noise. To this end, the motor driving the chopper blade, being necessarily close to the detector in a small instrument, is clockwork. This has two advantages: electrical noise from commutators and changing magnetic fields is obviated; and battery life is considerably lengthened. A major disadvantage is the variation in chopping frequency as spring tension alters, so that a narrow-band amplifier (with a corresponding low noise) cannot be used. However, this difficulty is overcome and, in fact, turned to advantage, by the use of a phase-sensitive rectifier in conjunction with a wide-band amplifier. This produces the required narrow bandwidth while the fundamental frequency can vary considerably. The output is in a form which can readily be turned into a meter reading.

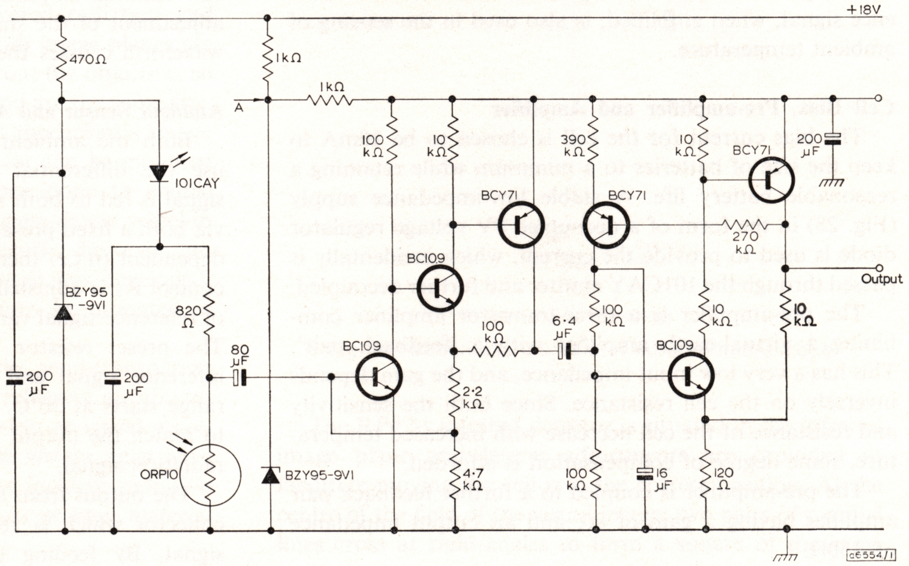

Fig. 28—Cell bias, pre-amplifier and main amplifier

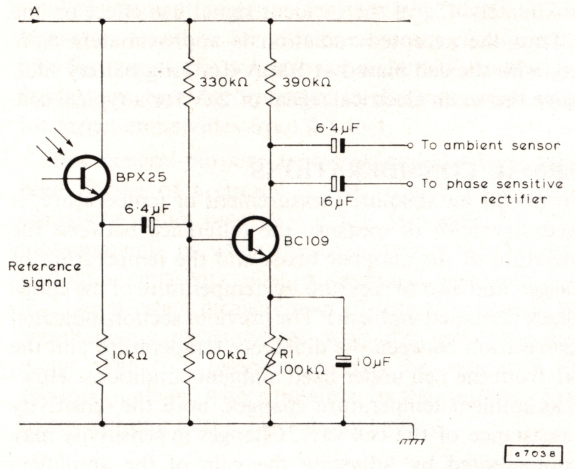
A
330kΩ
390kΩ
6·4μF
To ambient sensor
To phase sensitive rectifier
16μF
BPX25
6·4μF
BC109
Reference signal
10kΩ
100kΩ
R1 100kΩ
10μF
e7038

Fig. 29—Reference signal amplifier

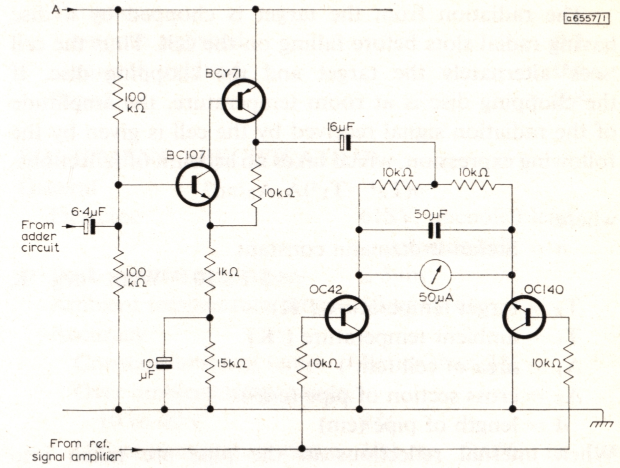
A
e6557/1
BCY71
100 kΩ
BC107
16μF
10kΩ
10kΩ
10kΩ
From adder circuit
6·4μF
100 kΩ
1kΩ
50μF
OC42
50μA
OC140
10 μF
15kΩ
10kΩ
10kΩ
From ref. signal amplifier

Fig. 31—Amplifier (×10) and phase sensitive rectifier

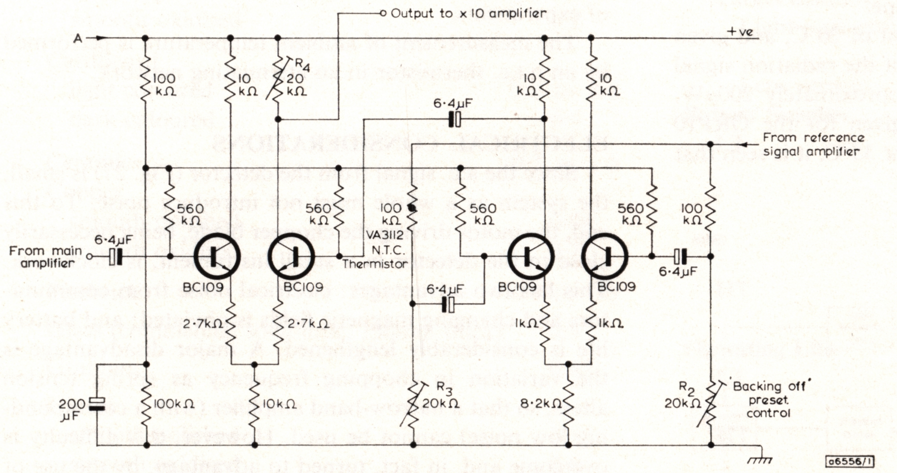
Output to ×10 amplifier
A
+ve
100 kΩ
10 kΩ
R4 20 kΩ
10 kΩ
10 kΩ
6·4μF
From reference signal amplifier
560 kΩ
560 kΩ
100 kΩ
VA3112 N.T.C. Thermistor
560 kΩ
560 kΩ
100 kΩ
From main amplifier
6·4μF
BC109
BC109
BC109
BC109
6·4μF
6·4μF
2·7kΩ
2·7kΩ
1kΩ
1kΩ
R3 20kΩ
8·2kΩ
R2 20kΩ
'Backing off' preset control
200 μF
100kΩ
10kΩ
e6556/1

Fig. 30—Ambient sensor and adder circuit

The phase-sensitive rectifier requires a reference signal which switches it at the correct phase relative to the chopper blade. This is provided by the two devices, the 101CAY, which is a gallium arsenide emitter, and the BPX25 phototransistor acting as the detector. The reference signal, when amplified, is also used in the sensing of ambient temperature.

Cell Bias, Pre-amplifier and Amplifier

The bias current for the cell is chosen to be 10mA to keep the size of batteries to a minimum while retaining a reasonable battery life. A stable low-impedance supply (Fig. 28) in the form of a decoupled 9V voltage regulator diode is used to provide the current, which incidentally is passed through the 101CAY emitter and further decoupled.

The pre-amplifier is a three-transistor amplifier combining a virtual-earth amplifier with a 'feedback pair'. This has a very low input impedance, and the gain depends inversely on the cell resistance. Since both the sensitivity and resistance of the cell decrease with increased temperature, some degree of compensation is afforded.

The pre-amplifier is coupled to a further feedback pair amplifier having a gain of 80, and an output impedance of 150Ω.

Reference Signal Amplifier

The chopped radiation falling on the BPX25 detector (Fig. 29) produces a signal of 10mV across the 10kΩ load resistor. This is amplified by a factor of 100 by a conventional amplifier. The preset emitter resistor allows adjustment of the shape of the output signal so that the waveform crosses the mean level symmetrically.

Ambient Sensor and Adder Circuit

Both the ambient sensor and adder circuit (Fig. 30) use the differential amplifier technique. The reference signal is fed to both sides of the first differential amplifier via both a fixed preset attenuator chain and a temperature dependent (n.t.c. thermistor controlled) chain. The preset control R_3 is adjusted to feed through the correct amount of reference signal variation relative to the radiation signal. The preset resistor R_2 is adjusted to back off excess reference signal and radiation signal so that the meter range starts at 30°C. A voltage gain of 5 is incorporated to match the output level of the ambient sensor with the radiation signal.

The output from the ambient sensor is taken from the collector which is 180° out of phase with the radiation signal. By feeding this and the radiation signal into opposite sides of the second differential amplifier, the output corresponds to the sum of the two signals. The preset control R_4 in the output collector provides adjustment of gain to set the meter range correctly.

This is followed by a feedback pair amplifier having a gain of 10 and low output impedance (100Ω) suitable for feeding the phase-sensitive rectifier.

Phase-sensitive Rectifier

The reference signal switches the transistors OC42 and OC140 on and off alternately, 180° out of phase since one is a p-n-p device and the other an n-p-n device (Fig. 31 and Ref. 2). When one is short-circuited, the signal current flows in one direction through the meter. At the end of half a cycle, the conditions are reversed, but so also is the sense of the signal. Hence signal current flows through the meter in the same direction at all times, except when the target temperature is lower than the 30°C threshold. The capacitor across the meter reduces the bandwidth of the system to about 10Hz with the result that noise is considerably reduced.

REFERENCES

1. Bowling-Barnes, R. 'Determination of Body Temperature by IR Emission', **J. App. Physiology**, Vol. 22, No. 6, June 1967.
2. Williams, P. 'An Improved Phase-sensitive Detector', **J. Sci. Instrum.**, Vol. 45, 1965.

Infrared Microscope for Temperature Measurement of Small Areas

T. J. Jarratt
Mullard Limited

INTRODUCTION

The infrared microscope described was developed primarily to examine the temperature distribution over the surface of transistors and integrated circuits. The instrument incorporates an RPY51 indium antimonide infrared detector.

MICROSCOPE LAYOUT AND OPTICAL SYSTEMS

The optical and mechanical arrangement of the system are shown in Fig. 32. The microscope optical system is very simple, consisting basically of a single objective and an eyepiece, through which the specimen is viewed in the ordinary way.

An infrared image is formed by interposing a semi-transparent mirror, angled at 45°C, in the microscope column: this mirror reflects the infrared radiation and transmits light for normal viewing. Both image planes are arranged to be at the same distance from the objective, so that the images are focused together and are the same size.

A second mirror is used to deflect the infrared image through 90° so that the RPY51 detector can be mounted in an upright position. This has been done to enable liquid nitrogen to be poured into the glass dewar vessel in which the cell is mounted. Subsequently, however, an automatic liquid nitrogen transfer system was developed, and the cell on the prototype may now be mounted in any position.

The reflecting material used on the semi-transparent mirror is a thin gold film. This is very reflective at infrared wavelengths and has a high transmission at visual wavelengths. All the mirror surfaces in the system must have the reflecting material deposited on the incident radiation side to prevent attenuation by the glass or base material of the mirror.

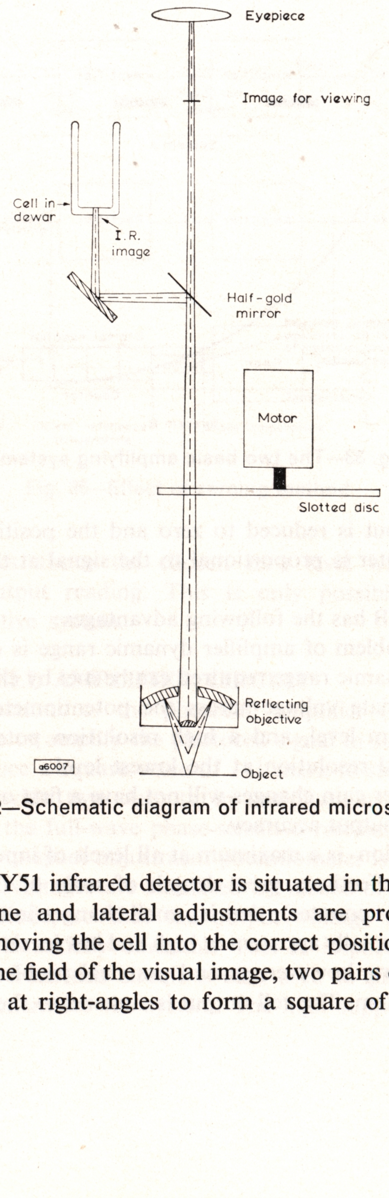
Eyepiece
Image for viewing
Cell in dewar
I.R. image
Half-gold mirror
Motor
Slotted disc
Reflecting objective
a6007
Object

Fig. 32—Schematic diagram of infrared microscope

The RPY51 infrared detector is situated in the infrared image plane and lateral adjustments are provided to facilitate moving the cell into the correct position. At the centre of the field of the visual image, two pairs of parallel lines cross at right-angles to form a square of the same size as the detector (the RPY51 is a 0·5mm square). The cell must be adjusted to occupy the same position in the infrared image as the crossed lines occupy in the visual image.

The type of objective used on the microscope is a Beck reflecting objective designed for use at 15× magnification. Because a mirror objective is used, the problem of finding a lens material of suitable transmission at the appropriate infrared wavelength (5μm) has been avoided.

A further addition to the normal microscope system is a chopper disc introduced into the microscope column. Because the chopper is used, the output of the RPY51 can be connected to an a.c. amplifier, so that a high degree of amplification can follow the cell. The edge of the disc is cut to have 16 radial slots which produce a signal of 1:1 mark to space ratio. The disc is driven by a synchronous motor running at 3000rev/min to give a basic signal frequency for the entire system of 800Hz.

DEVELOPMENT OF ELECTRONIC SYSTEM

When the type of amplification system to be used with the microscope was considered, it was decided that some form of nulling by feedback would be advantageous. The two possible lines of approach are shown in Fig. 33.

System A is the straightforward open-loop amplifier method; System B shows the nulling method where the meter output is reduced to zero and the position of the potentiometer is proportional to the signal at the nulling point.

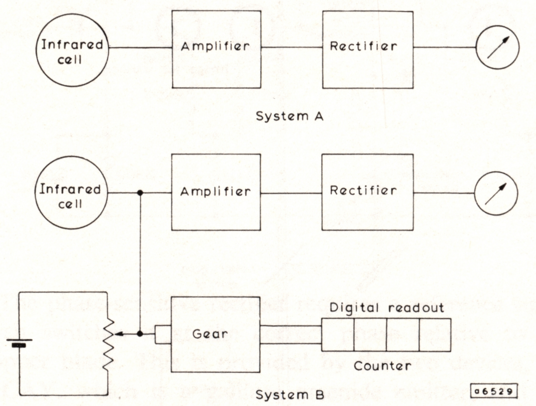

Fig. 33—The two basic amplifying systems

System B has the following advantages:

1) The problem of amplifier dynamic range is overcome. The dynamic range required can be met by choosing an appropriate voltage across the potentiometer for the maximum level, and a high resolution potentiometer for good resolution at the lowest level.
2) Amplifier gain changes will not have a first order effect on the output accuracy.
3) Resolution is a maximum at all levels of input because of the effectively great length of scale of the output meter (or counter); that is, small changes in cell output will be equally apparent at high and low levels of output.

There are, however, several practical problems with a nulling system. The cell output is a.c. and so the feedback signal must be an exactly similar waveform to produce zero input to the amplifier: at high cell output levels in particular, this is a difficult requirement to meet. Nulling will also be difficult if there is excessive noise at the amplifier output. It will therefore be necessary to limit the bandwidth to some extent.

To obtain a good zero, it was decided to make this a d.c. point. This immediately necessitates a compromise in that there must then be some amplification and rectification outside the loop, the system being dependent on this for accuracy.

The cell output level is too low for immediate rectification, and amplification is necessary first. The gain of this first amplifier should therefore be just sufficient to bring the signal up to a level suitable for rectification; this will then ease the problem of keeping the gain stable by application of negative feedback.

Use of Phase-sensitive Rectifiers

An ordinary diode bridge rectifier is not suitable for use in this circuit. The forward voltage drop of the diodes makes them unsuitable for low-level operation.

A phase-sensitive rectifier using transistors will function at the millivolt signal level and is ideally suited for this application. This type of rectifier also provides a convenient means of reducing the bandwidth to almost any desired degree.

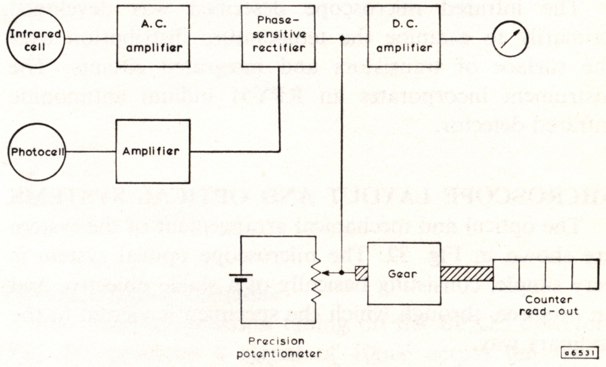

Fig. 34—Basic nulling system

The phase-sensitive rectifier requires an a.c. reference voltage which must be of the same frequency and in the same phase as the signal. This reference is available from the mechanical chopper disc when a lamp and photocell are arranged on either side of it at some suitable point to give the correct phase. This method of bandwidth limitation has the advantage that if the signal frequency alters, then the reference will also change, and there is no change in the d.c. output level of the rectifier. The whole system can therefore be made immune to changes in chopper frequency. To achieve this, however, there must be no phase shift in the amplifier preceding the phase-sensitive rectifier as this will cause a drop in the d.c. output. The bandwidth of the amplifiers must therefore be sufficient to ensure that over any possible change of chopper frequency, no phase-shift will be introduced. The basic block diagram has now been developed into that shown in Fig. 34.

Automatic Read-out

It is now an obvious step to close the mechanical loop by dispensing with the meter and substituting a motor which drives the potentiometer automatically to zero output, thus making a nulling servo-indicator. A small permanent-magnet d.c. motor is well suited to this application.

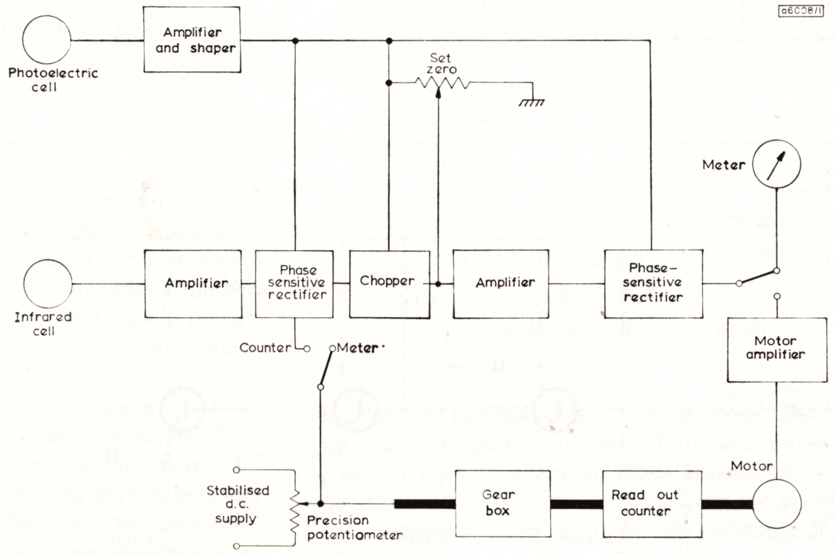

Fig. 35—Complete nulling system

In the system built, it was decided to use a commercially available mechanical digital voltmeter which contained the potentiometer, counter, motor, motor-amplifier and gearing. The motor used in the voltmeter is an a.c. 50Hz two-phase type.

Second Amplifier

The d.c. amplifier in Fig. 34 is of the same type as the first amplifier except that the input to it is chopped (modulated) and the output is phase-sensitive rectified. The modulators and phase-sensitive rectifiers have virtually the same circuit.

Meter Read-out

An independent meter readout was required and this was calibrated directly in temperature (black body). This is fed from a straight-through amplifier system with the potentiometer feedback switch out. The complete block diagram is shown in Fig. 35.

Zero Set

The reference signal is derived from the output of a phototransistor (BPX25) which is amplified and squared. There is also a preset control to adjust the mark-to-space ratio to be an exact square wave. The phase-sensitive rectifiers and modulators are all full-wave circuits, which means that two reference signals are required, one in anti-phase with the other. Their voltages are stabilised by a voltage regulator diode and suitably attenuated, and are used for zeroing the system.

The output from the cell depends on the difference between the radiation from the chopper blades and the radiation from the object under investigation. Since the system is phase-sensitive, if the infrared radiation from the object is less than that from the chopper blades, the output voltage will be negative; and if the object radiates more, the output will be positive (Fig. 36). Thus, if a square-wave 'backing-off' voltage is injected into the system, the system can be zeroed at any object temperature, so that any temperatures above the chosen zero level will give a positive output reading. This is only possible with a phase-sensitive system.

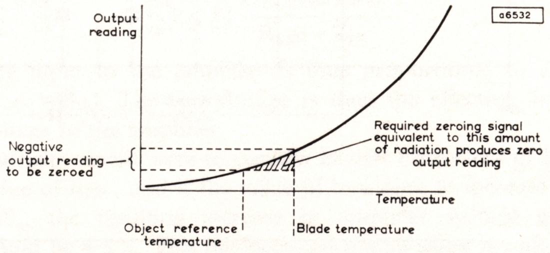

Fig. 36—Effect of zeroing method

PHOTOCELL AMPLIFIER CIRCUIT

The functions of the photocell amplifier (shown in Fig. 37) are to amplify the photocell signal in such a way as to produce a square wave of 1:1 mark-to-space ratio, and to provide two outputs in antiphase as reference signals for the full-wave phase-sensitive rectifier.

A mark-to-space adjustment potentiometer is included, and supply voltages are stabilised by means of a voltage regulator diode, so that the output voltage amplitude remains substantially constant. This is important since the output from this circuit is also used to provide the zero adjustment for the system. The high supply voltage

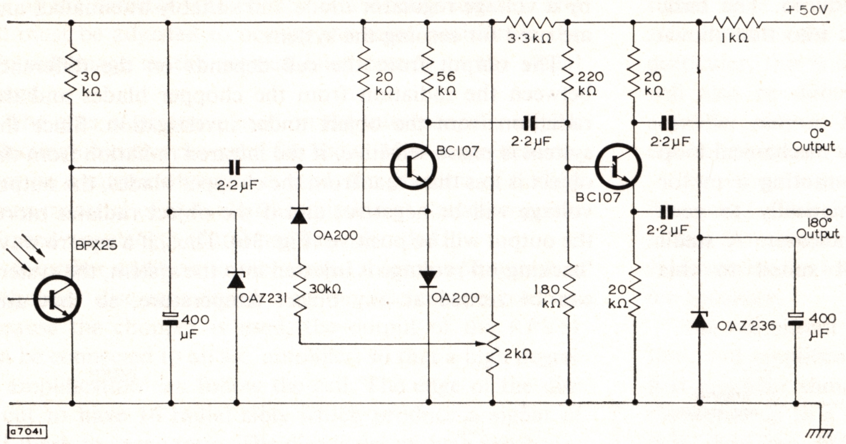

Fig. 37—Photocell amplifier and pulse shaper

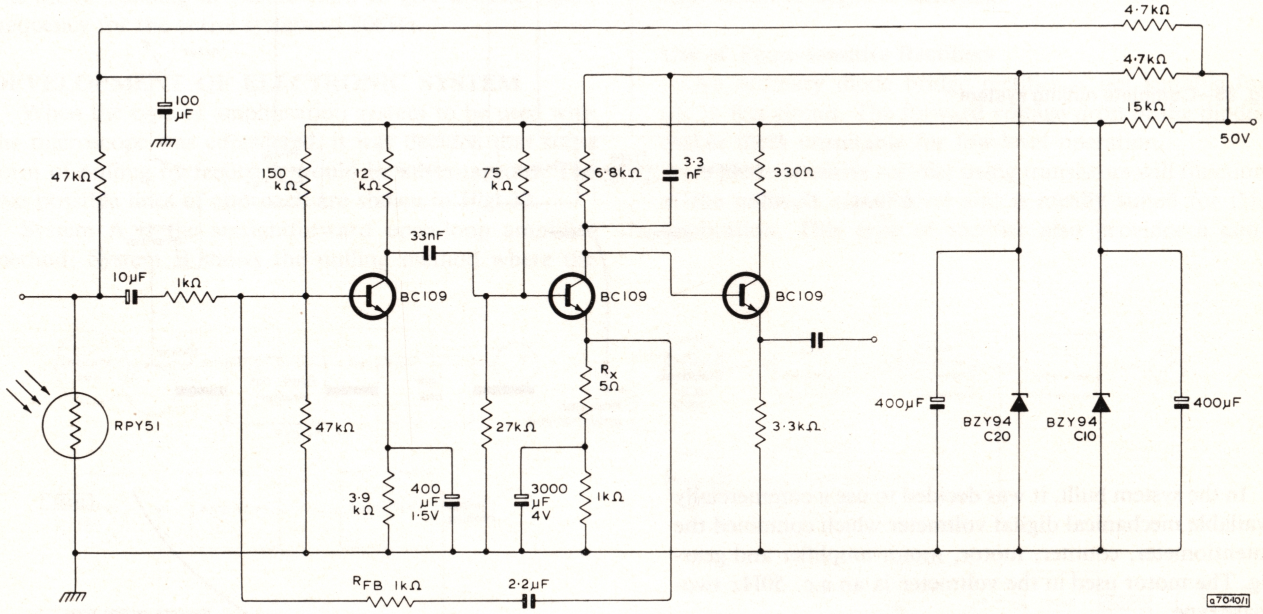

Fig. 38—Cell amplifier

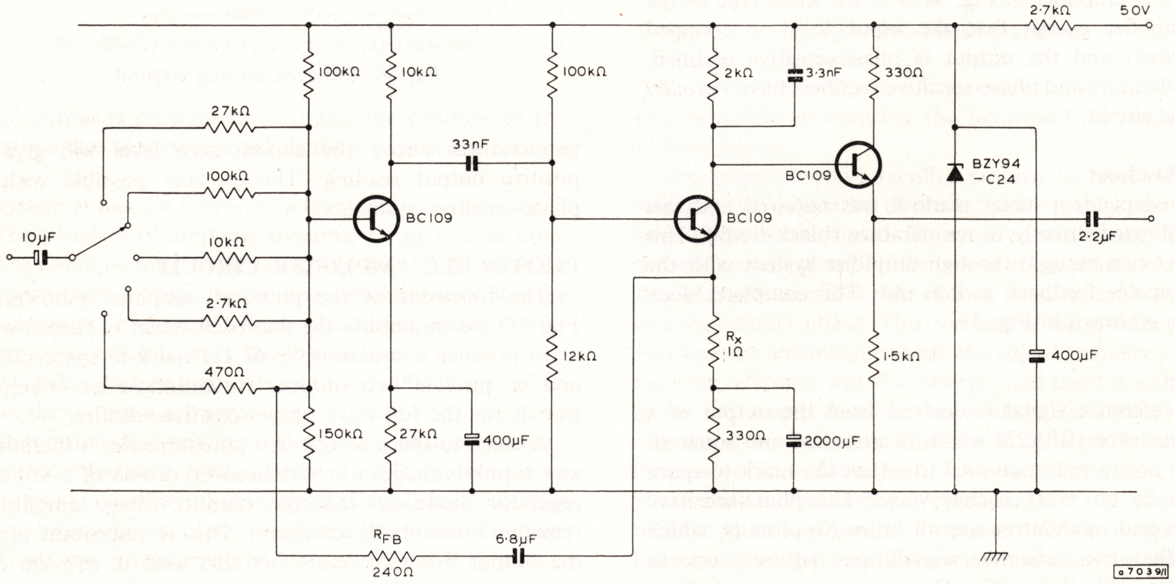

Fig. 39—Second amplifier

has been chosen because of the drive requirements of the insulated gate f.e.t. chopping transistors used in the phase-sensitive rectifiers.

AMPLIFIER CIRCUIT

The two amplifiers in the system are of similar design, and the circuits are shown in Figs. 38 and 39. The two major design considerations are low noise and stability of gain. BC109 transistors are used; these, when operated at a collector current of between 100μA and 200μA, and with an effective base-to-chassis impedance of 2kΩ, have a very good noise characteristic.

The resistance of the RPY51 is between about 1 and 2kΩ, so that this is suitable for feeding directly into the amplifier. Cell biasing is shown in Fig. 37 and this is simple constant-current feed from the stabilised 50V supply.

To achieve good gain stability, a large amount of negative feedback is essential. The accuracy of the basic two-stage amplifier is reasonably good. The stability of the current gain of the circuit is good, but this performance is degraded to some extent by the possibility of variations in input impedance. There is, however, some compensation for this effect, as the input to the amplifier from the cell does not represent a voltage drive. If it were a perfect current source then, of course, variations of input impedance would have no effect on amplifier gain.

In predicting what accuracy is to be expected in practice, it is necessary to decide on the worst-case conditions. Production spreads in transistor characteristics are such as to alter the gain of this type of amplifier by several percent, but since any instrument that is built will be calibrated, this effect was not included in the worst-case considerations.

The two factors affecting gain stability are temperature and ageing. Temperature will change the values of h_{FE}, r_e, and V_{BE}. The change in V_{BE} is -2mV/degC. The value of h_{FE} increases by 1% per degC. The value of r_e increases proportionally with absolute temperature. The change in r_e tends to reduce the effect of changes in h_{FE} and V_{BE}, the latter two tending to increase the stage gain, the former actually producing more negative feedback.

The expression for current gain G_i of this amplifier is:

$$G_i = \frac{A}{1+\dfrac{AR_x}{R_{FB}}},$$

where A is the open-loop current gain of the amplifier. To convert A to voltage gain G_v, the current gain G_i must be multiplied by the ratio of output resistance to input resistance. The input impedance Z_{in} to the amplifier is given by:

$$Z_{in} = R_{in} + \frac{r}{1+\dfrac{AR_x}{R_{FB}}},$$

where R_{in} is the external series resistance and r is the effective input resistance into the base of the transistor; at room temperature r is given by the equation:

$$r = 25/h_{FE}I_e$$

where I_e is measured in mA. The expression for Z_{in} shows that the summing point of the amplifier is not a perfect 'virtual earth'. Thus the true voltage gain G_v of the amplifier is given by:

$$G_v = \frac{G_iR_o}{R_{in}+\left(\dfrac{r}{1+\dfrac{AR_x}{R_{FB}}}\right)}$$

Variations in the voltage gain of the amplifier are caused partly by current gain variations in the amplifier and partly by variations in input impedance. These effects are additive. Thus, if amplifier gains fall slightly, the input impedance increases. However, because of the loading of the cell voltage by the amplifier input impedance, the cell output voltage rises, thus reducing the effect of gain variations. If the cell output were a constant current, changing input impedance would have no effect. This effect can be seen from the expression for cell voltage, V_{in}, in terms of cell resistance R_{cell}, and amplifier input impedance Z_{in}, given below.

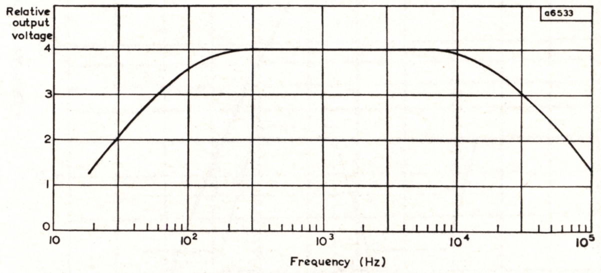

Fig. 40—Amplifier bandwidth

$$V_{in} = \frac{Z_{in}I_{bias}\Delta R_{cell}}{R_{cell}+Z_{in}}.$$

The input to the amplifier is thus proportional to $Z_{in}/(R_{cell}+Z_{in})$. The cell voltage is then the effective input voltage to the amplifier.

If the circuit were to contain BC109 transistors of low value of h_{FE}, and if the value of h_{FE} were to increase by 50%, the resulting increase in amplifier voltage gain would be 4·5%. This has been calculated using the above equations.

The bandwidth of the two a.c. amplifiers in the system is reduced to give the characteristic as shown in Fig. 40. This bandwidth was considered sufficient to ensure no amplitude or phase change through the amplifier at 800Hz±10%.

The top response is limited by the shunt capacitor across the collector load of TR_2 of each amplifier; the low-frequency response is limited by the amplifier input capacitor. The frequency characteristic of the amplifiers is equivalent to about a 15% fall-off in an 800Hz square wave at the output of the amplifier; this is considered to be acceptable for the waveforms in the system.

This amount of 'droop' in the waveform results in a change of d.c. output from a phase-sensitive rectifier, when there is a change of signal frequency. A frequency change of 6% (the most that would be expected of the 50Hz mains) would cause a change of output from a phase-sensitive rectifier of 0·5%.

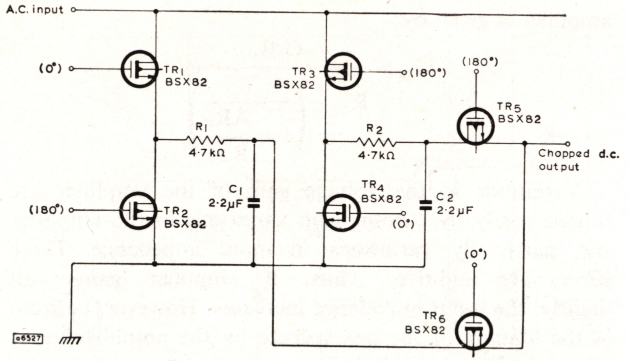

Fig. 41—Phase-sensitive filter

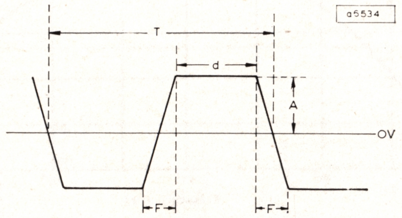

Fig. 42—Waveform of chopped radiation

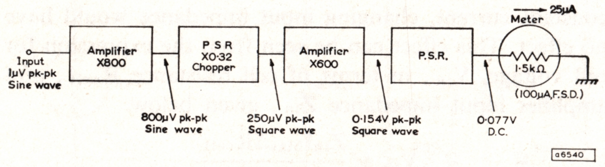

Fig. 43—Overall system gain

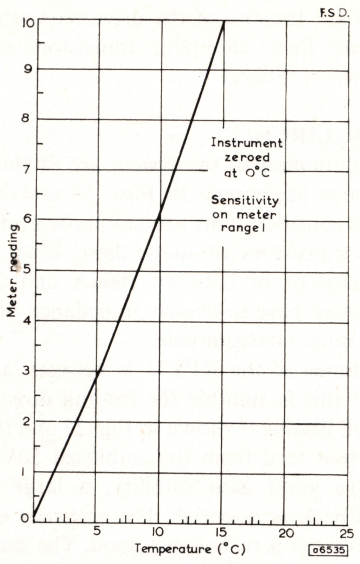

Fig. 44—Maximum sensitivity range

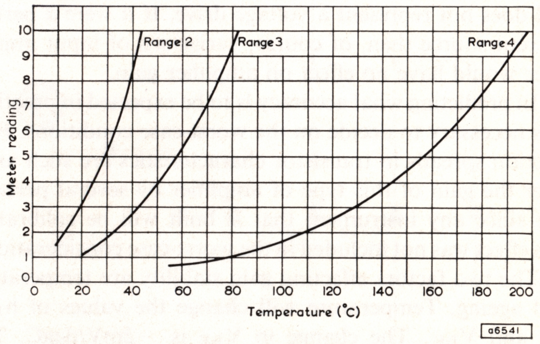

Fig. 45—Meter range curves

PHASE-SENSITIVE RECTIFIER AND CHOPPER

The type of phase-sensitive rectifier used consists of four switching transistors arranged in a bridge (Fig. 41). These operate in a similar manner to the diodes in a bridge rectifier, the difference being that, whereas the diodes are switched by the a.c. signal to be rectified, the transistors are switched on and off by an independent reference signal of fixed frequency and phase.

Thus, the phase-sensitive rectifier will produce a d.c. signal only from a signal of the same frequency and phase as the reference. The d.c. output from this circuit would normally have a floating level between the appropriate two points of the bridge. However, to obtain an output relative to chassis, two halfwave outputs are taken, as shown in Fig. 42, one being positive and the other negative.

The a.c. output from the first amplifier is fed into the phase-sensitive rectifier which then provides a d.c. signal which is used for comparison with the d.c. feedback from the potentiometer. The phase-sensitive rectifier also serves as a narrow-band filter when followed by a chopper and further a.c. amplification.

The type of transistor used is the insulated gate f.e.t. type BSX82. With the bridge arrangement and the following two chopper transistors, all the switching ON and OFF operations are carried out by one transistor in series and another in parallel. With this type of connection, noise generated when the series transistor is cut off is reduced by the parallel transistor being conductive.

The bandwidth of the circuit can be adjusted by altering the smoothing time-constant. The bandwidth is given by $1/2\pi CR$, and the bandwidth is defined as between the points where the d.c. level has fallen to 0·707 of the value at chopping frequency.

There is also a waveform change from the a.c. input to the a.c. output of the filter, the output always being a square wave.

If the input is assumed to be a sinewave of peak value V, then the d.c. output V_{dc} at each half-wave point is V/π. Since there is a positive and a negative output of this value, the peak-to-peak value of the output waveform is $2V/\pi$. Thus the attenuation of a sinewave input measuring peak-to-peak at input and output is $1/\pi$ or 0·32. This is correct only if the output loading is a high resistance compared with the resistance in the filter. The waveform from the cell is of the form shown in Fig. 42. The attenuation of this waveform by the phase-sensitive filter is given by

$$\frac{V_{out}}{V_{in}} = \frac{\left(\frac{F}{2}\right)+d.}{T}$$

The first phase-sensitive rectifier has RC values of 4·7kΩ and 2μF. This gives a calculated bandwidth of 15·5Hz each side of chopper frequency.

The bandwidth of the first amplifier is about 20kHz (see frequency characteristic in Fig. 40). Since noise voltage is proportional to the square root of the bandwidth, this phase-sensitive rectifier will reduce the noise by $(20\,000/30)^{\frac{1}{2}}$ or approximately 25 times.

GAIN OF COMPLETE SYSTEM

The open-loop microscope system gain from input to meter is shown in the block diagram in Fig. 43. The gain shown in the first phase-sensitive rectifier block is for a sinewave input. Thus, for a 1μV peak-to-peak sinewave input, the open-circuit output voltage is 77mV d.c.

If a 100μA meter having 1·5kΩ coil resistance is used at the output, and the output resistor of the phase-sensitive rectifier is 1·5kΩ also, then the output current will be given by the equation

$$I_{out} = \frac{0{\cdot}077}{3\times 103}A \simeq 25\mu A.$$

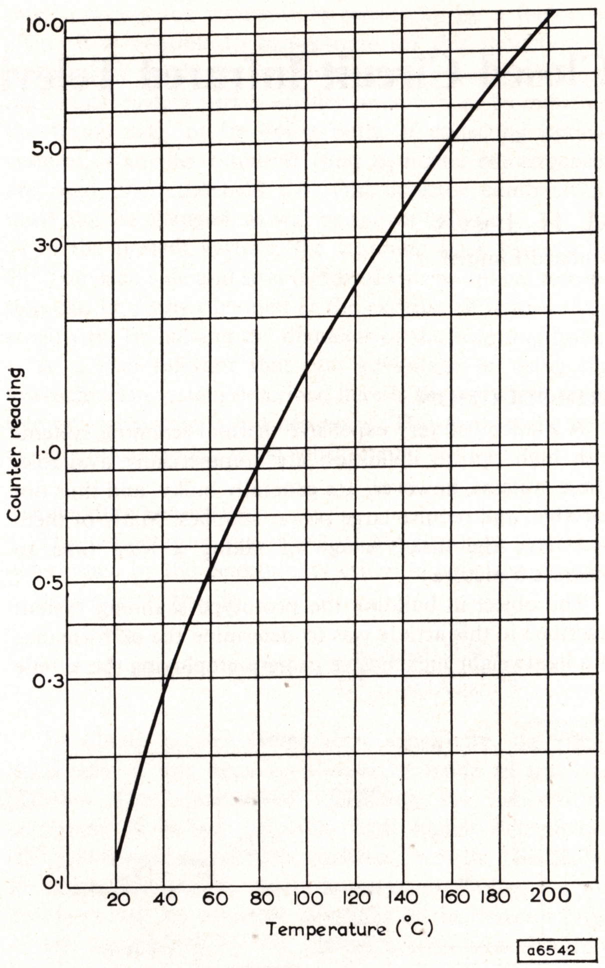

Fig. 46—Range of counter

EQUIPMENT SPECIFICATION

Detector

Type	RPY51, indium antimonide cell
Operating temperature	77°K
Cooling system	Drip-feed mechanism fed from liquid nitrogen dewar

Optical

Objective magnification	15×
Spot size	30μm
Visual field of view	1mm diameter
Working distance	24·3mm

Electrical

Bandwidth	
Normal chopping mode	4Hz
Transient measurement mode	50kHz

Performance

Temperature resolution* (Meter)	0·5degC at 25°C
Temperature range* (Meter)	
1	0 to 15°C
2	10 to 44°C
3	20 to 80°C
4	45 to 200°C
(See Figs. 44 and 45)	
Temperature range* (Counter)	15 to 150°C
(See Fig. 46)	
Cell response time	4μs
Spectral range	1·8 to 5·5μm

*Black-body calibration

Closed Circuit Infrared Television System

M. H. Jervis
Mullard Limited

INTRODUCTION

A number of very expensive thermal scanning systems with high optical definition are commercially available. These systems, however, are generally bulky, and thus not portable, and require large power supplies. Many of them also have the disadvantage of taking a long time to generate a picture.

The object in building the prototype scanning system described in this article was to determine the performance of a lightweight inexpensive camera employing the simple Nipkow disc as the scanning mechanism. This mechanism comprises a flat disc, perforated with a spiral of holes which, when rotated, generates 30 scanning lines. Since the disc, rotating at 1000 rev/min, is the only moving part, the camera is small in size, robust and has a low power consumption. The complete equipment consists of two parts, a camera head and an oscilloscope display, as indicated in Fig. 47.

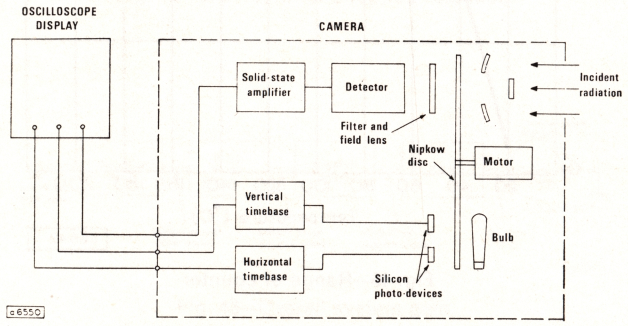

Fig. 47—Block diagram of system

The main problem of the Nipkow disc scanning mechanism is that the detector 'sees' any variation in the radiation emitted or reflected by the Nipkow disc, as well as that from the scene. In the first experiments, this variation produced a spurious signal level much greater than the signal from a room-temperature scene, but the problem was overcome by means of a specially constructed disc of black Perspex, so that the camera was limited by detector noise.

With the 30 line, 17 frames per second picture, the equipment has a temperature sensitivity of 0·5degC with a room temperature background. Thus, it can detect the presence and position of any 'hot spots' on moving and stationary objects within the field of view.

The detector is a Mullard 77°K indium antimonide photoconductive infrared detector which has an annular element to match the optical system. Cooling is achieved by using a liquid nitrogen drip-feed system supplied from a dewar vessel placed on the ground at the side of the camera. This enables the camera to be operated in any plane. If a Mullard room-temperature lead sulphide detector is used in place of the indium antimonide detector, the minimum detectable temperature becomes 120°C but detector cooling is then unnecessary.

THE DESIGN OF THE OPTICAL SYSTEM

The requirements of the equipment are that it should be portable and relatively inexpensive. This dictates the requirements of the optical system. A germanium lens could be used instead of the simple reflecting Cassegrainian system employed, but this would be expensive and therefore conflict with a basic requirement. The Nipkow disc scanning system, although not theoretically the most efficient, has the advantages of mechanical simplicity and ease of manufacture.

The optical system is shown in Fig. 48. The radiation from the scene is collected by the front-silvered concave mirror, focused via the front-silvered plane mirror onto the Nipkow disc, which has a spiral of 30 holes near its circumference. Each hole scans the image in turn, and the transmitted radiation is focused onto the annular detector by means of a field lens. The field lens projects an image of the effective annular shape of the collecting optics on to the detector element, and hence the radiation transmitted by a scanning hole is uniformly spread over the detector area.

A second set of holes in the Nipkow disc enables synchronisation pulses to be obtained, thus enabling the raster on the display oscilloscope to be triggered. The signal from the detector is used to intensity-modulate the electron beam of the oscilloscope, thus producing an image on the screen.

The design equation of the Nipkow disc is derived as Eq. 12 in Appendix 1. It is

$$\int_0^{\lambda_c} T_\lambda(Q_S - Q_B)d\lambda \geqslant \frac{K\lambda_1(A_D)^{\frac{1}{2}}(\Delta f)^{\frac{1}{2}}}{D^*_{\lambda 1} Jhc\sin^2\theta}.$$

From this equation the maximum temperature sensitivity of the camera using cooled indium antimonide and lead sulphide detectors is calculated. The temperature sensitivity for the indium antimonide detector is shown to be 0·5degC at 25°C, and this figure has also been obtained from actual measurements with the camera. For the lead sulphide detector, it is shown that a temperature difference of 80 degC between a black-body source and a room temperature should be detectable, and this again corresponds fairly closely to the easily observable 100degC difference measured with the camera.

VARIATIONS ON THE PRESENT DESIGN

The main parameters that can be varied in the Nipkow disc scanner are:

1) field of view,

2) optical resolution,

3) temperature resolution,

4) frame rate,

5) camera size and weight,

6) cost of system.

Each of these can generally be varied only at the expense of another: for example, the optical resolution can be increased at the expense of the temperature sensitivity and vice versa. The first three of these six variables are discussed below.

Field of View

The present 6° field of view of the system is most easily increased or decreased by using a collecting optical system of shorter or longer focal length. If the f-number of the optical system is kept constant, the convergence of the radiation at the Nipkow disc is constant and, hence, from Eq. 10 of Appendix 1, the temperature sensitivity remains the same.

Optical Resolution

The optical resolution of the present system (7mrad) is determined basically by the number of scanning lines, the field of view of the optical system, and the hole size in the Nipkow disc. It is given by the equation

$$\text{Optical resolution} = \frac{\text{Field of View}}{\text{Number of Holes}} \times \frac{\text{Actual diameter of holes}}{\text{Maximum diameter of holes with no overlap}} \quad \ldots(1)$$

If the optical resolution is doubled by doubling the number of scanning lines and the rest of the optical system is kept constant, then the diameter of the scanning holes must be halved and the electrical bandwidth increased.

The electrical bandwidth Δf required to give a square picture is given approximately by the equation

$$\Delta f \simeq \frac{Fn^2}{2}$$

where F is the frame rate and n is the number of scanning lines. This bandwidth is essentially the fundamental sine frequency generated by alternate picture elements being hot and cold.

It can be seen from the design equation in Appendix 1 that doubling the number of lines and keeping the rest of the system the same, reduces the hole area A_H by a factor of four and increases the bandwidth Δf by a factor of four, thus reducing the temperature sensitivity by a factor of eight. It is possible to compensate for this reduction in temperature sensitivity by using a more expensive collecting optical system with a smaller f-number, or by reducing the frame rate, or by doing both. If collecting optical systems of smaller f-number (that is, higher convergence) are used, then the field lens and detector combination must also be changed, as will be shown below.

In the present system, the scanning lines overlap by 50% on each side and so a factor of two in optical resolution can be easily obtained at the expense of temperature sensitivity, by halving the diameter of the scanning holes.

It is also relevant that one advantage of using the low-definition system described here is that an aberration-free optical system is not necessary. This enables the cost of the optical system to be substantially reduced.

Temperature Sensitivity

The temperature sensitivity of the scanning system is determined by the detectability criterion equation derived in Appendix 1; that is

$$\int_0^{\lambda_c} T_\lambda(Q_S - Q_B)D\lambda \geqslant \frac{K(A_D)^{\frac{1}{2}}\lambda 1(\Delta f)^{\frac{1}{2}}}{D^*_{\lambda(1)} hcJA_H\sin^2\theta}.$$

To obtain greater temperature sensitivity, the right-hand side of this equation should be made as small as possible. One method of increasing the temperature sensitivity is to use detectors with higher detectivities (D^*_λ) or longer wavelength response, or both. The degree to which this can be done, however, is limited by the detectors that are available. The area of the detector (A_D) is also determined by the optical system and therefore cannot be independently changed.

The two main ways of increasing the temperature sensitivity are:

1) to reduce the bandwidth Δf of the system by reducing the number of lines or the frame rate, or

2) to increase the optical efficiency, the hole size A_H, or the convergence of the radiation at the Nipkow disc.

As described in the previous section, either decreasing the number of scanning lines or increasing the hole size decreases the optical resolution.

The effect of reducing the bandwidth to below that given by $Fn^2/2$ is quite interesting. If the bandwidth is restricted at the high-frequency end, then the sharp edges of objects are blurred. If, however, the low-frequency end of the bandwidth is restricted, the edges of hot objects are accentuated and the temperature sensitivity of the system is increased. Restricting the low-frequency end of the bandwidth also enables hot and relatively cool objects to be seen in close proximity without overloading the picture. A useful bandwidth for the present system is from 300Hz to 5kHz.

OPTICAL SYSTEM OF THE EQUIPMENT

Because a small, inexpensive, portable scanning system was desired, the optical system also had to be readily available and inexpensive. The optical system finally chosen is shown in Fig. 48. It is a simple Cassegrainian system consisting of a 7·3cm diameter collecting mirror and a 4·7cm diameter plane mirror, to focus the image of the Nipkow disc. An arsenic trisulphide lens with a focal length of 1·4cm is then used to focus the radiation onto the detector. The detectors used are 8mm × 5mm diameter annular elements which are comparable with the shape of the collecting optical system. In the PbS camera, a 61SV detector can be used, but the field lens must be replaced by a cone channel optical system. The full details are:

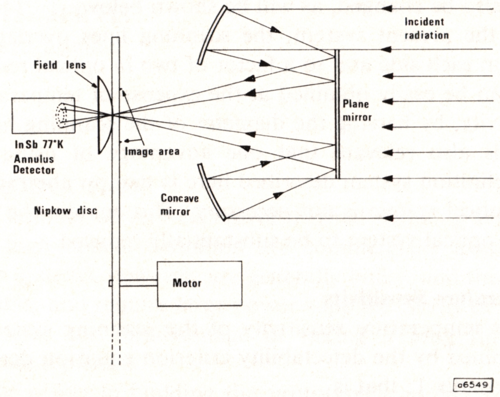

Fig. 48—Optical system of camera

Collecting mirror*:	Front-silvered, concave mirror 7·3cm diameter; 13cm focal length.
Plane mirror:	Front-silvered, plane mirror 4·7cm diameter (the area of concave mirror that is obscured is 5cm in diameter).
Nipkow disc:	A 19cm diameter disc of black Perspex. The scanning and synchronisation holes are 1mm in diameter.
Field lens:	Material, arsenic trisulphide; diameter, 2cm; focal length, 1·4cm.
Detector	
InSb:	8mm × 5mm diameter annulus, operating at 77°K. Type RPY56.
PbS:	8mm × 5mm diameter annulus, operating at room temperature. Type RPY57.

The focusing arrangement on the camera moves the whole collecting optics, thus enabling the scene to be continuously focused up in the Nipkow disc. The size of the detector is such that the image of the collecting optical system lies on the annular sensitive area for focusing distances between 1·2m and infinity.

Nipkow Disc

Nipkow disc scanning is a means of scanning in the image plane of a system. The disc has a spiral of 30 holes around its circumference as shown in Fig. 49, each of which scans across the image in turn. The radiation passing through these holes is focused on to the detector. The signal from the detector is then used to intensity-modulate the raster on the display oscilloscope. Secondary holes diametrically opposite the scanning holes are used to give pulses with which the line and frame timebases providing the raster are synchronised. The synchronisation pulses are produced by using a 12V festoon bulb and two BPX25 silicon phototransistors.

It is very important to align the synchronisation holes and the scanning holes on the same disc diameters, otherwise distortion will occur in the displayed picture.

The scanned image size on the Nipkow disc is approximately 1·5 × 1·5cm. The 30 scanning holes are placed on radii of the disc, such that angular displacement between any two consecutive radii is the same. Partly to compensate for the fact that the drilled scanning holes are round rather than square and partly to increase the temperature sensitivity, the scanning lines were made to overlap by 50% on both sides; that is, the holes were made 1mm in diameter.

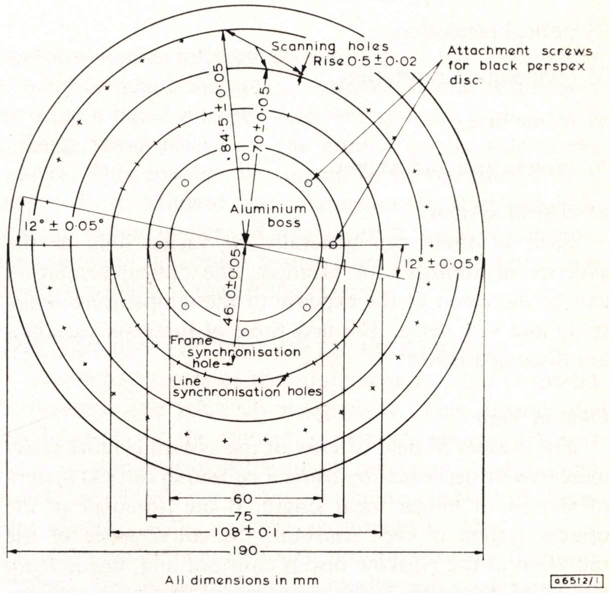

Fig. 49—Dimensions of Nipkow disc. The scanning and synchronisation holes are circular and 1·0 ± 0·05mm in diameter. The 30 scanning holes are placed in a spiral at 12° ± 0·05° intervals with a rise between two consecutive holes of 0·5 ± 0·02mm. The disc is constructed of $\frac{1}{8}$in black Perspex with a centre boss of aluminium. The scanning holes are countersunk, on the side facing the collecting optical system, to within 0·5mm of the other surface using a 5mm drill.

The main difficulty in making the Nipkow disc for the indium antimonide system was that the first discs produced a large spurious signal when rotated. The amplitude of this spurious signal was up to 50 times that of the noise from the detector and was caused by variations in reflectivity and emissivity, and by wobble along the surface of the discs. Various metal discs were made with polished or matt surfaces but, although the spurious signal was reduced, it was still much greater than the detector noise.

Finally, a different principle was tried. A disc was made of clear Perspex which, in thin sheets, transmits infrared out to 5·5μm. This disc was found to produce a very low spurious signal. Because most of the radiation is emitted from beneath the surface of the disc, surface imperfections and small scratches did not cause high standing signals as the disc was rotated. One problem that occurred on using clear Perspex, however, was that radiation from the bulb driving the phototransistors was channelled through the disc to the scanning holes, where it interfered with the video signal. This was overcome by using black Perspex.

The black Perspex discs still had, however, the wobble associated with the first discs. This produced a low-frequency spurious standing signal on the thermal picture. In order to reduce this to a minimum, the metal boss on the disc was extended as far as possible, and thicker Perspex discs were made. The loss of signal radiation was reduced to a minimum by counter-sinking the scanning holes on the side of the disc facing the collecting optics.

Complete elimination of the wobble was found to be unnecessary because of the other sources of low-frequency noise in the system, such as noise caused by the Leiden-Frost cooling system, and low-frequency noise in the indium antimonide annular detector.

All the sources of low-frequency noise were rendered almost unnoticeable by using a low-frequency (40Hz) cut in the system.

Should complete elimination of the wobble in the disc prove desirable, annealing the Perspex disc or, alternatively, coating a metal disc with Perspex or a similarly transmitting material, might prove satisfactory. Most of the effect of the wobble could also be removed by a form of black-level control in which the disc signal level would be measured before each line scan, thus enabling the cathode of the display oscilloscope to be clamped to the same d.c. level for each line and frame scan.

However, with this prototype equipment, it was found that very acceptable thermal pictures limited mainly by detector noise could be obtained with the indium antimonide detector by simply using the 40Hz low-frequency cut off. With the high-temperature, lead-sulphide version of the camera, the standing signal from the disc is of course negligible compared with the detector noise.

Field Lens

The purpose of the field lens is to focus the radiation from the scanned image on to the detector. This is achieved by imaging the collecting optical system on to the detector. Thus the field lens can be placed close to the Nipkow disc, enabling its diameter to be not much larger than the diameter of the image. This method also has the advantage that the radiation falling on any one point in the scanned image is spread uniformly over the detector, thus overcoming any non-uniformity of response problems in the detector.

The required diameter D of the detector is given by the equation:

$$D \simeq \frac{fd}{L\text{-}f}, \qquad \ldots(2)$$

where

f = focal length of the field lens,

L = separation distance of the field lens from the collecting optical system, and

d = diameter of the collecting optical system.

Cooling System for Indium Antimonide Detector RPY56

The indium antimonide detector used in the infrared camera is designed to operate at liquid nitrogen temperature (77°K). This is achieved by using a system which utilises the Leiden-Frost effect whereby beads of liquid nitrogen ride inside a layer of vapour in the transfer line. The vapour insulates the liquid beads from the walls of the transfer line; hence the length and material of the transfer line are not critical, and lengths up to two metres may be used. However, constrictions and sharp bends in the line must be avoided.

The actual system used consists of a 4 litre flask of liquid nitrogen which is coupled to the camera by a transfer line of p.v.c. tubing having a 3mm internal diameter. The flask is sealed with toggle clamps to generate enough pressure to force the liquid nitrogen beads through the transfer line. The actual rate of flow is controlled by restricting the vapour effluent from the cooling head in the detector.

The flow rate should be kept to the minimum required to cool the detector, which is generally about three-quarters of a turn of the needle valve used on the camera. If excess flow rates are used, then the beads may wet the wall of the transfer line, thus causing only nitrogen vapour to reach the detector.

The effluent vapour from the detector is heated to a few degrees below room temperature by the heatsink on the needle valve. It is then passed into the cavity between the detector and the field lens and subsequently blown onto the Nipkow disc. This use of the effluent gas serves several purposes:

1) to prevent the detector window and the field lens from misting up,
2) to cool the Nipkow disc and, therefore, cause it to emit less radiation,
3) to reduce the background radiation falling upon the detector and hence increase its detectivity.

Because the effluent gas is blown onto the Nipkow disc, it is important to switch the motor on before switching the cooler on, otherwise a large standing signal will occur from the cooled portion of the disc.

The 'stand-by' time of the 4 litre flask is approximately 60 hours, and the continuous running time is about 30 hours. Thus, under most conditions of intermittent use, 4 litre is enough for two days.

The main advantage of the Leiden-Frost cooling system is that it enables the camera to be used in any plane. Its main disadvantage is that the beads of nitrogen generate bursts of low-frequency noise as they are forced into the detector. This noise has largely been eliminated in the present camera by using a low-frequency cut of 40Hz.

ELECTRONICS

The basic functions of the electronic circuits are:

1) to generate the raster for the display oscilloscope,
2) to amplify the video signal from the detector and use it to modulate the picture brightness on the oscilloscope,
3) to control the speed of the motor to within ±10%.

---

*A shield is used on the concave mirror to prevent stray radiation from passing, unreflected, through the optical system.

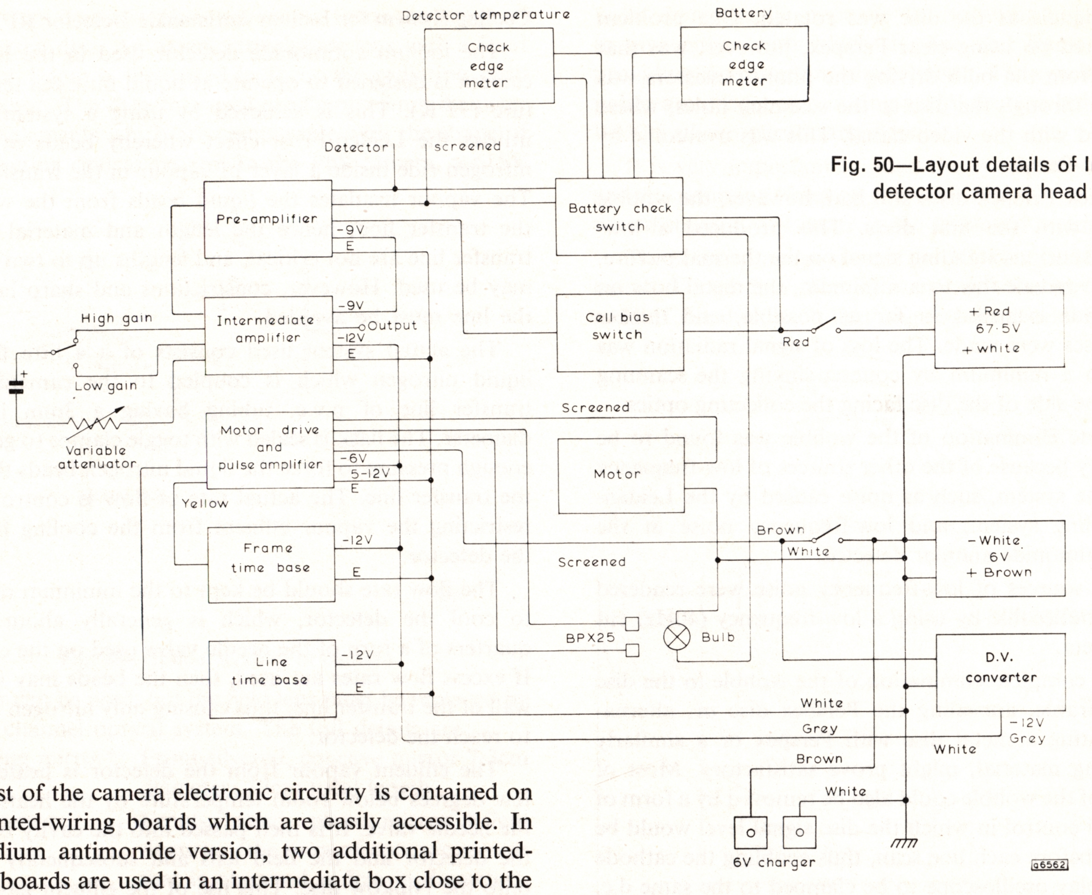
Detector temperature
Check edge meter
Battery
Check edge meter
Detector
screened
Pre-amplifier
-9V
E
Battery check switch
Cell bias switch
Red
+Red 67·5V +white
High gain
Intermediate amplifier
-9V
Output
-12V
E
Low gain
Variable attenuator
Motor drive and pulse amplifier
-6V
5-12V
E
Yellow
Screened
Motor
Frame time base
-12V
E
Brown
White
-White 6V +Brown
Screened
BPX25
Bulb
Line time base
-12V
E
D.V. converter
White
Grey
Brown
White
-12V Grey
White
6V charger
a6562

Fig. 50—Layout details of InSb detector camera head

Most of the camera electronic circuitry is contained on six printed-wiring boards which are easily accessible. In the indium antimonide version, two additional printed-wiring boards are used in an intermediate box close to the display unit; this box enables the video signal to be altered at the display end of the equipment. It includes a differential amplifier, which enables just the peaks of the video signal to be displayed, thus enhancing the temperature discrimination at temperatures other than room temperature. It also includes switching, by which the bandwidth of the video signal can be altered to show the importance of the video bandwidth on the visual display.

The layout of the electronic circuits in both versions of the infrared camera are given in Figs. 50, 51 and 52.

Display

Most oscilloscopes can be used as the display for this infrared camera. The line and frame camera timebases and the video signal are fed respectively onto the X, Y and Z inputs of the oscilloscope. However, most oscilloscopes suffer from certain limitations in this application.

1) They have phosphors which have too few 'grey tones'.
2) The low-frequency cut on the modulation is several hundred hertz.
3) They form a relatively expensive method of display since the camera timebases are used and most of the circuits within the oscilloscope become redundant.

However, acceptable thermal pictures can be obtained in spite of the above limitations. The frequency cut differentiates the picture; that is, it accentuates the edges of objects within the scene.

One type of oscilloscope which has been used with the present cameras is the E.M.I. oscilloscope type 101. This has a black and white phosphor, and has had the capacitors controlling the Z modulation temporarily changed to give a low-frequency cut of about 15Hz. This type of oscilloscope was used because of its portability, battery operation and price.

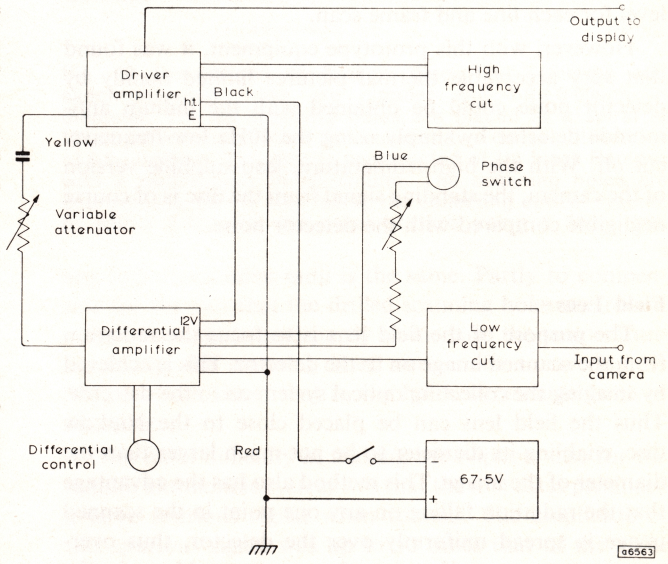
Output to display
Driver amplifier
ht
E
Black
High frequency cut
Yellow
Blue
Phase switch
Variable attenuator
Differential amplifier
12V
Low frequency cut
Input from camera
Differential control
Red
67·5V
a6563

Fig. 51—Layout details of InSb detector intermediate box

To make full use of the infrared cameras, a display is being developed to overcome the limitations described above and to provide a larger picture than the 75mm diameter tube of the type 101 oscilloscope.

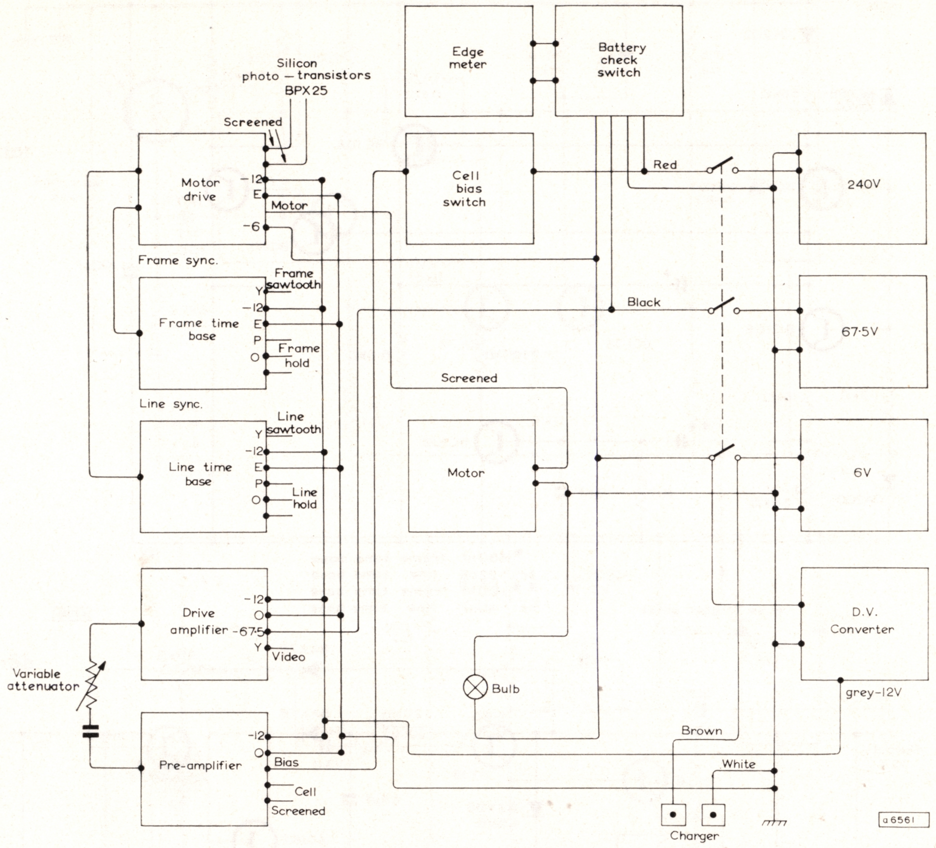
Silicon photo-transistors BPX25
Screened
Edge meter
Battery check switch
Motor drive
-12
E
Motor
-6
Cell bias switch
Red
240V
Frame sync.
Frame sawtooth
Y
-12
E
P
O
Frame time base
Frame hold
Black
67·5V
Screened
Line sync.
Line sawtooth
Line time base
Line hold
Motor
6V
Drive amplifier
-12
O
-67·5
Y
Video
D.V. Converter
grey -12V
Variable attenuator
Bulb
Brown
White
Pre-amplifier
Bias
Cell
Screened
Charger
a6561

Fig. 52—Layout details of PbS detector camera head

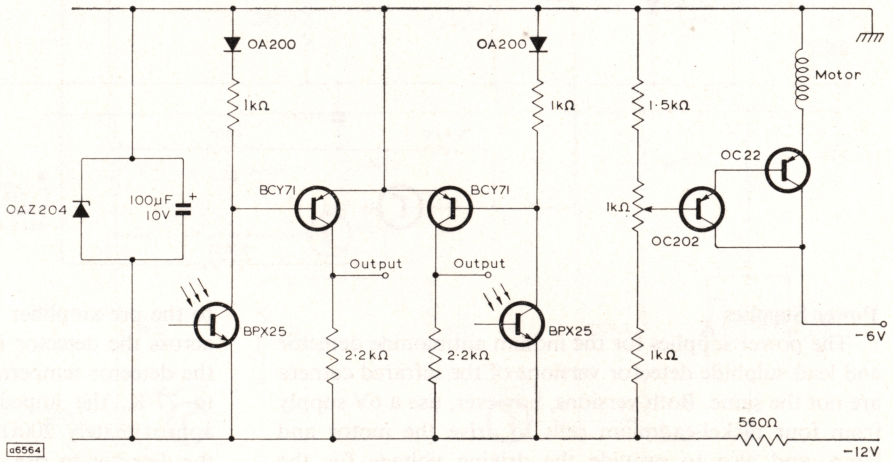
OA200
OA200
Motor
1kΩ
1kΩ
1·5kΩ
OC22
OAZ204
100µF 10V
BCY71
BCY71
1kΩ
OC202
Output
Output
BPX25
BPX25
2·2kΩ
2·2kΩ
1kΩ
-6V
560Ω
-12V
a6564

Fig. 53—Pulse amplifier and motor control

Pulse Amplifier and Motor Control

The circuit diagram for these parts of the system is given in Fig. 53. Synchronisation pulses are obtained by illuminating the inner ring of holes in the Nipkow disc with a 12V festoon bulb under-run at 6V. The radiation passing through is detected by two BPX25 silicon phototransistors, the resultant pulses being squared and amplified by the pulse amplifiers and then applied to the timebases. The motor drive circuit applied a constant voltage to the motor giving adequate speed control (±10%).

Timebases

The frame and line timebase circuits are basically similar sawtooth generators (see Fig. 54), with different timing capacitors to produce the appropriate sweep rates. Synchronisation is provided by the pulses already mentioned. The outputs from the timebases are fed directly to the X- and Y-inputs of the display oscilloscope to produce the raster.

Direct Voltage Converter

The direct voltage converter is a printed-wiring board similar to the one used in the Philips A.C. Millivoltmeter PM2451. It provides a stabilised output voltage of 11·7V for any driving voltage between 3 and 6V (Fig. 55).

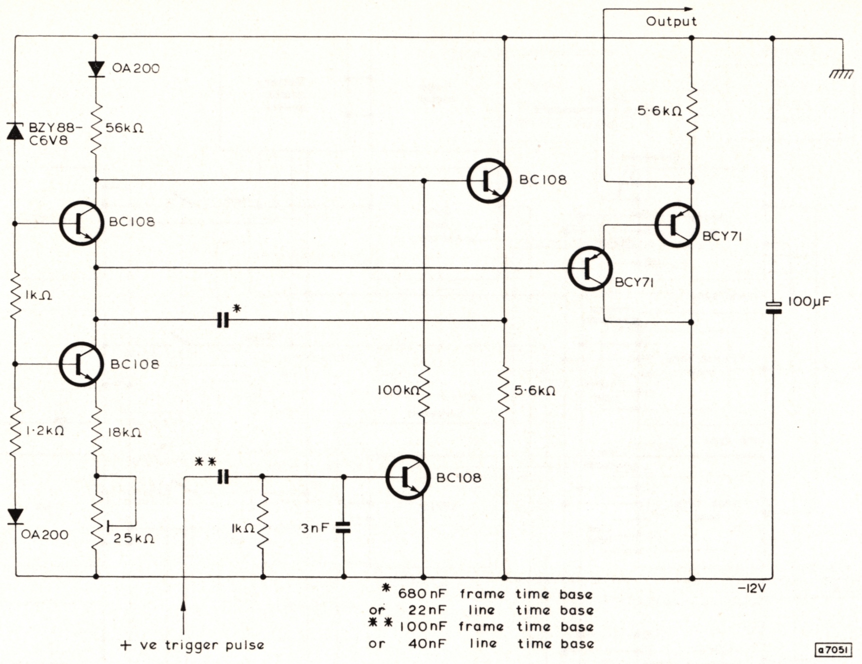
Output
OA200
BZY88-C6V8
56kΩ
BC108
BC108
BCY71
BCY71
1kΩ
*
100µF
BC108
100kΩ
5·6kΩ
5·6kΩ
1·2kΩ
18kΩ
**
BC108
25kΩ
1kΩ
3nF
OA200
−12V
+ ve trigger pulse
* 680nF frame time base
or 22nF line time base
** 100nF frame time base
or 40nF line time base
a7051

Fig. 54—Timebase circuits

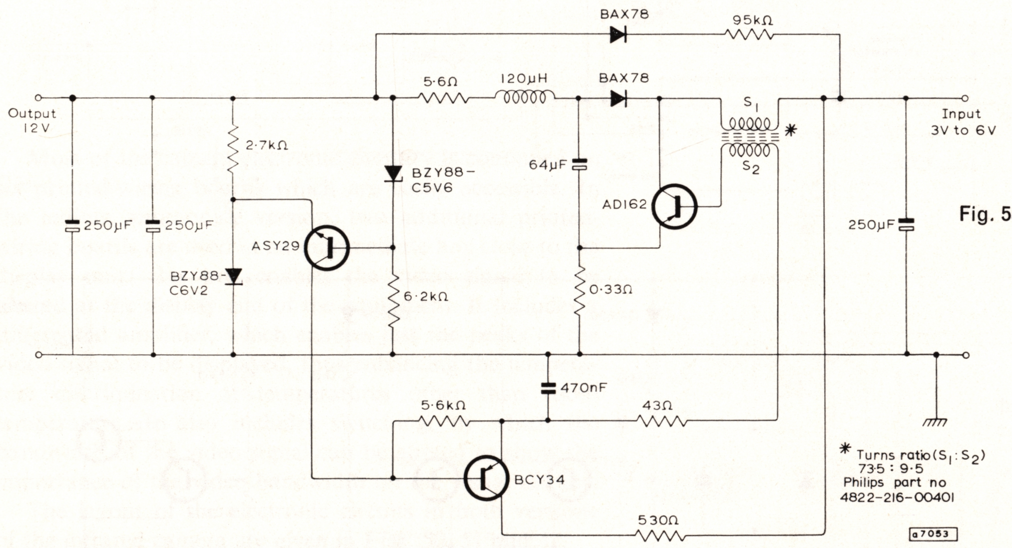
BAX78
95kΩ
5·6Ω
120µH
BAX78
S1
S2
*
Output 12V
Input 3V to 6V
2·7kΩ
BZY88-C5V6
64µF
AD162
250µF
250µF
250µF
ASY29
BZY88-C6V2
6·2kΩ
0·33Ω
470nF
5·6kΩ
43Ω
BCY34
530Ω
* Turns ratio (S1 : S2)
735 : 9·5
Philips part no
4822-216-00401
a7053

Fig. 55—Direct voltage converter

Power Supplies

The power supplies for the indium antimonide detector and lead sulphide detector versions of the infrared camera are not the same. Both versions, however, use a 6V supply from four nickel-cadmium cells to drive the motor and lamp, and also to provide the driving voltage for the direct voltage converter.

Both versions use a 67·5V supply from a B101 battery. In the indium antimonide detector version, it provides detector bias. In the lead sulphide detector version, it provides the high output voltage for the driver amplifier that is an integral part of the camera.

In the indium antimonide detector version, the intermediate box has a separate 67·5V, B101 battery as its power supply. The lead sulphide detector version requires a 240V supply from B127 batteries to bias the detector.

Video Amplifiers for Indium Antimonide Detector

Pre-amplifier

The signal from the indium antimonide detector is fed to the pre-amplifier board (Fig. 56), and the bias voltage across the detector is displayed on an edge meter. When the detector temperature changes from room temperature to 77°K, the impedance increases from a few ohms to approximately 200Ω and causes the bias voltage across the detector to rise, indicating that the detector is operational. The pre-amplifier has a gain of 220 and a bandwidth of 35kHz. The output is fed into the intermediate amplifier.

Intermediate Amplifier

The circuit of the intermediate amplifier is given in Fig. 57. It has a maximum gain of 100. Two stages of attenuation are provided on the input stage, one a fixed 10-to-1 attenuation and the other a variable 10-to-1 attenuation.

The output from the amplifier is the video output from the camera head which is then fed into the intermediate box.

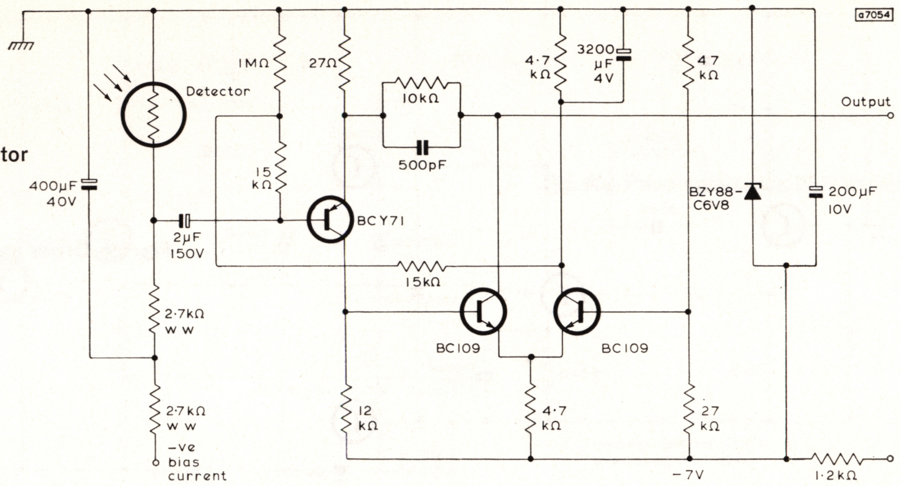
a7054
Detector
1MΩ
27Ω
10kΩ
500pF
4·7kΩ
3200µF 4V
4·7kΩ
Output
400µF 40V
15kΩ
2µF 150V
BCY71
15kΩ
BZY88-C6V8
200µF 10V
BC109
BC109
2·7kΩ w w
2·7kΩ w w
−ve bias current
12kΩ
4·7kΩ
27kΩ
−7V
1·2kΩ

Fig. 56—Pre-amplifier for InSb detector

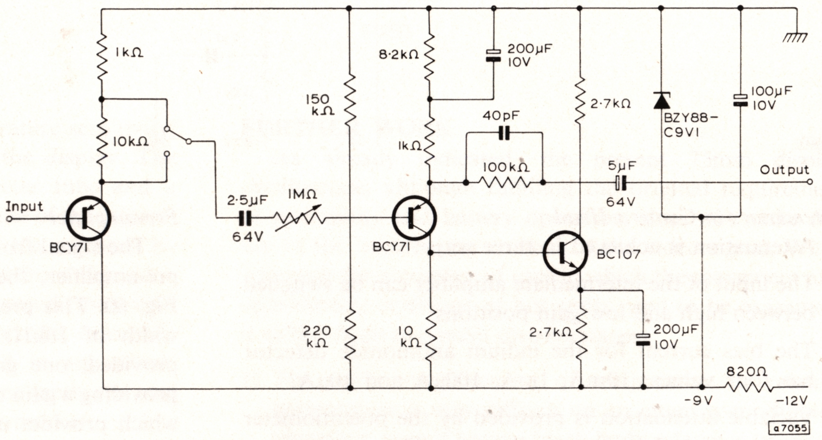
1kΩ
8·2kΩ
200µF 10V
150kΩ
40pF
2·7kΩ
BZY88-C9V1
100µF 10V
10kΩ
1kΩ
100kΩ
5µF 64V
Output
Input
2·5µF 64V
1MΩ
BCY71
BCY71
BC107
220kΩ
10kΩ
2·7kΩ
200µF 10V
820Ω
−9V
−12V
a7055

Fig. 57—Intermediate amplifier for InSb detector circuit

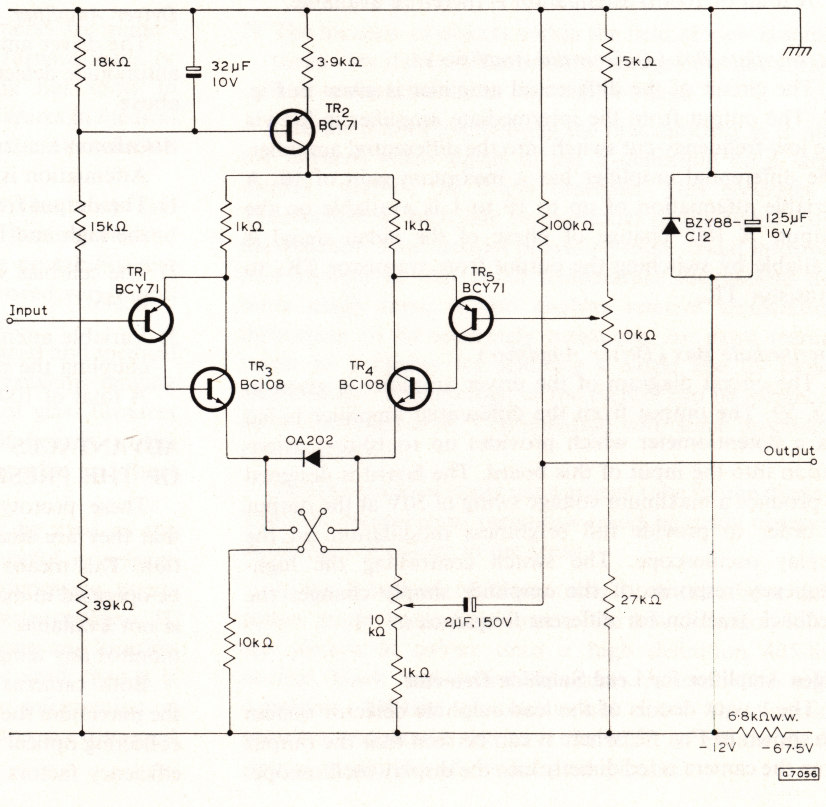
18kΩ
32µF 10V
3·9kΩ
TR2 BCY71
15kΩ
15kΩ
1kΩ
1kΩ
100kΩ
BZY88-C12
125µF 16V
TR1 BCY71
TR5 BCY71
Input
10kΩ
TR3 BC108
TR4 BC108
OA202
Output
39kΩ
10kΩ
10kΩ
2µF,150V
27kΩ
1kΩ
6·8kΩw.w.
−12V
−67·5V
a7056

Fig. 58—Differential amplifier for InSb camera

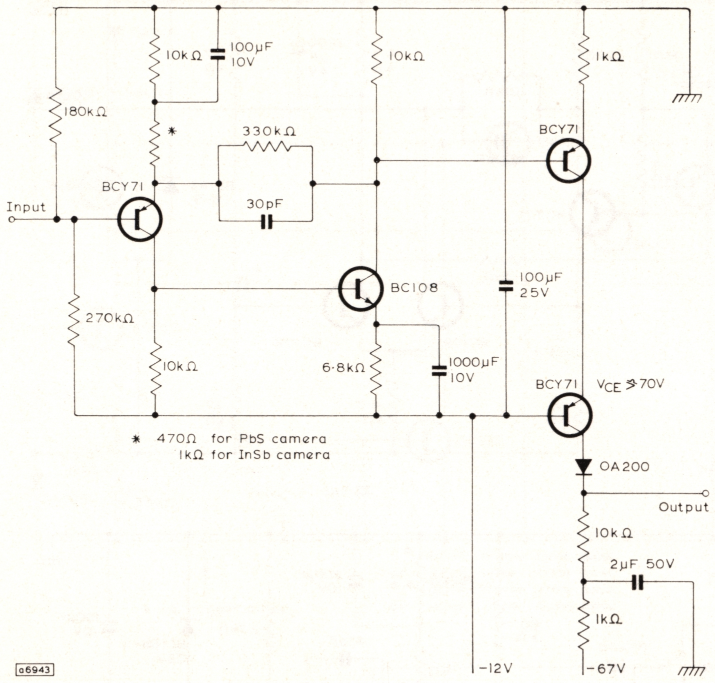

Fig 59—Driver amplifier

Attenuators in Camera Head

Attenuation is achieved in three ways:

1) The input of the intermediate amplifier can be switched between high and low gain positions.
2) The bias current for the indium antimonide detector has four values: 10mA, 1mA, 100μA and 10μA.
3) Variable attenuation is provided by the potentiometer on the input of the intermediate amplifier.

A total of 100dB attenuation is therefore available.

Intermediate Box (Differential Amplifier)

The circuit of the differential amplifier is given in Fig. 58. The output from the intermediate amplifier is fed via the low-frequency-cut switch into the differential amplifier. The differential amplifier has a maximum gain of 10. A variable attenuation of up to 10 to 1 is available on the output. A 180° change of phase of the video signal is available by switching the output from transistor TR_3 to transistor TR_4.

Intermediate Box (Driver Amplifier)

The circuit diagram of the driver amplifier is given in Fig. 59. The output from the differential amplifier is fed via a potentiometer which provides up to 10-to-1 attenuation into the input of this board. The board is designed to produce a maximum voltage swing of 50V at the output in order to provide full brightness modulation on the display oscilloscope. The switch controlling the high-frequency response of the amplifier simply changes the feedback fraction for different frequencies.

Video Amplifier for Lead Sulphide Detector

The layout details of the lead sulphide detector system are shown in Fig. 52, where it can be seen that the output from the camera is fed directly into the display oscilloscope.

Pre-amplifier

The signal from the lead sulphide detector is fed to the pre-amplifier, the circuit diagram of which is shown in Fig. 60. This pre-amplifier has a gain of 30 and a bandwidth of 16kHz, peaking at 10kHz. Two outputs are provided, one giving the maximum gain and the other providing a gain of 3. The output is fed via a potentiometer, which provides up to 10-to-1 attenuation, into the driver amplifier.

Driver Amplifier

The driver amplifier is the same as that for the indium antimonide detector version given in Fig. 59 and described above.

Attenuators

Attenuation is achieved in three ways:

1) The output from the pre-amplifier is switched between the high and low gain positions.
2) The cell bias voltage has four values: 240, 24, 2·4 and 0·24V.
3) Variable attenuation is provided by the potentiometer coupling the pre-amplifier and driver amplifiers.

A total of 100dB of attenuation is therefore available.

ADVANTAGES AND DISADVANTAGES OF THE PRESENT SYSTEM

These prototype cameras have the basic advantages that they are small, light, and have low power consumption. This means that the equipment is portable and can be operated in many difficult locations where mains power is not available. The prototypes are able to continuously monitor any temperature changes.

Both cameras have temperature sensitivities close to the maximum theoretically possible. It is felt that although collecting optical systems with smaller f-numbers or higher efficiency factors (or both) could be used to increase the number of lines or to increase the temperature sensitivity, the main area for improvement lies in the display. The present display with a three-inch diameter tube and a black/white phosphor does not make full use of the information potential of the cameras. Some of the methods by which more information can be obtained from the video signal are described in a later section. However, even with the present display, the cameras have proved extremely versatile and capable of being operated in any plane. Moreover, their potential cost is about one-tenth the cost of other thermal scanning systems on the market.

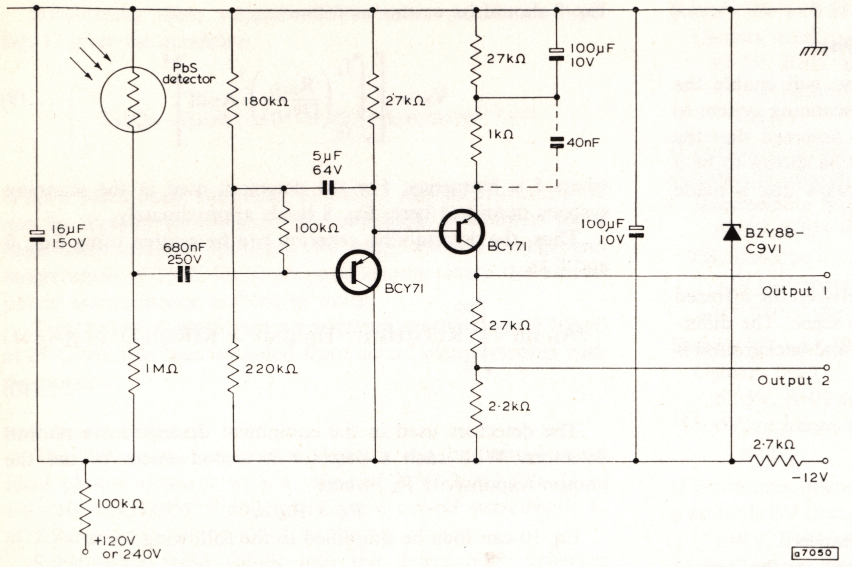

Fig. 60—Pre-amplifier for PbS detector

APPLICATIONS

The possible applications for both cameras are numerous. The most obvious are monitoring furnace walls or lagged pipes to detect faults; detecting hot spots in electronic circuits; measuring skin temperatures in medical applications where the condition of the patient is reflected in the temperature of the skin.

These cameras have the advantage that they can continuously monitor the movement of hot objects and the heat flow in stationary objects. The portability and battery operation of the cameras have proved very useful in both industrial and medical applications.

Both cameras have been used in industrial and medical applications, for the early diagnosis of problems ranging from the detection of flaws in the walls of glass furnaces and hot electronic components on circuit boards, to the examination of patients for cancerous growths and 'heat flow' in varicose veins.

The fact that most oscilloscopes can be used as the display for the cameras could be very useful in a large number of research projects where an inexpensive, versatile infrared camera is required to examine a problem. If, however, accurate temperature measurements and location of objects within the field of view are required, then it is possible that a display in which more information is presented would be necessary. Such displays are discussed in the next section.

FURTHER WORK

As already indicated, the present 75mm display oscilloscope, although fulfilling the original requirement of portability and battery operation, does not make full use of the information content of the video signal. While adequate for a number of uses in which the movement and approximate positions of hot spots need to be examined, it suffers from two main disadvantages:

1) The actual measurement of temperature or relative temperature is very difficult on an intensity-modulated phosphor, even if known black body reference temperature sources are included within the field of view.
2) The location of objects within the field of view is sometimes very difficult. The infrared image does not always bear a resemblance to the visible image.

One method of overcoming the first difficulty is to add the infrared video signal to the Y-deflection on a large display; that is, the frame timebase. This generates a Y-deflection of each line proportional to the signal from the detector. Thus besides providing more visual information content in that small temperature fluctuations are more easily seen, it also enables relative temperature differences to be accurately measured. An extra feature might be a facility for selecting a single line for closer examination. The contrast of the picture can be enhanced by a combination of Y-modulation with some brightness (Z) modulation.

Another method could use a colour-tube for the display. Then the temperature variations could be easily observed as changes of colour in the scene.

A third method of overcoming both the above difficulties might be to superimpose the low-definition infrared picture in colour onto a high definition 405-line normal black and white television picture. The high-definition 405-line picture would solve the location problem and would also have the effect of enhancing the optical resolution of the infrared picture.

APPENDIX 1

Design Equation of Nipkow Disc

The design equation of the Nipkow disc will enable the maximum temperature sensitivity of a given scanning system to be calculated. In this calculation it will be assumed that the system is limited by detector noise. This will be shown to be a justifiable assumption provided that the Nipkow disc is made of the right material and correctly balanced.

OPTICAL SYSTEM

The scanner must be able to distinguish between the infrared source of interest and the background in the scene. The difference between the radiant emittance of source and background is

$$W = \int_0^\infty (H_{S(\lambda)} - H_{B(\lambda)})d_\lambda \qquad \ldots(3)$$

where λ = wavelength

$H_{S(\lambda)}$ = source spectral radiant emittance

$H_{B(\lambda)}$ = background spectral radiant emittance.

A proportion of this radiation is collected by the optical system of the scanner and focused onto the Nipkow disc. From a basic theorem for ideal optical systems, the radiant power falling on a single scanning hole of area A_H in the Nipkow disc is given by

$$H_H = A_H\, W \sin^2\theta, \qquad \ldots(4)$$

where θ is the half angle of the cone of the convergence of the optical system at the Nipkow disc.

In practice, allowance must be made for the efficiency of the optical system (J), and for absorption and scattering by the atmosphere, which is a function of wavelength (T_λ).

Introducing these factors into Eqs. 3 and 4 gives

$$H_H = JA_H \sin^2\theta \int_0^\infty T_\lambda(H_S - H_B)d_\lambda \qquad \ldots(5)$$

DETECTOR

The radiant power passing through the scanning hole in the Nipkow disc is uniformly focused, by means of a field lens, on to the annular detector. The signal voltage V_S developed in the detector is given by

$$V_S = \int_0^\infty JA_H \sin^2\theta\, R_\lambda T_\lambda(H_{S(\lambda)} - H_B)d_\lambda \qquad \ldots(6)$$

where R_λ is the spectral responsivity of the detector; that is, the output voltage per unit of radiant power, as a function of wavelength.

The criterion for the detection of an object is that the difference signal between the source of interest and its background must exceed the system noise by a factor K. A value of 5 for this factor gives a high probability of detection.

Provided that the system is limited by detector noise, this noise (V_N) can be obtained from the area-normalised detectivity D^*_λ by the equation,

$$D^*_{\lambda(1)} = \frac{R_{\lambda(1)}}{V_N}(A_D\Delta f)^{\frac{1}{2}} \qquad \ldots(7)$$

where A_D is the detector sensitive area and Δf is the bandwidth. Therefore

$$V_N = \frac{R_{\lambda(1)}}{D^*_{\lambda(1)}}(A_D\Delta f)^{\frac{1}{2}}. \qquad \ldots(8)$$

If the detector noise V_N is dependent on frequency, then Eq. 8 should be written as follows:

$$V_N = \left[\int_{f_2}^{f_1}\left(\frac{R_{\lambda(1)}}{D^*_{\lambda(1)}}\right)^2 A_D df\right]^{\frac{1}{2}} \qquad \ldots(9)$$

where f is frequency. For the detectors used in the scanning systems described here, Eq. 8 holds approximately.

Thus, the detectability criterion can be written using Eqs. 6 and 8 as,

$$JA_H \sin^2\theta \int_0^\infty R_\lambda T_\lambda(H_{S(\lambda)} - H_{B(\lambda)})d\lambda \geqslant K(R_{\lambda(1)}/D^*_{\lambda(1)})(A_D\Delta f) \qquad \ldots(10)$$

The detectors used in the equipment described are photon detectors. With such a detector it is convenient to use the photon responsivity P_λ, where

$$P_\lambda = R_\lambda/\lambda.$$

Eq. 10 can then be simplified to the following form.

$$\int_0^\infty P_\lambda T_\lambda(Q_S - Q_B)d_\lambda \geqslant \frac{K\lambda_1 P_{\lambda(1)}(A_D\Delta f)^{\frac{1}{2}}}{D^*_{\lambda(1)}\, hc\, J\, A_H \sin^2\theta} \qquad \ldots(11)$$

where Q_S = source photon flux density per unit wavelength,

= $\lambda H_{S(\lambda)}/hc$,

Q_B = background photon flux density per unit wavelength,

= $\lambda H_{B(\lambda)}/hc$,

h = Planck's constant,

c = velocity of light.

For an ideal photon detector, P_λ is constant for wavelengths up to the cut-off wavelength λ_c, and is zero beyond. The detectability criterion then becomes:

$$\int_0^{\lambda_c} T_\lambda(Q_S - Q_B)d_\lambda \geqslant \frac{K\lambda_1(A_D)^{\frac{1}{2}}(\Delta f)^{\frac{1}{2}}}{D^*_{\lambda(1)}\, J\, hc\, A_H \sin^2\theta}. \qquad \ldots(12)$$

MAXIMUM TEMPERATURE SENSITIVITY

The design equation is applied to the scanning systems described in this article in order to calculate their maximum temperature sensitivities. The values of the following parameters in the criterion equation are:

Parameter	Value
Detector sensitive area, A_D	= 30·6mm² (annulus; 8mm outer diameter; 5mm inner diameter)
Bandwidth, Δf	= 8kHz
Area of scanning hole, A_H	= 7·85×10⁻³ cm² (1mm diameter hole)
Convergence, sin θ	= 0·2706
Planck's constant, h	= 6·625×10⁻³⁴ joule second
Velocity of light, c	= 3×10¹⁰cm s⁻¹
Efficiency of the optical system, J	= 0·51
Detectability criterion, K	= 5

InSb Detector System

The indium antimonide detector used in this system has a spectral responsivity that closely follows that of an ideal photon detector. In fact, it can be assumed to be an ideal photon detector with a value of D*(4·4μm, 800, 1) equal to 5×10¹⁰cm (Hz)$^{\frac{1}{2}}$ W⁻¹ and an effective cut-off wavelength λ_c of 5·5μm.

Substituting these values and the other parameters into Eq. 12 gives the condition

$$\int_0^{\lambda_c} T_\lambda(Q_S - Q_B)d\lambda \geqslant 3{\cdot}7\times10^{14} \text{ photons cm}^{-2}\text{ s}^{-1}.$$

With a black-body slide-rule, or with a similar instrument, it can be directly shown that this condition is satisfied for a black-body source temperature of 0·5degC above a background temperature of 25°C for short path lengths where the atmospheric transmittance is close to unity.

This figure of maximum temperature sensitivity of 0·5degC at 25°C has also been obtained from actual measurements with the camera.

PbS Detector System

The PbS room temperature detector can be treated as an ideal photon detector with a value of D*(2·3μm, 800, 1) of 1·8×10¹⁰cm(Hz)$^{\frac{1}{2}}$W⁻¹ and an effective cut-off wavelength λ_c of 2·8μm.

Substituting these values into the detectability criterion equation gives

$$\int_0^{\lambda_c} T_\lambda(Q_S - Q_B)d\lambda \geqslant 5{\cdot}5\times10^{14} \text{ photons cm}^{-2}\text{ s}^{-1}.$$

With a black-body slide rule it can be found that, for short optical path lengths (that is, $T_\lambda \simeq 1$) and allowing for the daylight filter transmission of 55%, a temperature difference of 80degC between a black-body source and a room temperature background is enough to satisfy this criterion. This figure again corresponds fairly closely to the easily observable 100degC difference measured with the camera.

APPENDIX 2

Equipment Specification

Picture quality	30×30 element raster generated at 17 frames per second
Field of view	6°×6°
Focusing range	60cm to infinity
Detector types	
Low temperature camera	RPY56 InSb detector cooled to 77°K annular element, 8×5mm
High temperature camera	RPY57 PbS detector operated at room temperature; annular element 8×5mm
Temperature ranges	
InSb detector	−40 to +800°C
PbS detector	+120 to several thousand degrees C, depending on optical attenuation filters used.
Temperature sensitivity	
InSb detector	±0·5degC at 25°C
PbS detector	±5degC at 200°C (accuracy, ±10%)
Effective spectral response	
InSb detector	3·0 to 5·5μm
PbS detector	2·0 to 2·8μm (Type G1 daylight filter incorporated)

Battery life with InSb detector	
Camera head	
67·5V, B101 supply	50h
6V, rechargeable NiCd supply	4h

(Continuous operation for up to 50h may be obtained using a suitable 6V charging unit during operation.)

Intermediate box	
67·5V, B101 supply	80h
Oscilloscope display	
12V rechargeable supply (or mains operated)	4h
Battery life with PbS detector	
Camera head	
67·5V, B101 supply	120h
6V, rechargeable NiCd supply	4h

(Continuous operation for up to 120h may be obtained using a suitable 6V charging unit during operation.)

240V, B123 supply	450h
Oscilloscope display	
12V, rechargeable supply (or mains operated)	4h
Power consumption	
Camera	3W
Oscilloscope display	20W

Coolant for InSb detector

Liquid nitrogen fed by Leiden-Frost drip-feed mechanism from dewar vessel.

Dewar capacity	4 litre
Cooling period (intermittent use)	2 days
Dimensions	
Camera	34×25×28cm
Intermediate box	23×15×14cm
Four-litre dewar	20cm high; 40cm diameter
Weight	
Camera	7·4kg
Intermediate box	2·1kg
Four-litre dewar	7·7kg

APPENDIX 3

Equipment Controls

Camera Controls

Focus	60cm to infinity in the directions shown (InSb equipment has a calibrated scale).
Attenuation controls	
Coarse	5 ranges each with an attenuation factor of approximately 10.
Fine	Variable attenuation factor of approximately 10.
Battery check	Enables condition of batteries to be ascertained; they should be either replaced or recharged when needle no longer lies in red region of scale.
Detector temperature check (InSb detector camera only)	Needle valve controlling flow of coolant should be turned approximately three-quarters of revolution, at which point needle should slowly move into red region of scale; flow rate may need adjusting from time to time but should be kept to minimum required to cool detector.

6V charging point	Enables 6V NiCd supply to be recharged, the charging period being 14 hours at maximum of 250mA; Philips charger, PM9000, is suitable.
Approximate black-body temperature calibration	When the oscilloscope display controls on PbS equipment are set as described below, an approximate effective black-body temperature calibration can be obtained by decreasing attenuation until the display phosphor just reaches its maximum brightness; temperature of object under consideration can then be read from instrument chart.
Outputs	Video signal and two timebase outputs are provided on B.N.C. sockets; screwdriver adjustments are provided for line and frame holds.

Intermediate Box Controls

(InSb detector camera only)

High-frequency cut	Enables 3dB point on video signal to be switched to 16kHz, 8kHz, 5kHz, 3kHz or 1kHz.
Low-frequency cut	Enables 3dB point on video signal to be switched to 15Hz, 45Hz, 100Hz, 300Hz, or 1kHz.
Phase switch	Enables phase of video signal to be changed by 180°; this reverses the 'white is hot' convention on display oscilloscope to 'black is hot'.
Differential control	Enables peaks of video signal to be displayed on oscilloscope; this enables fine detail on relatively-high-temperature object to be seen in sharp contrast.
Attenuation controls	Two variable attenuation controls are provided; each has maximum attenuation of approximately 10:1.

Oscilloscope Display Controls

Focus, brilliance, astigmatism	For calibration purposes on the high-temperature PbS equipment, these should be set with the white lines positioned centrally.
Y-amplifier	500mV/cm, d.c.
Sweep	X-input
Y-input	Frame timebase from camera
X-input	Line timebase from camera
Z modulation on back panel	Video signal
X- and Y-gain and shift	Should be adjusted until centrally positioned square picture is obtained.

SELECT BIBLIOGRAPHY

Simon, I., 'Infrared Radiation', Van Nostrand, 1966 (Paperback).

Smith, R. A., Jones, F. E. and Chasmar, R. P., 'The Detection and Measurement of Infrared Radiation', O.U.P., 1957.

Conn, G. K. T., and Avery, D. G., 'Infrared Methods', Academic Press, 1960.

Haughton, J. T., and Smith, S. D., 'Infrared Physics', O.U.P., 1966.

Kruse, P. W., McGlauchlin, L. D. and McQuistan, R. B., 'Elements of Infrared Technology', Wiley, 1962.

Holter, M. R., Nudelman, S., Suits, G. H., Wolfe, W. L. and Zissis, G. J., 'Fundamentals of Infrared Technology', Macmillan, New York, 1962.

Jamison, J. A., McFee, R. H., Plass, G. N., Grube, R. H., and Richards, R. G., 'Infrared Physics and Engineering', McGraw-Hill, 1963.